Skoltech
Skolkovo Institute of Science and Technology

Skolkovo Institute of Science and Technology

DEVELOPMENT OF MESSENGER RNA DELIVERY SYSTEM VIA VIRUS-LIKE PARTICLES

Doctoral Thesis

by

YULIA ZHITNYUK

DOCTORAL PROGRAM IN LIFE SCIENCES

Supervisor

Professor Konstantin Severinov

Moscow - 2019

Table of Contents

Abstract

Applying messenger RNA (mRNA) has become a promising therapeutic modality in various spheres ranging from basic science to biotechnology. Introducing mRNA into cells allows to express a certain protein of interest thus making it a viable tool for gene therapy and vaccine development. mRNA delivery is advantageous over DNA delivery as it is transient and does not carry the risk of genomic DNA integration. However, few efficient mRNA delivery options are currently available thus new delivery methods are required. This problem becomes even more complicated for hard-to-transfect cell types. To this end, we have established a novel mRNA delivery system utilizing chimeric virus-like particles (VLPs). We generated a novel type of VLPs by fusing protein G of Vesicular stomatitis virus (VSV-G) with a ribosomal protein L7Ae of *Archeoglobus fulgidus*. This system ensured the efficient delivery of EGFP and SpCas9 mRNA which was independent of BoxC/D motif in the mRNA sequence. We demonstrated that incorporating messenger RNAs inside virus-like particles of VSVG-L7Ae occurs via binding with some endogenous kink-turn motif. Our VSVG-L7Ae VLPs-based system demonstrated a high transduction efficacy in hard-to-transfect cell lines, such as human induced pluripotent stem cells (iPS cells) and monocytes. In summary, this platform may serve as an efficient and transient transgene delivery tool for any mRNA of interest.

Publications

Zhitnyuk Y, Gee P, Lung MSY, Sasakawa N, Xu H, Saito H, Hotta A. Efficient mRNA delivery system utilizing chimeric VSVG-L7Ae virus-like particles. Biochem Biophys Res Commun. 2018 Nov 10;505(4):1097-1102. doi: 10.1016/j.bbrc.2018.09.113. Epub 2018 Oct 10

Musharova O, Vyhovskyi D, Medvedeva S, Guzina J, Zhitnyuk Y, Djordjevic M, Severinov K, Savitskaya E. Avoidance of Trinucleotide Corresponding to Consensus Protospacer Adjacent Motif Controls the Efficiency of Prespacer Selection during Primed Adaptation. MBio. 2018 Dec 4;9(6). pii: e02169-18. doi: 10.1128/mBio.02169-18

Acknowledgments

Creation and exploration are probably two of the most enriching and satisfying activities in life, and I was lucky enough to be engaged in both of them, while engineering the delivery system and then trying to elucidate its unexpected mechanism of action.

I would like to warmly and sincerely thank the following people without whom my PhD would have been impossible, who greatly helped me in one or the other along the way:

Prof. Konstantin Severinov, Prof. Akitsu Hotta, Prof. Aleksander Kuleshov, Prof. Konstantin Lukyanov, Prof. Timofei Zatsepin, Dr. Naga Vara Kishore Pillarsetty, Professor Yuri Kotelevtsev, Prof. Kaspars Tars, Prof. Anna Derevnina, Dr Matthew Mulherin, Dr. Nina Popova, Dr. Dmitry Artamonov, Dr. Anna Nikolaeva, Dr. Peter Gee, Dr. Mandy Lung, Dr. Huangang Xu, Noriko Sasakawa, Dr. Mio Iwasaki (Proteomic analysis), InSyoBio labs (RNA-seq analysis), Prof. Svetlana Dubiley, Dr. Olga Musharova, Dr. Alexey Kulikovskiy, Dr. Anastasia Sharapkova.

I wish them all the best, and my gratitude is beyond any possible expression.

Abbreviations

7SL lnc RNA- long non-coding RNA of Signal Recognition Particle RNP complex

Aa-amino acids

ACE- A/C rich exon enhancer

CA - Capsid (p24) Lateral connections between MA and NC

CPP- cell-penetrating peptides

CCR5- chemokine receptor type 5

CSD - Cold shock protein RNA-binding domain of YB-1

CTD - C-terminal RNA-binding domain of YB-1

CXCR4 - chemokine receptor type 4

dsDNA- double-stranded DNA

ER- Endoplasmic Reticulum

FRET- fluorescence resonance energy transfer

gRNA - genomic RNA (of retro-and lentiviruses)

HCV- Hepatitis C virus

HBV- Hepatitis B virus

HER2- Human epidermal growth factor receptor 2

HIV-1- Human Immunodeficiency Virus type I

HSV- Herpes simplex virus

hTERT- human telomerase reverse transcriptase

hTR- human telomerase RNA

iPS cells- induced pluripotent stem cells

IRAK1- Interleukin-1 receptor-associated kinase 1

KLF-4 - Kruppel-like factor 4

LMWP-low molecular weight protamine

lncRNA-long con-coding RNA

MA- Membrane associated (Matrix) protein (gp17)

MCP- MS2 coat protein

MDA-5- Melanoma Differentiation-Associated protein 5

MFI-Mean Fluorescence Intensity

MLV- murine leukemia viruses

NC- nucleocapsid

PABP- Poly-A Binding Protein

PBMC- Peripheral Blood Mononuclear Cell

PFV-Prototype Foamy Virus

PIV5-Parainfluenza virus type 5

RIG-I- retinoic acid-inducible gene 1

RNC- ribosome-nascent chain complexes

RNP- Ribonucleoprotein complex

RRM- RNA-Recognition Motifs

rRNA- ribosomal RNA

SaCas9 - CRISPR- associated protein from *Staphilococcus aureus*

SeMV- Sesbania mosaic virus

siRNA - small interfering RNA

snoRNA - small nucleolar RNA

snRNA - small nuclear RNA

SpCas9 - CRISPR- associated protein from *Streptococcus pyogenes*

SRP - Signal Recognition Particle

ssDNA - single-stranded DNA

SYNCRIP - Synaptotagmin binding, Cytoplasmic RNA-interacting protein

TALENs - Transcription Activator-like Effector Nuclease

TF - Transcription Factor

TLR-Toll-like receptor

tRNA - transfer RNA

VLPs - Virus-like Particles

VSV - Vesicular Stomatitis Virus

VSVG-G -Vesicular Stomatitis Virus Protein-G

YBX-1 -Y-box binding protein

1.1 Messenger RNA delivery as an appearing novel therapeutic modality.

Messenger RNA applications are shaping up to become a ubiquitous tool not only in basic research but also in a therapeutic sector. Exploiting mRNA as a message carrier provides a solution to numerous biological problems [Stanton et al, 2018]. For instance, when introduced into a cell it allows a protein of interest to be specifically expressed thus making it useful for gene therapy and vaccine development [Kaczmarek, Kowalski, Anderson, 2017]. Moreover, mRNA enables the defective protein to be replaced to cure genetic diseases. Applying mRNA can serve as a therapeutic tool for introducing the genome- editing platforms/ presenting disease-associated proteins or antigens to the immune system [Kaczmarek et al, 2017].

Other conventional means of expressing the desired protein in cells are as following: introducing plasmid DNA or protein. Yet, the plasmid DNA poses a significant risk of genome integration and consequent mutations, thus implying certain limitations in using it in therapy. mRNA is advantageous over the conventional means not imposing such limitations. Furthermore, mRNA exposition provides for transient expression which can be desirable, for example, in introducing genome editing platforms due to the decreased risk of off-target effects [Pattanayak et al, 2013]. Localization of mRNA in the cytoplasm ensures rapid protein production and evades the challenge of intranuclear delivery [Tavernier et al, 2011]. Moreover, mRNA expression does not depend on cell cycle, and mRNA-mediated protein production can be predicted and described by modelling [Leonhardt et al, 2014].

Another conventional method to manipulate the protein outcome is cell protein transfer. This method has been developed as a valuable direction in both: basic research and gene therapy for decades now [D'Astolfo et al, 2015]. It enables a transgene to be transiently expressed with no risk of insertional mutagenesis what makes it similar to mRNA methods. However, as compared to protein delivery, mRNA provides an enhanced and prolonged performance, since one

molecule of mRNA gives rise to multiple protein products through translation by polysomes. Another interesting advantage of introducing mRNA rather than proteins, is that it allows the protein expression to be programmed by introducing regulatory sequences in the 5' or 3' UTR of mRNA, for example MS2 stem loops or kink-turn motifs. This allows the translation to be subtly manipulated by supplying the corresponding MS2 or kink-turn binding protein to prevent ribosomal binding and thus halt the translation [Stapleton et al, 2012; Saito et al, 2010]. This approach enables on- and off- systems to be produced. Interestingly, exploiting mRNA rather than protein in bioengineering permits devising the microRNA switches. In this case mRNA contains a complementary region to be targeted by a certain microRNA, predominantly expressed in a particular cell type. MicroRNA switches encoding an apoptotic protein can serve as a cell sorting tool, as a cell survives only in case it contains the required microRNA to degrade mRNA transcript and therefore to prevent the apoptotic protein from translation and functioning [Miki et al, 2015].

Messenger RNA stability. The only problem using mRNA for therapeutic purposes is its low stability. To execute the full potential of mRNA cytoplasmic expression and to eliminate potential obstacles towards mRNA-based therapies, mRNA stability should be increased. Hence, a few ways to enhance mRNA stability were developed. First, chemical modification of 5'-cap has substantially decreased the transcript degradation by RNA SpDcp1/2 decapping complex. Second, an enhanced mRNA translation was observed due to an increased cap interaction with the major transcription factor 4E [Strenkowska et al, 2016]. Another efficient means of influencing the mRNA transcript stability is optimizing the codon when the rare codons are replaced by more common synonymous codons [Presnyak et al, 2015] or utilizing circular mRNA molecules with IRES elements [Chen, Sarnow, 1995].

Immunogenicity. RNA molecules are recognized by certain types of pathogen recognition receptors (PRR) within immune cells. These include endosomal membrane-associated TLR-3, 7 and 8 (Toll-like receptors) and cytosolic sensors: RIG-I, MDA-5, and LGP-2 receptors. RIG-I

(retinoid-inducible gene I) was known to detect dsRNA with a bare triphosphate group at the 5' end, where the 5' end nucleotide is involved in the base pairing with the complementary chain of the dsRNA [Schlee et al, 2009; Schmidt et al, 2009]. However, recent studies demonstrate that dsRNA bearing m7-guanosine triphosphate cap is also recognized by RIG-I [Schuberth-Wagner et al, 2015].

MDA-5 and LGP-2 signal after identifying dsRNA, which should either have a long double-stranded area (over 2 kb for MDA-5) [Pichlmair et al, 2009] or double-stranded regions on the ends (for LGP-2) [Li et al, 2009]. On the contrary, TLR7 and 8 can detect ssRNA, although the mechanisms of discriminating between self versus non-self are poorly understood. One of the ways for TLR 7 and 8 to sense RNA and activate the downstream signaling cascades is when these RNAs contain UA-rich regions [Heil et al, 2004]. Interestingly, pseudouridylation of mRNA was demonstrated to decrease the potential activation of innate immune receptors and thus immunogenicity [Andries et al, 2015]. Another approach to modify RNA nucleotides and to decrease their immunogenicity is methylation of cytosine residues. Combining these modifications in IVT-transcribed mRNA was demonstrated to decrease the immune destruction yielding the detectable levels of proteins and their proper functioning after naked mRNA intramuscular injection in mice. Following along with this approach, Kormann et al. delivered erythropoietin and surfactant-B mRNAs with a consequent increase in systemic hematocrit. This lead to the mice survival due to a lethal lung disease [Kormann et al, 2011]. Erythropoietin is a hormone secreted by kidneys, which stimulates the red blood cells production, for example, in hypoxic conditions, while surfactant is a mixture of proteins that allows alveoli in the lung not to shrink under the negative pressure of pleural cavity. The increased hematocrit and mice survival in acute pulmonary disease proved that mRNA of erythropoietin and surfactant B was successfully delivered and due to chemical modifications of uridines and cytosines avoided the immune-mediated instability.

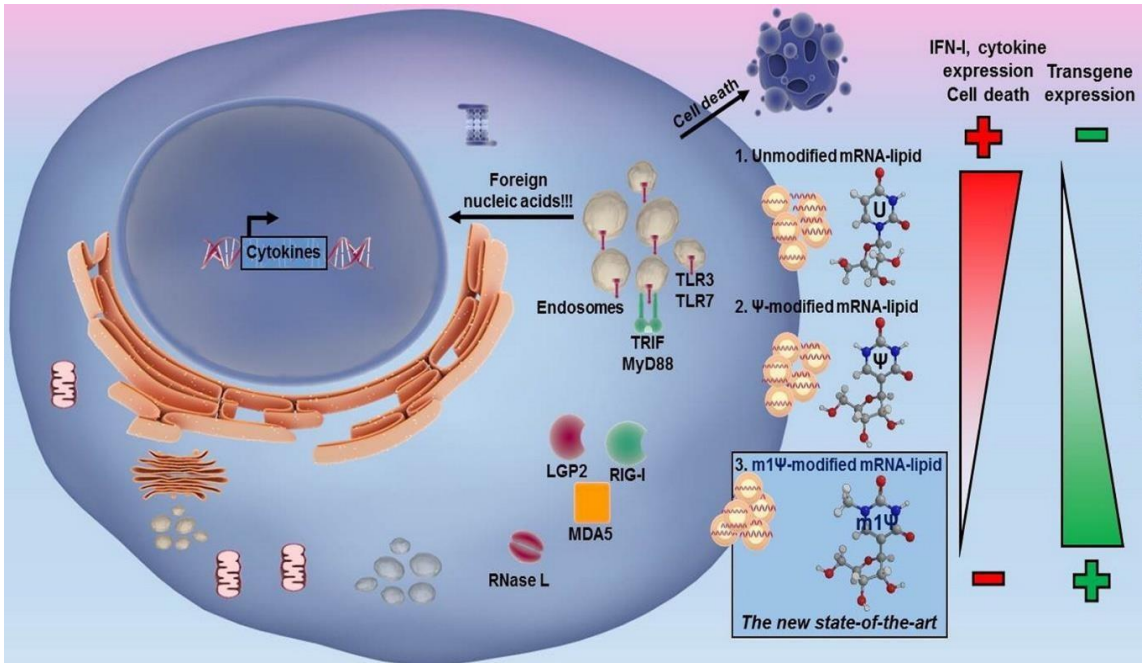

Figure 1.1 Innate immune receptors and chemical mRNA modifications.
Figure adapted from the reference Andries et al, 2015.

1.2 Applications of mRNA delivery.

mRNA delivery may be applied to various areas simplifying and making the previous methods more effective, precise and long-lasting. The applications may be as following: to devise viral vaccines, to generate autologous dendritic cell vaccines for cancer immunotherapy, to replace disease-related defective protein in gene therapy, and to introduce genome-editing platforms to cells.

1.2.1 Immunotherapy with autologous Dendritic Cells *ex vivo* transfected by electroporation with mRNA of tumor antigens.

The technique of introducing a tumor-specific antigen to dendritic cells *ex vivo* with a consequent injection of these antigen-exposed dendritic cells back to a patient has already appeared in the

late 20th century [Boczkowski et al, 1996; Hsu et al, 1996]. Dendritic cells are innate immune cells serving as the major link between the innate and adaptive branches of the immune system. DCs belong to the class of antigen-presenting cells (APCs) that are capable of engulfing the antigen, digesting it and presenting it on their surface in a complex with MHC class II receptor to be introduced to the T helper cells, or even B-cells and thus initiate adaptive immune response. Autologous dendritic cells are taken from the patient, *ex vivo* transfected with either protein [Hsu et al, 1996] or mRNA [Koido et al, 2000] of tumor-associated antigen and administered to the patient by intravenous/ intranodular (inside lymph nodes) or intradermal routes (Figure 1.2).

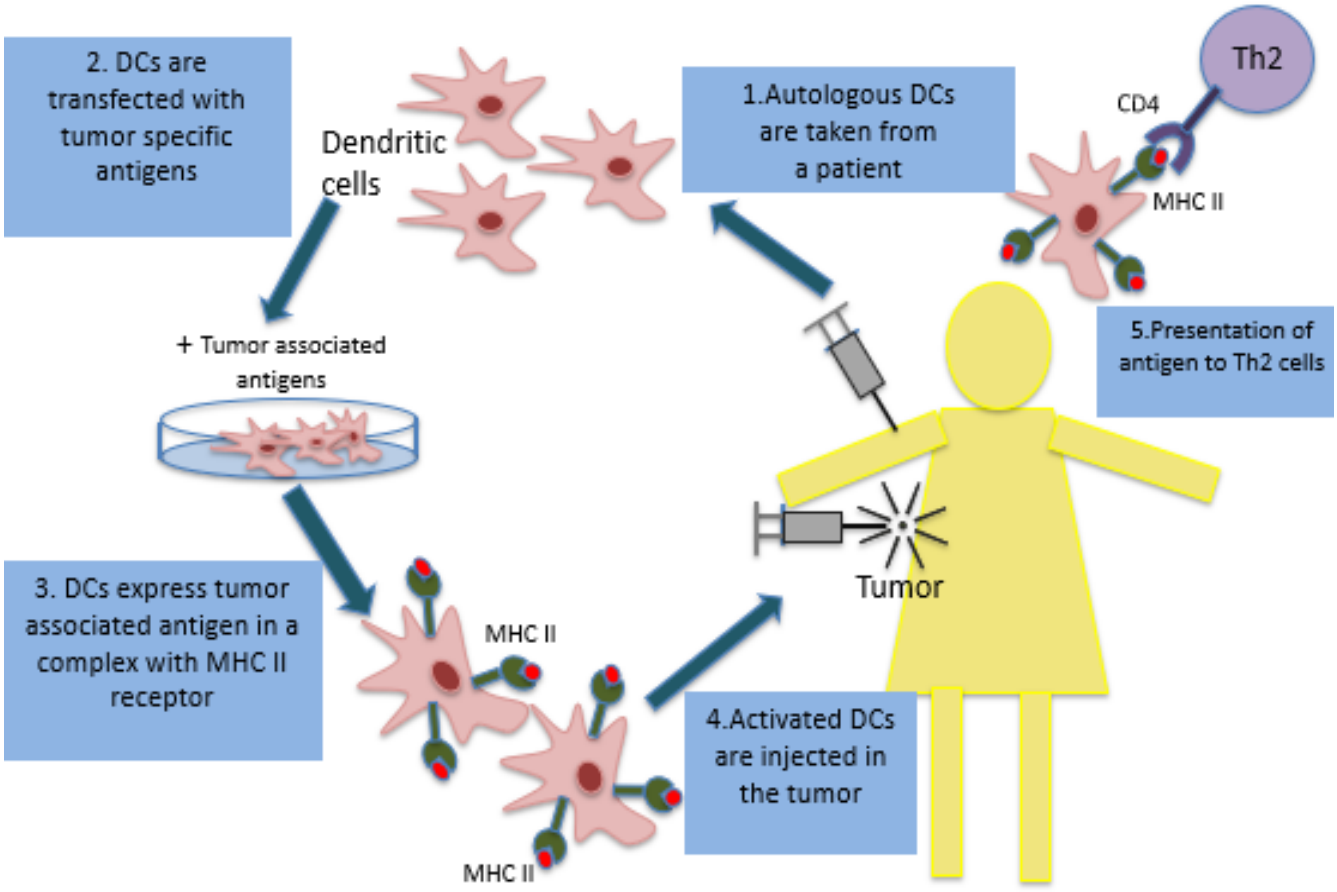

Figure 1.2 Dendritic cells vaccination

The autologous dendritic cells are taken from a patient. Then in a dish they are exposed to either ligands that stimulate receptors of the innate immunity (TLRs, PRRs) or transfected with tumor-associated antigens. This enables the activation of the dendritic cells and further signal presentation to Th2 cells. Lastly, activated dendritic cells are injected back to the lymph nodes

or tumor itself of the patient.

Dendritic cell vaccination with mRNA of tumor-specific antigens is undergoing the clinical trials for the following malignancies: renal cell carcinoma (mRNA AGS-003, clinical trials #NCT00678119) [Amin et al, 2015], acute myeloid leukemia (AML) (mRNA encodes for WT1 (Wilm's tumor 1) protein, clinical trials #NCT01686334) [Van Tendeloo et al, 2010], multiple myeloma (a cocktail of mRNAs encoding CT7, MAGE-A3, and WT1, clinical trials # NCT01995708), prostate cancer (mRNAs for hTERT and survivin, clinical trials # NCT01197625), melanoma (IVAC MUTANOME mRNA, a polyepitopic RNA based on individual patient tumor mutations and tumor marker expression, clinical trials # NCT02035956), breast cancer (ARM1 IVAC_W_bre1_uID encoding for individual tumor-associated antigens plus p53 mRNA, clinical trials # NCT02316457), solid tumors and lymphomas (mRNA-2416 encoding OX40L, a ligand for CD134 receptor on a particular subtype of dendritic cells promoting and amplifying Th2 immune response. As a lipid nanoparticle, this RNA is injected into the solid tumor (Clinical trials # NCT03323398).

Moreover, dendritic cells can be utilized in HIV-1 vaccine development. iHIVARNA-01 represents targeting dendritic cells *in vivo* by simultaneous administration of a cocktail made up of DC and mRNA molecules encoding HIV-associated antigens (16 joined fragments from Gag, Pol, Vif and Nef) and mRNA molecules triplet trimix including transcripts encoding antigen-presenting cells stimulating molecules (Clinical trials # NCT02888756).

Another exciting field of vaccine development is directly injecting mRNA to elicit immune response by stimulating RNA-sensing pathogen-recognition molecules, for example TLR-7 [Fotin-Mleczek et al, 2011]. There are several anti-viral vaccines harnessing mRNA being investigated and tested in clinical trials. Examples of such vaccines are those against Zika virus (mRNA 1325, clinical trials # NCT03014089), rabies (CV7201 encoding a part of rabies virus glycoprotein, clinical trials #NCT02241135), and CMV (mRNA-1647 and

mRNA-1443 , clinical trials #NCT03382405) [John et al, 2018].

1.2.2 Substitutional therapy for genetic diseases. Other than in vaccine development or autologous dendritic cell-based vaccine development, mRNA can serve either to replace a deficient protein or to increase the expression of a protein beneficial for a particular pathological condition. For instance, a prolonged hyperglycemia (elevated glucose concentrations in the blood) in patients with Diabetes Mellitus type II induces the non-enzymatic glycosylation of various structures leading to endothelium dysfunction and hypercoagulability state. This ultimately impairs a blood flow to peripheral tissues and leads to ischemic (restrained from blood flow) ulcers formation. In this case, introducing VEGF to the ischemic area promotes the growth of new vessels and ultimately restoring the blood flow. This also opens up promising ways of treating the ischemic heart disease after myocardial infarction or after the heart failure, since neovascularization promotes oxygen and thus nutrient delivery to the heart muscle [Zangi et al, 2013]. One of mRNAs that is supposed to serve this purpose is AZD8601 (modified VEGF-A RNA). Its intradermal injections in forearm have been tested in patients with Diabetes Mellitus type II (Clinical trial # NCT02935712).

Deficient enzyme replacement therapy by introducing mRNA encoding human methylmalonyl-coenzyme A mutase is applied to treat a rare liver disease called methylmalonic acidemia. This trial has only been recently launched by Moderna and therefore has not been attributed a number yet. Still it illustrates that mRNA expression may serve as a powerful tool of protein-replacement therapy in enzyme deficiencies.

Other examples of protein-replacement therapy include introducing mRNA as a part of lipid nanoparticle (LNP). Ramaswami et al. treated Hemophilic B mice *in vivo* with mRNA encoding for human Factor X (hFIX). The group used LUNAR lipid nanoparticles, which consisted of a proprietary Arcturus therapeutics' lipid (ATX), cholesterol, a phospholipid 1,2-distearoyl-sn-glycero-3-phosphocholine (DSPC), and a pegylated lipid [Ramaswamy et al, 2017]. This

approach allowed Factor IX to be efficiently delivered to the liver of hemophilic mice and to restore the coagulation profile. In another study, a systemic delivery of chemically modified [Kormann et al, 2011] and unmodified [Thess et al, 2015] mRNA of erythropoietin in mice and non-human primates was confirmed through the increased hematocrit level.

1.2.3 Genome editing.

While gene therapy is required to replace a defective gene product, genome editing allows the mutation to be permanently corrected at the gene level. The discovery type II bacterial CRISPR-Cas9 system (clustered regularly interspaced short palindromic repeats (CRISPR)–CRISPR-associated (Cas9) genome editing system) as a genome editing tool was a breakthrough in the field of genome engineering. CRISPR-Cas9 platform demonstrated an increased performance over the other genome editing platforms such as ZNFs and TALENs in terms of engineering simplicity and efficiency [Doudna, Charpentier, 2014]. To facilitate applying this RNA-programmable nuclease Cas9 in laboratory conditions, scientists devised a chimeric single guide RNA (sgRNA) functionally similar to crRNA:tracrRNA complex in bacteria and archaea (Figure 1.3).

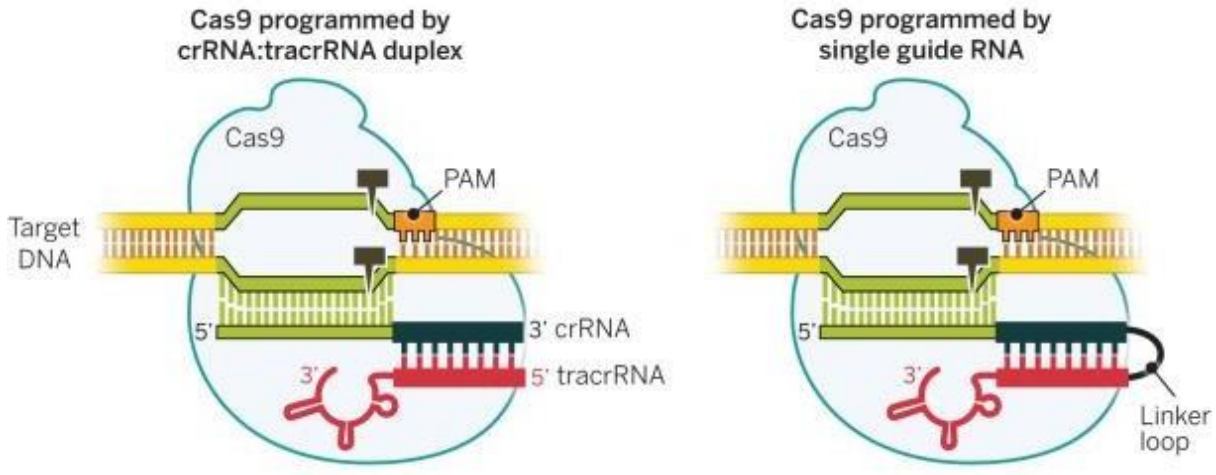

Figure 1.3 CRISPR-Cas9 system with separate crRNA and tracrRNA and sgRNA. The

figure is adapted from reference Doudna, Charpentier, 2014

After matching with the neighboring downstream PAM (protospacer adjacent motif), sgRNA binds to the 20 nt-long target DNA sequence via Watson-Crick base paring. Cas 9 proteins were obtained from bacterial type II CRISPR-Cas system. Cas9 executes DNA unwinding and performs a double-strand break (DSB) being led by sgRNA to the necessary spot in the genome. DSB can be restored by several DNA repair pathways: i) generally occurring non-homologous end-joining pathway followed by insertion or deletion (indels) leading to a gene knockout (KO) (Figure 1.4) or ii) homology-directed repair (HDR) which requires a DNA template [Iliakis et al, 2004].

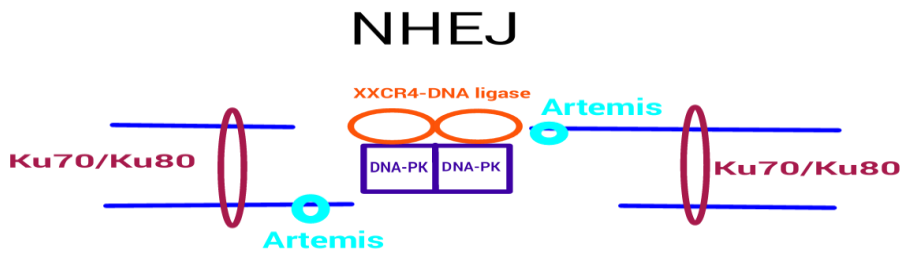

Figure 1.4 The mechanism of NHEJ. DSB is juxtapositioned and stabilized by Ku70/Ku80 complex and DNA-PK. Artemis processes cleaves damaged nucleotides. XXCR4-DNA ligase dimmers ligate ends of DSB.

Using ssODN (single-stranded oligodeoxynucleotides) together with CRISPR-Cas9 system as a template stretch can shift the preference of the repair pathway towards HDR [Tycko et al, 2016]. As a genome editing tool CRISPR-Cas9 system proved to be effective and efficient in mammalian cells and tested on numerous organisms including mice and rats **[**Doudna, Charpentier, 2014**]**. However, several major limitations of the system include the following: a

high risk of off-target effects [Tycko et al, 2016], a low level of HDR-mediated genome editing in comparison to NHEJ [Doudna, Charpentier, 2014], and delivery challenges [Moreno, Mali, 2017]. Multiple diseases have recently been treated by CRISPR-Cas9 *in vivo* using the animal models. Some of these include Duchenne muscular dystrophy [Long et al, 2016, Nelson et al, 2016], hereditary tyrosinemia [Yin et al, 2016], ornithine transcarbamylase (OTC) deficiency [Yang et al, 2016], amyotrophic lateral sclerosis (ALS) [Gaj et al, 2017], hemophilia B [Singh et al, 2018], Rett syndrome [Swiech et al, 2015], alpha1-antitrypsin deficiency [Song et al, 2018], and Leber congenital amaurosis [Ruan et al, 2017].

1.2.4. RNA-based reprogramming

In addition to the vaccine development and genome editing, mRNA delivery is used for the reprogramming. Introduction of Yamanaka's factors Oct4, Sox2, Klf, and c-myc to the cells enables their reprogramming to iPS cells [Takahashi and Yamanaka, 2006]. Delivery of mRNA allows the escape the nuclear phase and, therefore, favors the safety concerns as the risk of genome integration is very minor. A common way to introduce mRNA for the reprogramming purposes is by using Sendai viral (SeV) vectors [Bernal, 2013]. SeV is a negative strand enveloped RNA virus. By the means of incorporating mRNA of interest to the viral RNP complex, Yamanaka's factors were used to obtain iPS cells from fibroblasts, CD34 positive cord blood cells [Nishishita, 2011], and T-lymphocytes. [Seki, 2010]

1.3 Virus-like particles as delivery systems.

Recent advances in the field of vaccine development and gene therapy have attracted attention to virus-like particles as a tool either to introduce the antigen to the immune system or to deliver the necessary/required protein/mRNA/genome-editing platform. In general, virus-like particles are the viral coat proteins lacking viral nucleic acids. VLPs can be divided into two distinct categories: derived from either enveloped (1) or naked (2) viruses.

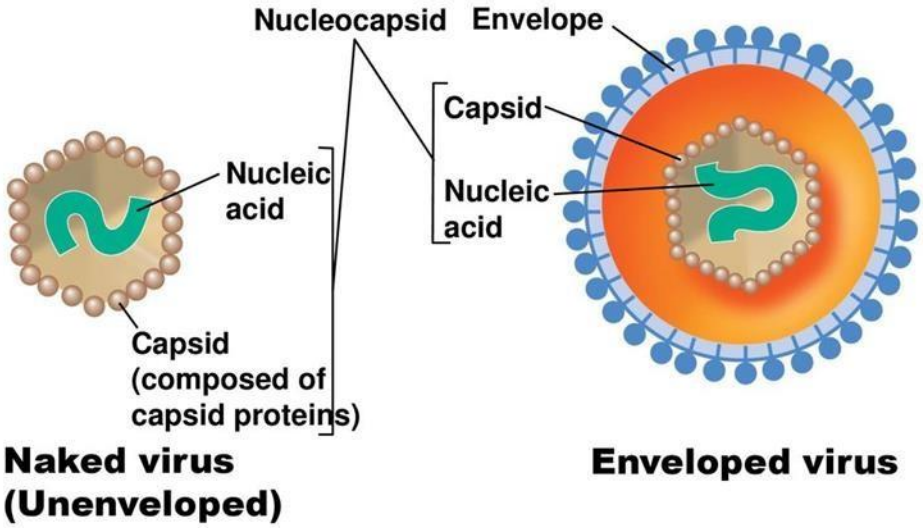

Figure 1.5 The difference between naked and enveloped VLPs
[https://slideplayer.com/slide/13806387/]

Since these categories are structurally divergent, their application as well as pros and cons vary. VLPs obtained from the enveloped viruses consist of one or more glycoprotein that enveloped viruses exploit to bud off from the host cell. VLPs of this type are surrounded by the lipid bilayer membrane of the host cell which they derived from. A mammalian host cell culture is essential to produce the enveloped VLPs. The great advantage of these systems lies in their ability to incorporate large molecules such as peptides and ribonucleoprotein complexes in large amounts sufficient for transfecting recipient cells. The second category of VLPs is comprised of viral capsid proteins. These are the actual capsid proteins serving as a shield to protect viral genetic material. In addition, these viral capsids may have a lipid bilayer membrane around. Capsids consist of repetitive peptide monomers, called ‘capsomers’. The great advantage of these VLP systems is their ability to assemble on their own in a cell-free environment thus being devoid of the unwanted producer cell material otherwise co-incorporated into VLPs together with the cargo of interest. The limiting factor though, is that the self-assembly of capsomers in cell-free conditions may become impaired if loaded with an overwhelming amount of cargo. Hence, peptides or nucleic acids are more preferable candidates for delivery than proteins. Nevertheless,

it is not the case for generating VLPs via bacteria/yeasts being the production systems as was demonstrated by Abraham et al. [Abraham et al, 2016]. In their study SeMV VLPs (30 nm in size) fused with the B-domain of *Staph. aureus* M protein (antibody-binding domain, 58 AA) and additionally loaded with antibodies of interest (discussed further) showed sufficient delivery load to various cell types [Abraham et al, 2016]. Another important distinction between these two groups is the ability of the latter to enter via host cell membranes. VLPs from the enveloped viruses carry the enveloped glycoproteins that bind with the host cell receptors and become internalized. In this regard, capsid proteins of VLPs derived from naked viruses, especially bacteriophages, are far less efficient due to the absence of a biological need for bacteriophages to enter mammalian cells. Hence for the most systems an additional entry booster becomes necessary / essential, such as commonly used cell-penetrating peptides (CPP) [Pan et al, 2012]. However, when target cell internalization is not required, and it is sufficient for the peptide to be exposed on the surface of VLPs to bring about the production of antibodies, bacteriophage-derived VLPs can be successfully used without CPP [Caldeira et al, 2010; Caldeira et al, 2015; Crossey et al, 2015].

As my project aims to develop a viable VLP delivery system, here I will discuss some examples of VLP-based systems and how these delivery vehicles were utilized in lab practice to transfer cargoes *in vitro* or *in vivo*. VLPs are widely used in the field of vaccinology. By carrying certain epitopes on their surface, VLPs can introduce antigens to the immune cells, and thus elicit immune response and production of antibodies. However, this application of the VLPs is beyond the scope of my project. The platforms carrying the cargo of interest inside the particles and designed only to deliver various types of loads, such as RNAs/ proteins/ RNP (Ribonucleoprotein complexes) inside the cells/ *in vivo* are described further.

1.3.1 Enveloped VLPs

1.3.1.1 Paramyxoviruses

Paramyxoviruses are the enveloped negative-sense RNA viruses. Like other enveloped viruses, they are equipped with glycoproteins (F and HN/G) necessary to incorporate into the lipid bilayer membrane, yet by contrast to other enveloped viruses, these VLPs also bear capsids inside the enveloped particle. Glycoproteins involved in the envelope formation are often termed as "spike" glycoproteins arising from a characteristic shape under the electron microscope [Harrison et al, 2010].

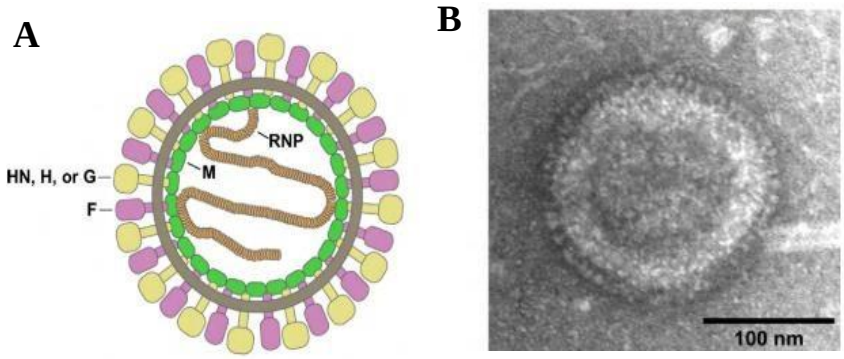

Figure 1.6. Schematic structure of paramyxovirus (A) and its electronic photograph (B) [Harrison et al, 2010]

These glycoproteins are responsible for the cell entry by attaching to sialic acids of the host (HN/G) and consequent fusion (F-protein) that united them with other types of envelope glycoproteins. M-proteins are the matrix proteins concentrated together with the capsid proteins at the potential budding site underlying the membrane being penetrated with the envelope

glycoproteins. M-proteins serve as adapters between the viral glycoproteins and the capsid proteins orchestrating the viral assembly and playing a major role in it. Consequently, for the most types of paramyxoviruses (hPIV-1, Sendai, NDV, Measles, and Nepah) only M-protein alone expressed within the host cells is sufficient to produce non-infectious VLPs [Harrison et al, 2010]. Yet such VLPs require glycoproteins to attach (HN) to and fuse (F protein) with the host cells to be exploited as a delivery vehicle. Smitt et al. utilized this strategy to develop a universal protein delivery tool working with any type of cells. To enable the protein of interest to incorporate into the VLPs, the authors fused it with the 15-residue DLD-containing domain of the C-terminal region of the Nucleocapsid protein of Sendai virus or PIV5 (Parainfluenza virus-5). C-terminal domain of the nucleocapsid (NC) was reported to be essential for binding with the M-protein of the corresponding virus [Schmitt et al, 2010]. This interaction allows the viral material to be packaged during the virus assembly. Schmitt et al. developed a delivery VLP-system consisting of 4 core elements: Glycoproteins required for entry (1), attachment (2), M protein, required for VLP formation (3), and the protein of interest, fused with a 15-residue C-terminal end of NC protein. Taking advantage of this combination, the authors managed to demonstrate a successful delivery not only of the marker proteins such as luciferase, but also, importantly, of highly applicable nowadays SpCas9/ SaCas9/Cpf1 as well as RNP complexes of SpCas9 with sgRNA if the latter was preliminary expressed in the producer cells. An important advantage of this VLP-based delivery tools is that through the fusion proteins VLPs insert their constituents right into the cytoplasm of the recipient cell bypassing the endosomal pathway.

1.3.1.2 Retroviral VLPs

Retroviruses are single-stranded positive sense RNA-viruses. The prototypical example of these viruses is HIV-1 (Human Immunodeficiency Virus type I). The main HIV-1 structural component is gag protein. It is translated as a precursor polypeptide chain, consisting of 6

proteins, and requires the viral protease mediated cleavage to release its constituents. The gag protein is comprised of MA (Membrane associated, or Matrix protein), Sp1-spacer protein 1, CA-capsid protein, Sp2-spacer protein two, NC (nucleocapsid), and p6 protein.

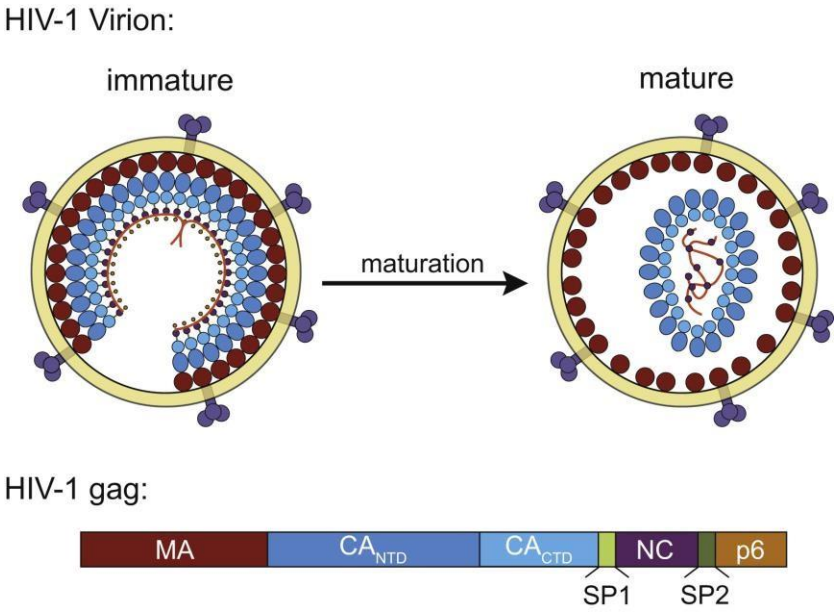

Figure 1.7 HIV-1 particle structure and maturation [**Monroe et al, 2010**]

These proteins work in the following way: the membrane protein is required to anchor the rest of the particle in lipid membrane via myristoyl group, the capsid protein enables interaction between outer protein (matrix) and inner protein (nucleocapsid), nucleocapsid incorporates gRNA via psi signal, and p6 located at the C-terminus of the polypeptide chain and required to release virions. P6 mediates the excision of the particle from the host membrane. The gag protein alone was reported to be sufficient to produce the virus-like particles. In this case they cannot mature, a viral protease essential to cleave the gag polyprotein is absent. The minimal combination of gag constituents still capable of forming virus-like particles was defined to be as following: N- terminal 12- amino-acid remnant of Matrix protein, C-terminal domain of capsid protein with Spacer 1 protein, and a leucin-rich domain of nucleocapsid protein [Accola et al, 2000]. Retroviruses are one of the most powerful and viable toolboxes among others in

gene therapy research. Nevertheless, insertional mutagenesis due to a random choice of inclusion sites and potential involvement of the oncogene loci and other important sites remain serious constraints on their application.

Retroviral delivery of mRNA

It was observed by Rulli et al. that plenty of host intracellular RNA molecules were co-packaged with viral RNAs and delivered to the recipient cells inoculated with retroviral particles [Rulli et al, 2007]. Consequently, Hamann et al. [Hamann et al, 2014] decided to estimate whether lentiviral particles lacking viral RNA can indeed deliver any of the RNA molecules overexpressed in the host cell to the target cells. They used three types of lentiviral particles: MLV, HIV-1, and FM (foamy viruses) to compare the delivery of a fluorescent marker. All types of lentiviruses possess the gag protein that enables incorporation and packaging of viral RNA. Although the full mechanism of this process remains to be completely elucidated, at least two factors enabling the incorporation of viral nucleic acids are known. Firstly, there are non-specific interactions between the positively charged gag protein and negatively charged nucleic acids. Secondly, there is a specific interaction between genome packaging sequence (Psi) on the viral acid sequence with His-Cys motives in gag protein [Hamann et al, 2014]. Interestingly, the gag protein of foamy viruses does not possess His-Cys motives but instead has Glycine-Arginine-rich motifs at the C-terminal end essential to package viral nucleic acids [Müllers, 2013]. The authors of this study aimed to deliver the cargo to the recipient cells and compare MLV, HIV-1, and PFV (Prototype foamy virus) VLPs side-by-side. All particles were assembled similarly: env+gag+pol+ GFP construct was overexpressed in the host cell. Although all VLPs efficiently delivered GFP to the target cells (HEK293T), PFV VLPs demonstrated the highest efficiency as shown by MFI (mean fluorescent intensity) of the target cells (10-folds higher than in the other two groups). The authors additionally investigated the minimal constituent components required to deliver the cargo by PFV and found that only envelope glycoprotein+ gag + transgene were sufficient to transfer VLP. Pol (viral polymerase) was not a dispensable element, although its absence in the VLP structure decreased the delivery rate.

The authors also demonstrated that the transgene delivery is mRNA-mediated, since the translation inhibitor in the recipient cells drastically decreased MFI levels. In addition, this study indicated the potential application of these VLPs as an efficient delivery tool for Cre-recombinase RNA. The efficiency of consequent genome editing was as high as 75-85%. Lindemann's group achieved transient expression of fluorescent proteins *in vivo* by injecting VLPs in the mouse brains. Yet, for these types of VLPs, incorporating RNA into the assembled VLPs is limited to two molecules per VLP due to a dimerization of viral RNA with *psi* sequence of the gag protein during the viral assembly [Souza, Summers, 2005]. To overcome this obstacle, Prel at al. utilized bacteriophage coat protein and cognate MS2 stem loops cloned into transgene RNA to be incorporated into the particle [Prel et al, 2015]. MS2 coat protein (MCP) is a bacteriophage MS2 nucleocapsid protein capable of binding to MS2 stem loops (hairpins) of mRNA replicase initiation codon in order to maintain its concentration in the infected cell on the required level [Pickett, Peabody, 1993]. By fusing MCP with lentiviral nucleocapsid and combining 12 stem loops of MS2 in a luciferase construct, the authors enhanced the incorporation of mRNA and efficiently delivered cargoes such as the reporter protein, Cre- recombinase, differentiation factors (RUNX2, DXL5) to hematopoietic CD34+ cells, iPS cells (induced pluripotent stem cells), mesenchymal stem cells, and, importantly, into mice models (by caudal vein delivery).

Retroviral delivery of protein

Another method to achieve the transient transgene expression is via protein delivery. In fact, protein delivery into the cytoplasm of the target cell can ensure a rapid action as well as less efficient innate response. Innate response is based on nucleic acid sensors which can identify a foreign nucleic acid and degrade transgene RNA (these receptors include MDA-5, RIG-I, TLR-3,7) [Peretti et al, 2005]. Kaczmarczyk et al. exploited avian retrovirus to achieve an extremely efficient delivery of proteins to the cytoplasm and the nucleus of the target cells. For this purpose, VLPs consisting of envelope glycoprotein commonly used for pseudotyping of retroviruses, VSV-G (Vesicular Stomatitis Virus Protein G), and the gag protein fused with the protein of interest (GFP, Cre- recombinase, Caspase 8) were applied. Since the authors encoded protease in the gag, when the fused polypeptide chain was cleaved, the protein of interest was

released. Transduction of the recipient cells (PC3) by VLPs bearing gag-GFP reached almost 100 per cent. Interestingly, the authors used the combination of envelope protein VSV-G and GFP construct without fusion with Gag protein as a negative control and did not observe any fluorescent GFP-positive recipient cells. Mangeot et al. published their pioneer work on protein transfer by "Gesicles"- VLPs comprised of envelope VSV-G glycoprotein of zoonotic Vesicular Stomatitis Virus [Mangeot et al, 2011] (discussed further). Kaczmarczyk et al. [Kaczmarczyk et al, 2011] compared the efficiency of gag-Cre in the complex of VLPs with VSV-G with another method of protein delivery by cell-penetrating protein Tat. The fusion of Cre-Tat and cell treatment with these constructs did not yield any detectable gene-recombination events in comparison with VSVG-gag-Cre VLPs. This demonstrated that VLPs have a better potency for the endosomal escape in comparison with cell-penetrating peptide Tat-system earlier demonstrated to be entrapped within the endosomes [Richard et al, 2003]. Similar works exploiting the same principle of protein transfer followed harnessing the structure of MLV (Murine Leukemia Virus). Wu and Roth generated a stable cell line secreting such VLPs for large-scale protein VLPs production [Wu, Roth, 2014]. This approach currently remains in the focus of attention as Robert et al. [Garcea , Gissmann, 2004] have recently utilized this system from HIV-1 to deliver transcription factors (cTA and KLF4) to the recipient cells [Robert et al, 2017].

1.3.2 Naked VLPs

Naked viruses lack lipid bilayer membrane forming the outer layer of enveloped VLPs. Being on average 30 nm in size, naked viruses are smaller than the enveloped ones (100 nm in size). Another difference is that naked VLPs require CPP displayed on their capsids to enter the cells. Naked VLPs are exploited to deliver short RNAs (siRNAs/microRNAs) since they cannot efficiently incorporate large volumes of cargo. Broadly speaking, a VLP system produced from a naked virus contains the nucleocapsid of a bacteriophage (MS2/PP7), RNA interacting with the

internal side of NC via the *pac* sites, and CPP on the outer surface of NC to enter the target cell.

1.3.2.1 MS2 bacteriophage system

MS2 coat protein of MS2 bacteriophage (MCP) consists of 180 capsomers when assembled from *E.coli.* Viral RNA is packaged within the capsid by means of *pac* sites interacting with capsid proteins and enabling encapsulation [Zhan et al, 2009]. The ability of MCP to encapsulate RNAs with *pac* sites on both ends was utilized by Pan et al. [Chen, Li, 2010] to create MS2 VLPs bearing pre-microRNA 146a. Interestingly, in another study the same research group managed to incorporate RNA of 3034 nt in length [Zhan et al, 2009].

To allow the internalization of the desired cargo into the target cells, CPPs (cell-penetrating peptides), in particular, 11-residue cationic polypeptide derived from Tat (Tat 47-57) was used. This polypeptide was previously shown to effectively penetrate lipid cell membraines [Fawell et al, 1994]. Such VLPs demonstrated a potent down-regulation of microRNA-146a targeting IRAK 1 (interleukin- 1-associated tyrosine kinase). MicroRNA-146a is down-regulated in lupus as it targets pro- inflammatory pathways. Moreover, it was shown to be involved in the pathogenesis of autoimmunity as well as that of myeloproliferative disorders and cancers [Boldin et al, 2011].

Hence enhancing levels of microRNA-146a by VLP delivery seemed to be a reasonable approach. The authors demonstrated down-regulation of IRAK-1 *in vitro* and *in vivo* (VLPs were injected into the tail vein of C57BL⁄ 6 mice) [Pan et al, 2012]. In the consequent study they applied this system for the *in vivo* treatment of lupus-prone mice (BXSB, Jackson laboratories). After the injection, large amounts of MS2-VLPs were detected in PBMCs (peripheral blood monocytes), as well as in the lung, spleen and kidneys. Importantly, a consequent decrease of auto-antibodies – anti-dsDNA and ANA (antinuclear antibodies) – as well as a drop in pro-inflammatory cytokines involved in SLE pathogenesis (IFN-α, TNF-α, IL-1β, and IL-6) was observed [Pan et al, 2012].

Similarly to these studies, Wang's group consequently utilized the same delivery vehicle and the same cargo – pre-micro-RNA-146a – to affect osteoclast differentiation and its downstream effects. Applying MS2-VLPs to PBMC resulted in increased levels of microRNA-146a, down-regulation of its targets – EGFR (epidermal growth factor receptor) and TRAF6 (tumor necrosis factor (TNF) receptor-associated factor 6), and decreased osteoclast formation from PBMC demonstrated by immunohistochemistry and bone resorption assay [Yao et al, 2015]. Further attempts of the same group to improve this system included displaying the Tat protein on the MCP surface instead of chemical crosslinking. By these means the authors demonstrated the delivery of microRNA-122 to the hepatocellular carcinoma cell lines (Hep3B, HepG2, and Huh7) and related mice models [Wang et al, 2016]

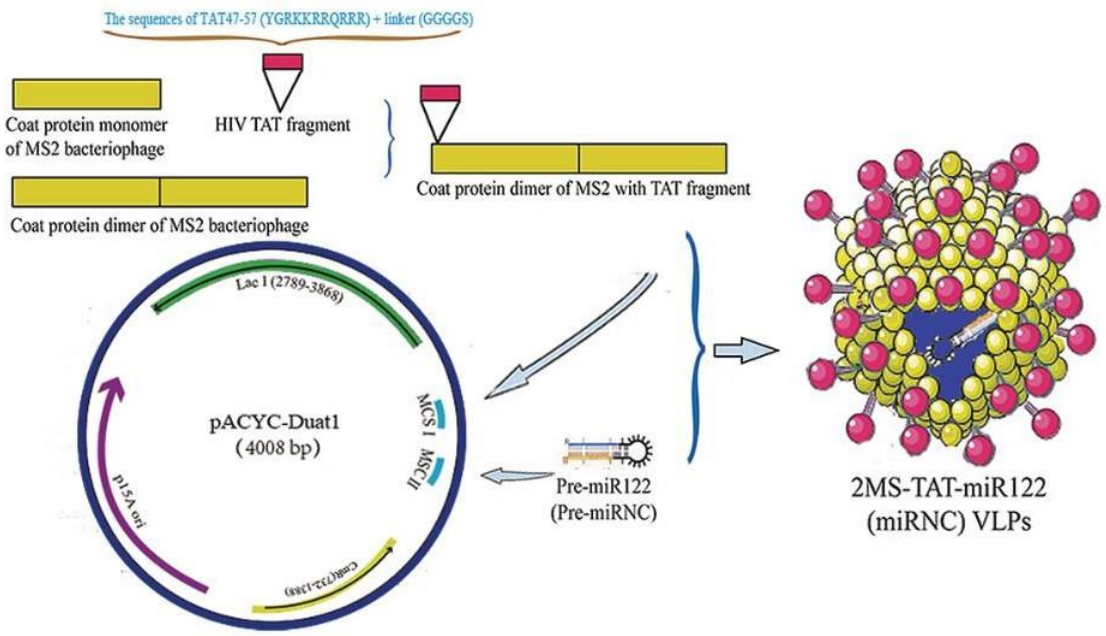

Figure 1.8 Schematic diagram of construction and preparation of 2MS-Tat-Mir-122 VLPs
Figure is adapted from reference Wang et al, 2016.

1.3.2.2 PP7 bacteriophage system

Similar approach was applied to deliver EGFP mRNA via bacteriophage PP7. Like that of MS2 bacteriophage, PP7 capsid can also self-assemble and incorporate mRNA. Another type of CPP was exploited to enable cell entry, namely low molecular weight protamine (LMWP) displayed

on the PP7 capsid surface (it was inserted between the 10th and the 11th amino acid residues of the 2nd subunit of the PP7 coat protein) [Caldeira et al, 2015]. This study was the first to demonstrate that LMWP displayed on the surface of PP7 bacteriophage capsid protein maintained its cell-penetrating functions and hence could be successfully adopted as a delivery tool. In another work, Sun and colleagues utilized a similar approach to deliver pre-micro-RNA-23b into SK-HEP-1 cell line by packaging it into MS2 bacteriophage and displaying Tat 47-57 protein on its surface. [Sun et al, 2017].

1.3.3 VLPs derived from plant viruses

SeMV (Sesbania Mosaic virus) [Abraham et al, 2016] is a positive-sense RNA plant virus. Unlike other plant- derived virus-like particles requiring expression in planta and further purification, SeMV can be expressed in and purified from *E coli* with a sufficient yield.

Abraham et al. used Sesbania Mosaic virus to produce antibody-bearing VLPs, in particular, IgG. SeMV enters the cell via binding to vimentin, a cytoskeleton protein present in a wide range of cell types (i.e. in mesenchymal cells). Further trafficking of SeMV VLPs revealed that after entering the cell through caveolae-dependent endocytosis they enter the endosomal pathway [Plummer et al, 2012]. SeMV VLP system is a remarkable tool due to its high bioavailability *in vivo* and *in vitro*. Abraham et al. used B-domain of *Staphylococcus aureus* A protein capable of binding Fc and Fab fragments of antibodies. By inserting this 58AA-domain into the loop of the helix formed by SeMV capsid, the authors managed to drastically increase the antibody-binding capacity of the VLPs. The increased bound antibody level compared with that of a single-domain molecule of *Staphylococcus aureus* was explained by multimeric assembly of the VLPs. When VLPs were loaded with antibodies designed to initiate apoptosis, the cell viability drastically decreased as a result of successful delivery.

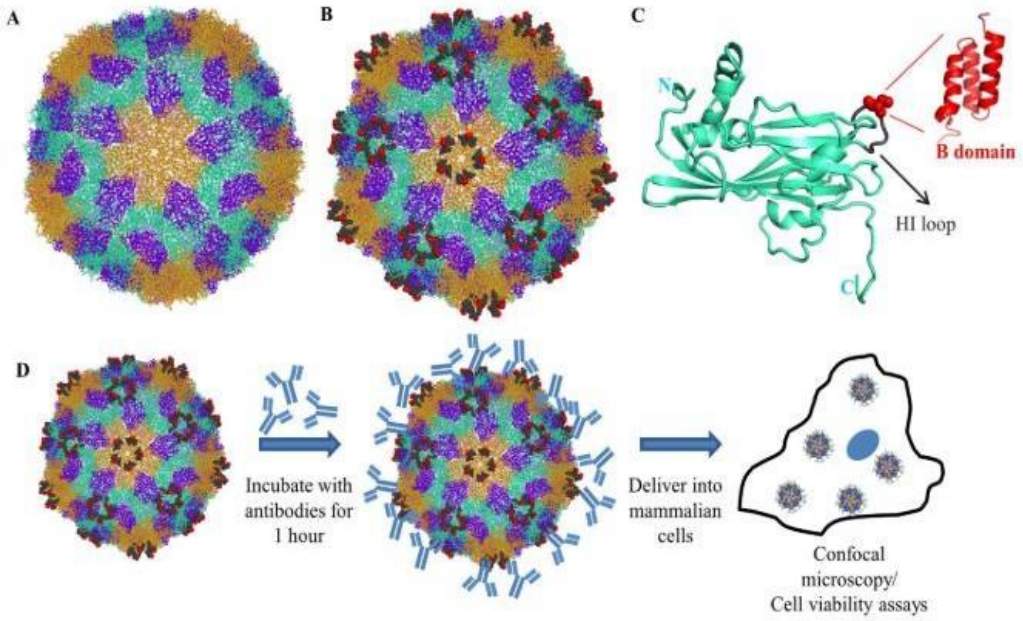

Figure 1.9 Design of SeMV CP based chimera
Figure is adapted from reference Abraham et al, 2016.

The therapeutic potential of antibodies is based on their ability of binding to pathogen/ tumor cell receptors, coating (opsonizing) them and thus facilitating their elimination by the immune system cells. Under these circumstances, antibodies are bound externally; however, in some cases internalization of antibodies is essential. Intracellular localization of antibodies enables vital pathways to be halted and rapidly leads to detrimental outcomes for the malignant cell. For these purposes, delivery platforms for intracellular targets demonstrate higher cell toxicity and thus enhance the therapeutic potential of such treatment. Hence this platform based on SeMV chimeric Protein A-B-domain seems to be promising for applying these VLPs for cancer treatment.

1.3.4. Other categories of VLPs

Here, we have discussed some examples of purely enveloped or naked VLPs. However, as was briefly mentioned above, there may be defined an additional third branch of this classification, which includes VLPs that possess both: nucleocapsid and outer membrane surface. These include

VLPs of Hepatitis B virus (HBV) comprising HBV core antigen and lipid membrane envelope. HBV VLPs are capable of entering the cell due to the presence of positively charged arginine-rich domain A. They were utilized for oligonucleotide delivery to a wide range of cells [Cooper et al, 2004].

1.3.5 Targeted VLPs delivery

To narrow down VLP tropism to the target cells of interest rather than to all cells expressing the co-receptor for the VLPs fusion and entry, a number of techniques have been implied. Peretti et al., for example, created lentiviral VLPs based on HIV-1 structural protein Nef, bearing thymidine kinase from the HSV (Herpes Simplex Virus). The latter enzyme is essential to activate the antiherpetic drugs such as acyclovir and ganciclovir via phosphorylation. When the enzyme is activated, nucleotide triphosphate is formed, which terminates DNA replication in a chain fashion E [Moolten et al, 1986]. In all cells possessing HSV-derived tyrosine kinase treating with either acyclovir or ganciclovir results in impaired DNA synthesis and consequent cell death. To exclusively target cells infected with HIV-1 and thus expressing HIV-1 proteins (for example, gp120, required for viral entry) on their surface Peretti et al. engineered VLPs with CD4+ CCR5/CXCR4 receptors on their surface, pseudotyped with VSV-G. CCR5 and CXCR4 are receptors on CD4+ cells and macrophages which HIV-1 exploits for viral entry and further spread. By “reverse fusion” the authors managed to enhance selective targeting of only virus- infected cells.

Fusion with antibodies

The authors of the paper fused the Polyomavirus coat protein VP1 with the antibody-binding domain of *Staphylococcus aureus* engineered protein Z. Chimeric VLPs still maintained their ability to form pentameric VLP structures *in vitro* with all Z-domains bound to an antibody molecule. Such antibody-bearing could efficiently target (at least by binding, but also by internalizing) any cells exposing a cognate antigen receptor on their surface. Gleiter et al.

[Gleiter, Lilie, 2001] demonstrated it by delivering rhodamine-labelled cDNA by VLP-Z VLPs carrying Herceptin (Antibodies against Her2) to SK-BR-3 cell line with Her2 antigen. In contrast, the delivery to the Her2-deficient cell line (MCF-7) failed to provide an evidence of targeted delivery.

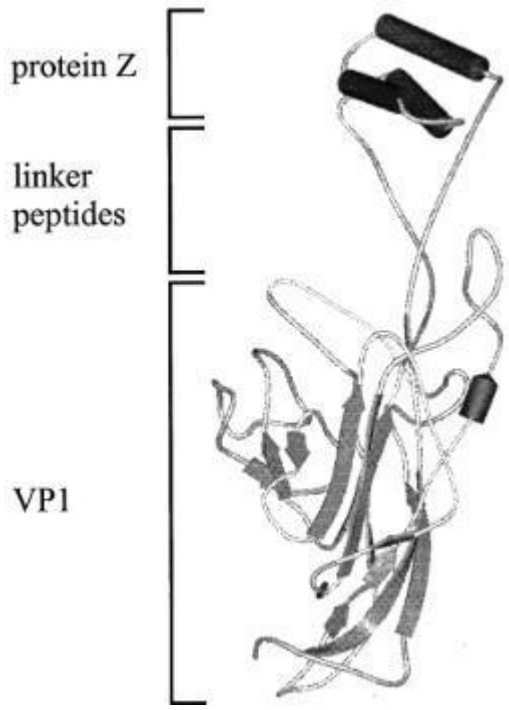

Figure 1.10 Scheme of the fusion protein VP1-Z
Figure is adapted from reference Gleiter, Lilie, 2001

Another example of effective therapeutic delivery to Her-2-positive cancer cells *in vitro* and *in vivo* was demonstrated by Suffian et al. [Suffian et al, 2017]. Here, the authors attached the Z-domain of the aforementioned antibody-binding protein A of *Staph. aureus* to anti-Her2 antibodies. In addition, the authors deleted the arginine-rich domain, which normally ensures broad cell tropism to increase the restriction of targeting to cancer cells expressing Her-2 receptor. In cancer mice models (IP and MFP) intraperitoneal injection of such chimeric VLPs resulted in significantly higher accumulation in comparison with HBC-VLPs without any modifications. This suggests that this vehicle can be exploited to deliver anti-cancer therapies to

HER positive tumors. To conclude, VLPs are a rapidly emerging platform for the delivery of molecular loads such as RNAs, proteins, and polypeptides. VLPs can exhibit broad tropism when necessary (to target virus-infected cells) or narrow tropism to specifically target cancer cells. Despite being used as vaccine platforms for decades, VLPs have only recently gained a tremendous interest as delivery vehicles.

Chapter 2

Materials and methods

2.1. Constructs: design and cloning

2.1.1. Polymerase chain reaction (PCR)

PCR is a widely established technique based on the ability of DNA polymerase to synthesize a DNA strand complementary to a template strand. Specifically designed primers can be used to delineate a specific region of the template in order to amplify it and thus accumulate a large number of copies of this which can be viewed on an agarose gel.

Forward and reverse primers were designed using PrimerBlast and checked for specificity using the USCS genome browser. 2.5µl of cDNA was aliquoted into new clean tubes. The following mixture was prepared:

5X buffer	5µl
Forward primer	0.5µl
Reverse primer	0.5µl
Taq enzyme	0.125µl
Water	16.375µl

22.5µl of this mixture was then aliquoted into small tubes containing cDNA. The samples were heated as follows (annealing temperature was determined after primer optimization).

95 °C Denaturation	8 min	
95 °C Denaturation	30s	
Tm-10 °C Annealing	30s	35-40 cycles
72 °C Elongation	30s	
72 °C Elongation	10 min	

2.1.2. Gel electrophoresis of PCR products

A 1% agarose gel was prepared by diluting 0.3 g of agarose in 35ml of Tris acetate –EDTA (TAE) buffer in a glass flask and heated until all the agarose was fully dissolved. 3.5ml of Sybr Safe DNA Stain (Invitrogen) was added to the flask and this mixture was then poured into a suitable gel cassette with an appropriate well comb. Once set, the gel was placed in a gel rig and the gel was further covered over with TAE buffer. The gel was run at 120 V for 30 min.

2.1.3 Cloning design

2.1.3.1. Cloning of VSVG-MS2BP, VSVG-L7Ae, and VSVG-L7KK

MS2BP cDNA was PCR amplified from pMS2CP-myc-T2A-tagRFP [80] (Appendix A). L7Ae cDNA fragment from *Archaeoglobus fulgidus* was PCR amplified from pcDNA3.1-CMV-L7Ae-myc-His6-pA [8](Appendix A). L7KK cDNA was PCR amplified from pL7KK-myc-T2A-tagRFP [81] (Appendix A). The PCR amplicon (either MS2BP, L7Ae, or L7KK) was cleaned up

by Wizard SV Gel and PCR Clean-Up System (Promega) and inserted into HindIII site just before the stop codon of the pENTR-VSVG-pA by In-Fusion HD Cloning Kit (Cat.639650, Clontech). We inserted a flexible Gly-Ser linker sequence between the VSV-G and MS2BP/L7Ae/L7KK.

Digestion reaction (20µl) with Hind III (5'-A/AGCCT-3') was performed at 37 ℃ for 60 minutes in the following mixture:

Vector DNA	X µl (1 µg)
Enzyme buffer	2 µl
Restriction enzyme	1 µl
Nuclease-free Water	to 20 µl
Total Volume	**20µl**

The product of digestion was run on the gel for 40 minutes at 120 V side-by-side with its uncut corresponding vector. The digested product (linearized pENTR-VSVG-pA) was cleaned up by Wizard SV Gel and PCR Clean-Up System (Promega). In-fusion reaction was performed for 30 min at 56 ℃. The concentrations of the vector and the insert were calculated using Takara In-Fusion molar ratio calculator (https://www.takarabio.com/learning-centers/cloning/in-fusion-cloning-tools/in-fusion-molar-ratio-calculator) at 1:2 molar ratio as the following mixture:

Linearized vector	X µl
Insert with Hind III overhangs	Y µl
In-fusion ligase	1 µl
Nuclease-free Water	10 µl -X µl -Y µl

Total Volume	**10µl**

The resulting constructs, pENTR-VSVG-MS2BP [Saito et al, 2010], pENTR-VSVG-L7Ae [Saito et al, 2010] and pENTR-VSVG- L7KK [Saito et al, 2010], were transferred into pHL-EF1a-GW-A [Li et al, 2015] by a LR Clonase II reaction (Gateway LR Clonase II, Cat 11791-020, Invitrogen). LR recombination reaction between an attL-containing pENTR-VSVG-MS2BP/L7Ae/L7KK entry clone and an attR-containing destination pHL-EF1a- GW-A vector was performed in the following mixture:

Entry clone (supercoiled, 100-300 ng	1-10 µl
Destination vector	150 ng/µl (1 µl)
5X LR Clonase	1 µl
TE Buffer, pH 8.0	4 µl
Total Volume	**10 µl**

The reaction mixture was incubated at 25°C for 1 hour. Then 2 µl of 2 µg/µl Proteinase K solution was added to the reaction and incubated at 37°C for 10 minutes.

Transformation of competent *E. coli* DH5α cells.

Competent *E. coli* DH5α were taken from minus 80 °C and thawed on ice for 20 minutes. 1 µl of the reaction mixture was added to *E.coli* tube, gently pipetted and kept on ice for another 30 minutes. Then competent cells were incubated at 42 °C for 30 seconds and placed back on ice for another 30 seconds. Next, preheated to 37 °C 1 ml of SOC medium was added to the competent cells and the tube was shaken for another hour at 37 °C and plated on Ampicillin agar plates.

The next day five colonies from each plate were picked, and colony PCR was conducted. The same primers as for the amplification of PCR products of VSVG-MS2BP/L7Ae/L7KK were used for colony PCR.

The final constructs obtained were pHL-EF1a-VSVG-MS2BP-pA, pHL-EF1a-VSVG-L7Ae-pA and pHL-EF1a-VSVG-L7KK-pA.

2.1.4 Cloning of MS2 stem loops in pHL-EF1a-EGFP-pA

pHL-EF1a-SphcCas9-A vector [Li et al, 2015] was digested at BglII (5'-A/GATCT-3') and BamHI sites (5'-GGATCC-3'). Digestion reaction (20µl) was performed at 37 ℃ for 60 minutes in the following mixture:

Vector DNA	X µl (1 µg)
Enzyme buffer	2 µl
Restriction enzyme Bgl II	1 µl
Restriction enzyme Bam HI	1 µl
Nuclease-free Water	to 20 µl
Total Volume	**20µl**

The product of digestion was run on the gel for 40 minutes at 120 V side-by-side with its uncut corresponding vector. The digested product (linearized pHL-EF1a-SphcCas9-A) was cleaned up by Wizard SV Gel and PCR Clean-Up System (Promega).

Oligonucleotides containing 2 copies of modified MS2SL sequence [80] (underlined) flanked with BglII(5'-A/GATCT-3') and BamHI (5'-G/GATCC-3'). sites 5'-Gaaccgtcagatctgctacgatccggtgaggatcacccatcgagatccggtgaggatcacc catcgagatccaccggatcccaccat-3' were annealed in a thermocycler machine.

At first, equal volumes of oligonucleotides were mixed in a PCR tube.

The following thermal profile was used to achieve the annealing:

Temperature	**Time**
Heat to 95 °C	For 2 min
. Cool to 25 °C	For 45 min
Cool to 4 °C	For 5 min

The product of reaction was subjected to electrophoresis on the gel for 30 minutes at 120 V and purified by Wizard SV Gel and PCR Clean-Up System (Promega).

Linearized pHL-EF1a-SphcCas9-A and the product containing MS2 SL were mixed in T4 ligation reactions in the following mixture:

T4 DNA Ligase Buffer (10X)	2 µl
Vector DNA (4 kb)	50 ng
Insert DNA (1 kb)	37.5 ng
Nuclease-free water	to 20 µl
T4 DNA Ligase	1 µl
Total Volume	**20µl**

The mixture was left for overnight ligation at 16°C using T4 DNA ligase (NEB, Cat. M0202M). The resulting vectors pHL-EF1a-SpCas9-MS2SLx2/x4-pA were sequenced and underwent a Gateway BP reaction to replace SpCas9 cDNA with ccdB-CmR cassette from pDONR221 using Gateway BP Clonase II Enzyme mix kit (Cat 11789-020, Invitrogen) to generate pHL-EF1a-ccdB-MS2SLx2/x4-pA vector. BP recombination reaction between an attB-containing pDONR221 donor clone and an attP-containing vectors pHL-EF1a-SpCas9-MS2SLx2/x4-pA

destination vector was performed in the following mixture:

Entry clone (supercoiled, 100-300 ng)	1-10 µl
Destination vector	150 ng/µl (1 µl)
5X BP Clonase	1 µl
TE Buffer, pH 8.0	4 µl
Total Volume	**10 µl**

The reaction mixture was incubated at 25°C for 1 hour. Then 2 µl of 2 µg/µl Proteinase K solution was added to the reaction and incubated at 37°C for 10 minutes.

Further a Gateway LR reaction to replace ccdB-CmR cassette with EGFP cDNA from pENTR2B-EGFP with Gateway LR Clonase II Enzyme mix kit (Cat 11791-020, Invitrogen) was performed using the same protocol for LR reaction as described above.

2.1.5. Cloning of BoxC/D in pHL-EF1a-EGFP-pA

The BoxC/D motif [8] (underlined) containing oligonucleotides Fwd: 5'-gtacagatctggatcgggcgtgatccgaaaggtgaccctaggcttaagtata-3' and Rev: 5'-tatacttaagcctaggggtcacctttcggatcacgcccgatccagatctgt-3' was annealed in TE buffer. The following thermal profile was used to achieve the annealing:

Temperature	**Time**
Heat to 95 °C	For 2 min
. Cool to 25 °C	For 45 min

Cool to 4 °C	For 5 min

Annealed oligonucleotides were run on the gel for 30 minutes at 120 V, purified by Wizard SV Gel and PCR Clean-Up System (Promega) and inserted into BlnI (AvrII) (5'- C/CTAGG-3') site of the pHL-EF1a-EGFP-pA [Li et al, 2015] vector by In-Fusion HD Cloning (Cat.639650, Clontech) using the same Infusion protocol and 2:1 molar ratio as described above.

2.1.6 Cloning of MS2SL and BoxC/D in sgRNA (*DMD1*)

Oligonucleotides containing 2 copies of modified MS2SL sequence [Endo et al, 2013] (underlined) flanked with BglII and BamHI sites 5'-Gaaccgtcagatctgctacgatccggtgaggatcacccatcgagatccggtgaggatcacccatcgagatccaccggatcccaccat-3' were annealed in a thermocycler machine. The following thermal profile was used to achieve the annealing:

Temperature	**Time**
Heat to 95 °C	For 2 min
. Cool to 25 °C	For 45 min
Cool to 4 °C	For 5 min

The annealed oligonucleotides were run on the gel for 30 minutes at 120 V and purified by Wizard SV Gel and PCR Clean-Up System (Promega) and inserted into BamHI (5'-G/GATCC-3') into pHL-H1-sgRNA-DMD –Rih constructs [Li et al, 2015] on BamHI site (downstream the target sequence) by In-fusion reaction as described above. pHL-H1-sgRNA-DMD1-MS2SLx1/x2-

mEF-Rih were obtained. sgRNA was previously designed in the lab to target 45th exon of *DMD* gene [Li et al, 2015].

2.2 Cell culture

Human embryonic kidney HEK293T cells (Cat. CRL-3216, ATCC) and THP-1 cells (Cat. RCB1189, Riken Cell Bank) were maintained in RPMI 1640 media (Cat. 11875-119, Life Technologies) supplemented with 10% fetal bovine serum (FBS), penicillin and streptomycin. Human iPS cells 404C2 (a kind gift from Dr. Keisuke Okita) were cultured on plates coated with iMatrix-511 (0.25–0.35 μg/cm^2) (Cat. 892012, Nippi) in StemFit AK03N medium (Ajinomoto). To indicate that the cells were still iPS cells, their morphological characteristics such as the number of colony-forming units was used. To ensure that the cell cultures were mycoplasma-free, all the cell types were regularly tested using a MycoAlert Mycoplasma Detection Kit (Cat. LT07-218, Lonza).

2.3 VLP production and inoculation

293T cells were seeded in a 6-cmplate at a density of 1.9-2.2 × 10^5 cells in 3 ml of DMEM medium supplemented with 10% FBS, penicillin and streptomycin.

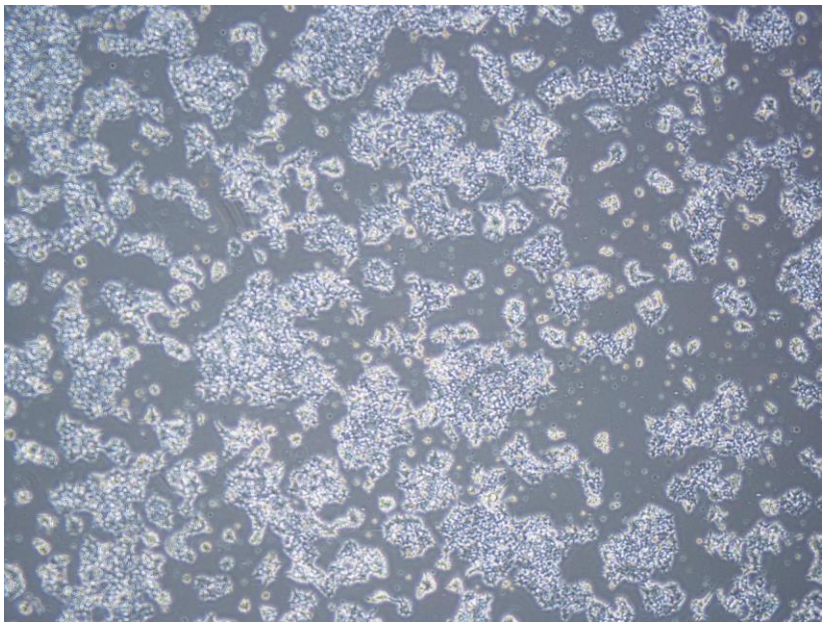

Figure 2
The figure depicts HEK 293T cells that are plated at a density of 1.9-2.2 × 10^5 cells/3mL for the VLP production.

The next day, 3 µg of VSVG plasmid (pHL-EF1a-VSVG-pA, pHL-EF1a-VSVG-L7Ae-pA, or pHL-EF1a-VSVG-L7KK-pA) and 5 µg of EGFP plasmid (pHL-EF1a-EGFP-pA, pHL-EF1a-EGFP-MS2SL×2/×4-pA, or pHL-EF1a-EGFP-BoxC/D-pA) were transfected by lipofectamine 2000 (Cat.11668019, Thermo Fisher Scientific) in Opti-MEM media (Cat. 31985-062, Life technologies) according to the manufacturer's instructions. Between 8 to 12 hours after transfection, the medium was changed to fresh DMEM medium (4 ml per 6-cm plate). Two days post-transfection, VLP-containing medium was collected, filtered through a 0.45 µm-pore syringe filter (Cat.16555K, Sartorius), and concentrated by centrifugation with LentiX concentrator (Cat. 631231, Takara Clontech) according to the manufacturer's instructions or by ultra-centrifugation. For ultra-centrifugation, we centrifuged the harvested medium for 3 hours at 24,000 rpm at 4ºC. The supernatant was discarded, and the pellet was incubated with 90 µl of HBSS (Hanks' balanced salt solution, Cat. 14175-095, Thermo Fisher Scientific) for 5-12 hours. Afterwards, VLPs were resuspended by pipetting 20 times. Resuspended VLPs were either

immediately inoculated onto target cells or stored at −80°C until further use. Recipient HEK293T cells were seeded at a density of 5.0×10^4 cells per well in a 48-well plate one day prior to inoculation. VLPs were inoculated directly onto target cells and the recipient cells were harvested 24 hours post-inoculation to assess EGFP delivery. EGFP-positive cells were measured by flow cytometry analysis using a BD LSR Fortessa (BD Biosciences). For human iPS cell transduction, the cells were treated with ROCK inhibitor Y-27632 (final 10 µM, Cat. 08945-42, Wako) for 1 hour at 37ºC prior to the inoculation with the VLPs and collected for flow cytometry analysis 24 hours post-inoculation.

2.3.1 Inhibition of the exosomal production

Exosome inhibitor Spiroepoxyde, 5uM or GW4869, 2 uM [Essandoh et al, 2015] were added to the cell medium of the producer cells 6 hours post-transfection with fresh medium. VLPs were collected and concentrated as described above (Section 2.3)

2.3.2 Production of retroviral particles

293T cells were seeded in a 6 cm-plate at a density of 2.2×10^5 cells in 4 ml of DMEM medium supplemented with 10% FBS, penicillin and streptomycin. The next day, the following plasmids PL-sin-Eip- vector- 2.4ug, Gag-pol-1.44ug, Tat-1.44ug, Rev-1.44, VSVG-A- 0.72 ug /HL-EF1a-VSVG-L7Ae-myc-6His-iP-pA-0.72ug were transfected by lipofectamine 2000 (Cat.11668019, Thermo Fisher Scientific) in Opti-MEM media (Cat. 31985-062, Life technologies) according to the manufacturer's instructions. For MLV VLPs the following list of vectors was utilized: pMX- 2.4ug, Murine Gag-pol-1.44ug, Tat-1.44ug, Rev-1.44. VSVG-A-0.72 ug /HL-EF1a-VSVG-L7Ae-myc-6His-iP-pA-0.72ug

2.4. qRT-PCR

2.4.1. mRNA extraction using TRIZOL

Cells or VLPs were homogenized in 1ml of Tri-reagent (Sigma) for 5 min at room temperature. 0.2ml of chloroform was added to the samples, and eppendorfs were shaken vigorously for 15s and incubated at room temperature for 2-3min. The samples were spun at 12,000 x g for 15min at 4°C which caused samples to separate into a lower red phenol-chloroform phase containing cellular proteins, an interphase containing the DNA and a colorless upper aqueous phase containing the RNA. The upper aqueous phase was transferred to a clean eppendorf, and 0.5ml of isopropyl alcohol was added to this solution/mixture. The samples were incubated for 10 min at room temperature and spun at 12,000 x g for 10 min at 4°C. Supernatant was removed, and the RNA pellet was washed with 1 ml of 96% ethanol. The sample was mixed well by vortexing and spun at 7500 x g for 5 min at 4°C. The supernatant was removed, and the RNA pellet was allowed to air dry. The RNA was then dissolved in 30µl of RNase-free water and the concentration was determined on the Nanodrop before storage at -80°C until needed. An A260/A280 ratio of 1.8-2 is indicative of pure RNA.

2.4.2. mRNA extraction using NucleoSpin RNA kit

Total RNA extraction from producer cells or VLPs was performed by NucleoSpin RNA kit (Cat.74095,5, Macherey-Nagel) according to the protocol of the manufacturer.

2.4.3 Reverse transcription

Reverse transcription (RT reaction) is a process in which single-stranded RNA is reverse transcribed into complementary DNA (cDNA) by using total cellular RNA or poly(A) RNA, a reverse trancriptase enzyme, a master mix of random hexamer primers, dNTP (deoxyribonucleotides-building blocks of DNA), and a RNase inhibitor (inactivates any enzymes

that can destroy the RNA). The resulting cDNA can be used in qRT-PCR reactions. The reaction was set up as follows:

5x RT Master Mix	2µl
RNA template	0.8 µg
Nuclease-free Water	Up to 10µl
Total Volume	**10µl**

Extracted RNAs were quantified, and the same amount (0.8 µg) was reverse-transcribed by ReverTra Ace enzyme (Cat. FSQ-201, TOYOBO).

2.4.4 qRT-PCR

Briefly, 1µl of cDNA was added in triplicate to an optical 96-well reaction plate. RT-PCR was performed using a SYBR Select Master Mix (Cat.4472908, Life Technologies). The following master mix was prepared on ice:

Sybr Mix	10µl
Forward primer	1 µl(10pmol)
Reverse primer	1 µl(10pmol)
Water	8 µl

StepOnePlus thermal cycler (Life Technologies) was utilized for quantitative analysis. Primers used for the qRT-PCR are listed in Appendix B.

2.5 Western Blot

VLP producer cells or VLP samples were lysed in Lysis buffer (20 mM Tris-HCl pH 7.5, 150 mM NaCl, 2% Triton X-100, 1 mM EDTA) containing complete Inhibitor Cocktail protease (Roche), incubated on ice for 10 min, and centrifuged for 30 min at 4ºC at 15,000 rpm. The supernatant was assessed for protein concentration by BCA assay (Cat. 23225, ThermoFisher Scientific). Equal amounts of protein (5 µg) were loaded onto a precast SDS polyacrylamide gel (4-12%, Cat. M41215, GenScript), and run for 1 h 30 min at 120 V. The gel was then incubated in blotting buffer, followed by transfer onto a nitrocellulose membrane using a Trans-Blot Electrophoretic Machine (Bio-Rad). The gel was placed on a layer of filter paper and sponge overlaid with the PVDF. A second piece of filter paper was placed on top followed by a second sponge. The entire assembly was placed in a cassette and in the Trans-blotting machine for 15 min.. Then the membrane was extracted, rinsed by 5 mL of PBS and placed in 10 mL of transfer buffer with shaking.

2.5.1. Antibody Blotting

Nitrocellulose membranes were blocked for non-specific binding by incubation in blocking buffer (Fast Western Blot kit, Cat. 35050, ThermoFisher Scientific) at 4°C overnight or at room temperature for 1h. The membrane was then incubated at 4°C overnight or at room temperature for 1h with the primary antibody of interest: anti-VSV-G (Cat. V5507-100UL, Sigma) or anti-ACTB antibodies (Cat. A5441, Sigma) at 1:500 to 1:1000 dilutions, respectively. The membrane was washed 3 x 10 min in 5mL of washing buffer (Fast Western Blot kit, Cat. 35050, ThermoFisher Scientific) and incubated with appropriate horseradish peroxidase (HRP)-linked secondary antibody (1:10000) for 1h at room temperature. Again, the membrane was washed 3x 10 min in 1% TBS. Blots were imaged on an ImageQuant LAS4000 to detect the protein by chemiluminescence (Cat. 35050, ThermoFisher Scientific).

2.7 CLIP (Cross-linking immunoprecipitation) assay

HEK 293T were transfected with 3µl of lipofectamine and 2 µg of total plasmid DNA (VSVG and EGFP) in a 6-well plate and harvested 48 hours post-transfection. The medium was removed, and the cells were rinsed with ice-cold PBS. The plastic lid was removed and cells were placed on a tray of ice and irradiated 365 nm UV once with 150 mJ/cm^2. The cells were harvested, spinned down at 4ºC, 5,000 rpm for 5 min, then PBS supernatant was discarded. The cell pellet was re-suspended in 200 µl lysis buffer (20 mM HEPES pH 7.5, 100 mM KCl, 5 mM $MgCl_2$, 1 mM DTT, 5% glycerol, 1% Triton X-100, and Ice-cold protease inhibitor (Cat. 29442-14, Nacalai tesque) added, then placed on ice for 10 min. RNA-protein complexes were solubilized using mild sonication by Bioruptor UCD-250 at 4ºC for 5 min at 250 W (30 sec sonication with 30 sec intervals). The cells were spinned at 20000 g for 30 min at 4ºC then the supernatant was collected. The cell lysate was incubated with anti-VSVG antibodies added at the concentration of 1 µg/µl. Afterwards, the lysates were incubated overnight at 4ºC with a microcentrifuge tube rotator. Meanwhile, 50 µl of Protein A/G Dynabeads (Cat. 88002, ThermoFisher Scientific) were washed ×3 times on a magnetic stand with Lysis buffer. After removing lysis buffer from the beads, cell lysates with anti-VSVG antibody were added to the beads and incubated at 4ºC with rotation for another 4 hours. After the incubation, one quarter of the lysate was run on the Western blot to assess VSVG protein immunoprecipitation. The rest three quarters were washed ×6 times on a magnetic stand with freshly prepared Lysis buffer (no proteinase inhibitor added). Protein-RNA complexes on the beads were dissociated from possibly bound RNA by adding 100 µg/ml Proteinase K (Cat. 29442-14, Nacalai tesque) in TE with 0.5% SDS, for 1 hour at 37ºC in the incubator with rotation. The supernatant containing eluted RNA was purified by Trizol (as described above). The amount of RNA in the supernatant was evaluated by qRT-PCR as described above.

2.8. Statistics

P values were calculated by GraphPad Prism program (unpaired t-test/ one-way ANOVA tests).

Chapter 3

Results

3.1 VSVG-L7Ae VLPs demonstrated higher transduction performance than VSV-G or VSVG-MS2 VLPs

We planned that fusing VSV-G with either MS2BP or L7Ae and cloning the cognate motifs in the mRNA structure would facilitate its incorporation into the VLPs and hence the delivery to the target cells. The whole process of VLPs production is a 3-step course. At first, VLPs of either VSVG-MS2BP or VSVG-L7Ae are generated after transfecting the producer HEK293T cells with the appropriate set of plasmids. This set also includes the cargo of interest (EGFP/Cas9) with the inserted motif for binding with L7Ae (BoxC/D) or with MS2BP (MS2SL). These motifs are cloned into 3'UTR. Shortly after transection of the producer cells, VLPs are generated. These VLPs are comprised of a cell lipid bilayer membrane penetrated with either VSVG-MS2BP /VSVG-L7Ae. RNA-binding domains are located inside the vesicles and are supposed to interact with the cognate binding motif and thus incorporate mRNA molecules inside (Figure 3A).

To facilitate EGFP mRNA packaging into VLPs, we fused either MS2BP or L7Ae with the C-terminus of VSV-G. Modified MS2SLs (×2 and ×4) or BoxC/D (×1) were also cloned into the 3'-UTR of EGFP (Figure 3B).

A

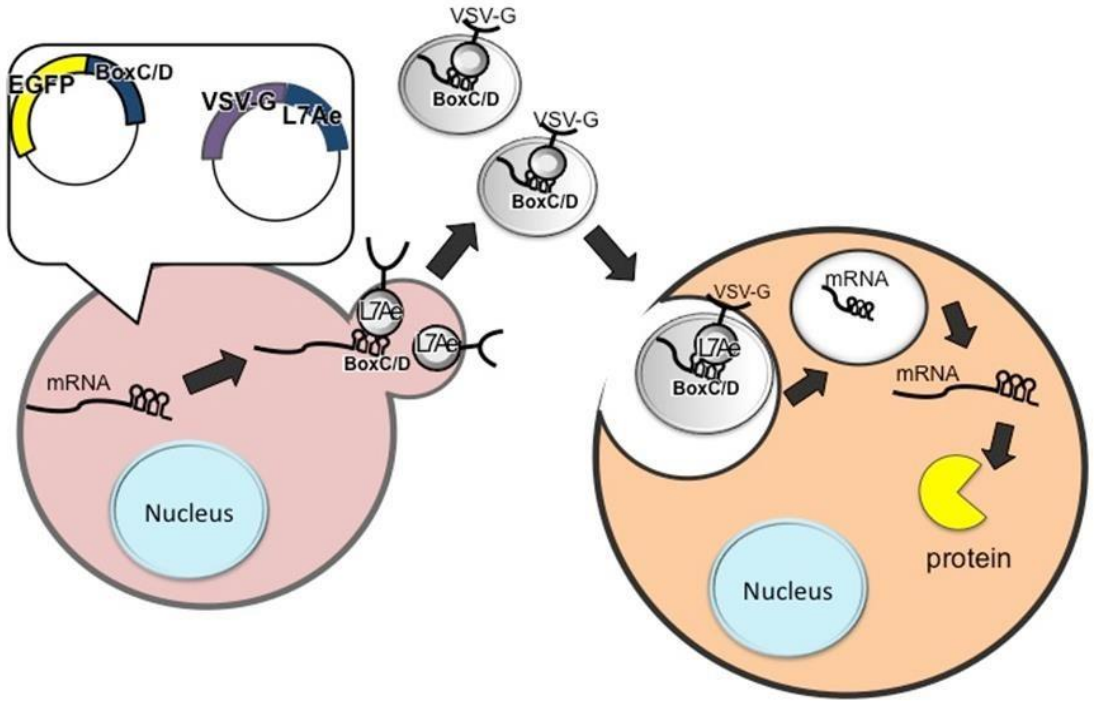

B

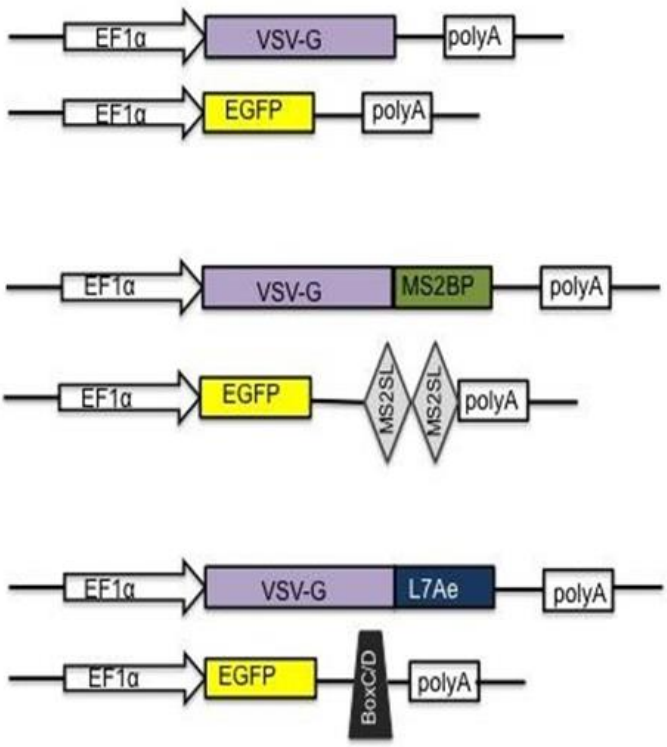

Figure 3 Schematic representation of chimeric VSVG-L7Ae VLPs system (A) and constructs design (B).

Delivery efficiency of VLPs was analyzed by flow cytometry 24 hours after inoculation onto HEK293T cells (Figure 3.1 A and B). Control VLPs with wild-type VSV-G and EGFP demonstrated modest EGFP fluorescence, whereas the VSVG-MS2 system failed to deliver detectable EGFP. In contrast, VSVG-L7Ae showed higher EGFP expression in comparison with the VSVG-WT and VSVG-MS2 samples.

A

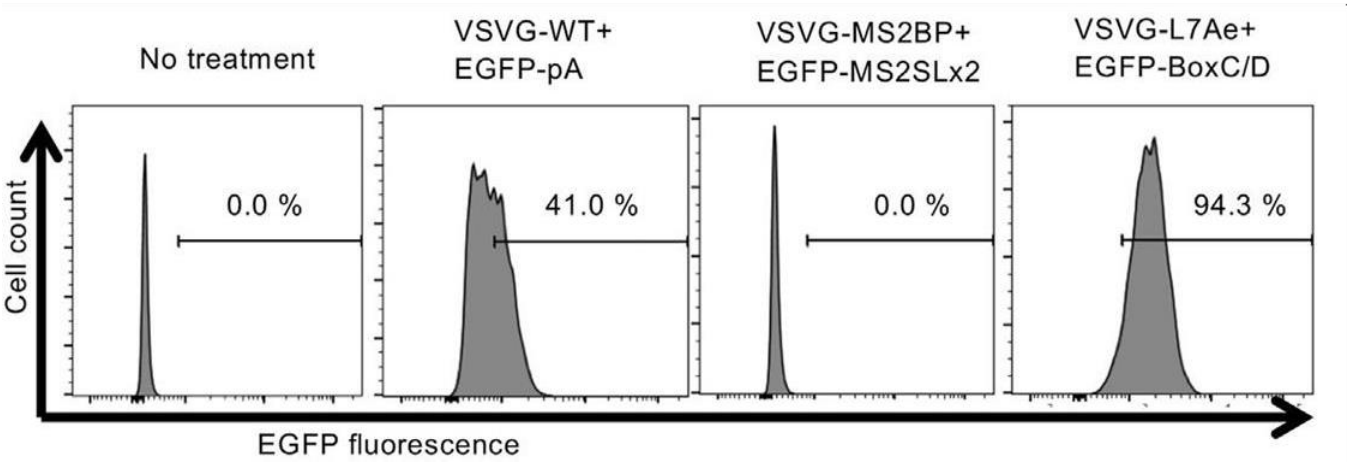

B

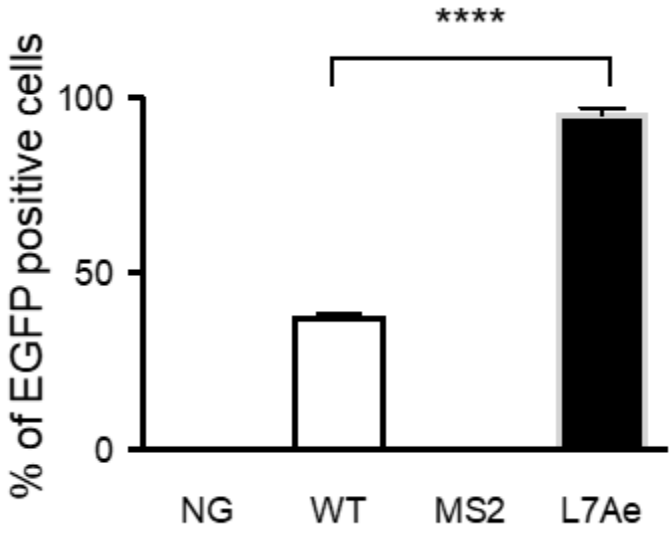

Figure 3.1 VSVG-L7Ae VLPs demonstrated higher transduction performance than VSV-G or VSVG-MS2 VLPs

EGFP fluorescent HEK293T cells were inoculated with three sets of VLPs and analyzed by flow cytometry. Histogram (Figure 3.1 A) and a bar graph (Figure 3.1 B) are presented. These

data represent technical triplicates (n = 3, ± S.D.).

To check the loading of target EGFP mRNA into VLPs, we lysed each type of VLPs and quantified the incorporation of EGFP mRNA by qRT-PCR (Figure 3.2). In line with flow cytometry analysis results, the level of EGFP mRNA in VSVG-L7Ae VLPs was significantly upregulated in comparison with VSVG-WT or VSVG-MS2BP VLPs.

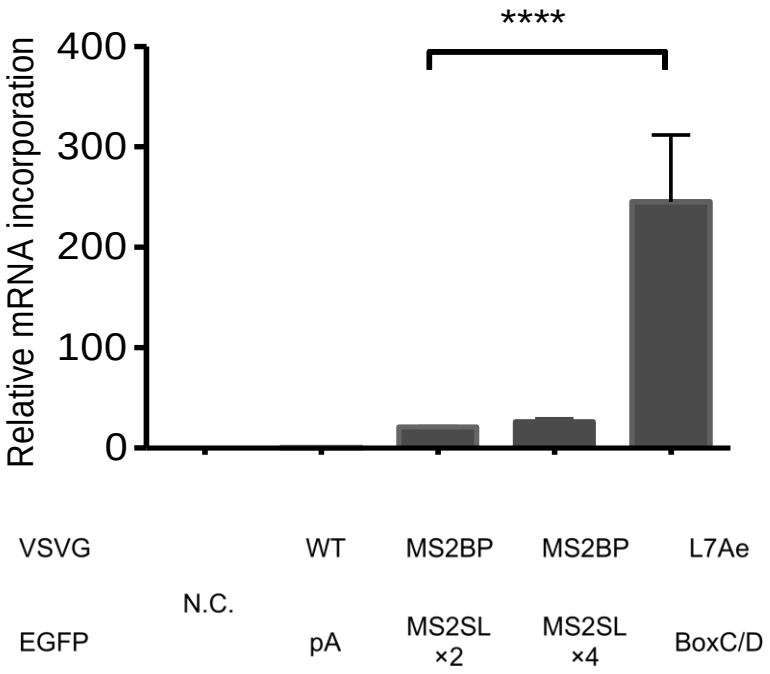

Figure 3.2 VSVG-L7Ae VLPs demonstrated higher EGFP mRNA incorporation than VSV-G or VSVG-MS2 VLPs
qRT-PCR analysis of the amount of EGFP mRNA with or without BoxC/D motif incorporated into VSVG-WT or VSVG-L7Ae VLPs (n = 3, ± S.D.).

To test whether the fusion of VSVG-WT with either MS2BP or L7Ae could have impaired VSV-G protein expression and/or stability, we examined VSV-G protein levels in the producer cells by Western blotting. Each fusion protein exhibited the expected molecular weight (VSVG-WT, 57.5 kDa; VSVG-MS2BP, 72 kDa; and VSVG-L7Ae, 73 kDa), but we noted that the expression of VSVG-L7Ae was lower than that of VSVG-WT, despite higher transduction efficiency (Figure 3.3) The expression of VSVG-MS2BP was lower in comparison with VSVG-WT and VSVG-L7Ae, which might explain the low transduction efficiency of the VSVG-MS2 VLPs. Hereafter, we concentrated primarily on VSVG-L7Ae VLPs due to its superior transduction efficiency.

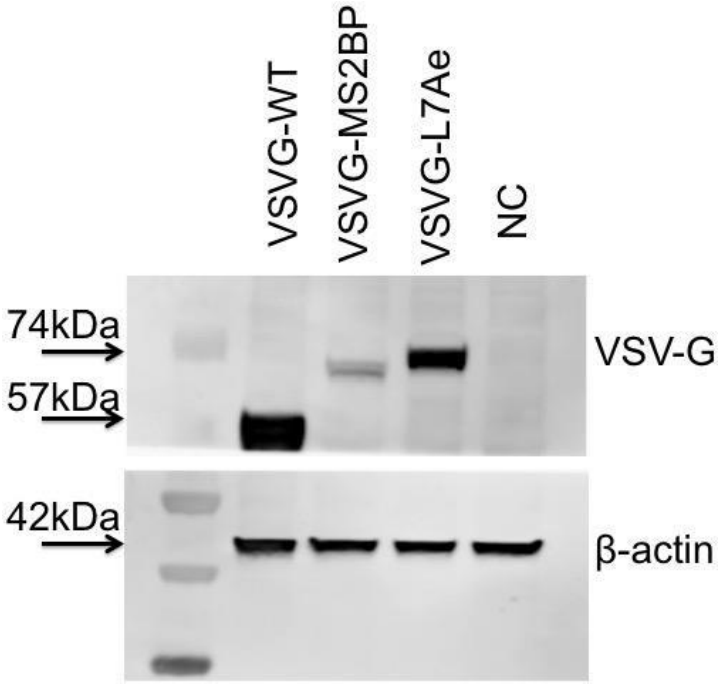

Figure 3.3 Western blot analysis of VSVG-MS2BP and VSVG-L7Ae expression in the cells

Western blot analysis of the VSV-G protein expression in the producer HEK293T cells. The same membrane was cut, and upper portion was incubated with an anti-VSV-G antibody while the lower part was incubated with β-actin for loading control.

3.2 Delivery by VSVG-L7Ae VLPs is BoxC/D-independent

Next, we set out to evaluate the impact of the BoxC/D motif on VSVG-L7Ae mediated EGFP delivery. We produced VSVG-WT and VSVG-L7Ae VLPs in combination with EGFP mRNA either containing or not containing the BoxC/D motif. The superiority of the VSVG-L7Ae EGFP delivery over VSVG-WT was reproducible, but surprisingly, EGFP-pA mRNA without a BoxC/D motif demonstrated the delivery efficiency comparable with that of EGFP-BoxC/D when packaged with VSVG-L7Ae (Figure 3.4, A).

Independence of VSVG-L7Ae efficiency from BoxC/D presence in the structure of EGFP mRNA appeared thought-provoking. We were wondering if it was something special about EGFP itself, or this result would be reproducible with another type of load. To elucidate this, we utilized SpCas9 vector without or with BoxC/D motif. We exploited HEK293T EG_FP stable

cell line permanently expressing sgRNA which targets *DMD* gene (exon 45). This target sequence was interspaced in-between EGFP gene thus preventing its expression and green fluorescence of the cell line. However, if SpCas9 was introduced into the cells, and in case genome got edited, *EGFP* gene was ultimately restored. We created pairs of VLPs in a similar manner as we did with EGFP. The only difference was that we had to wait for 72 hrs after inoculating VLPs onto target reporter cell line to allow gene recombination and EGFP translation to occur. Having performed this experiment, we observed the same pattern: the delivery by VSVG-L7Ae system was considerably more potent than that by WT-VSVG (Figure 3.4, B). In addition, it did not require corresponding motif (BoxC/D) to be present in the structure of the cargo molecule (Figure 3.4, B).

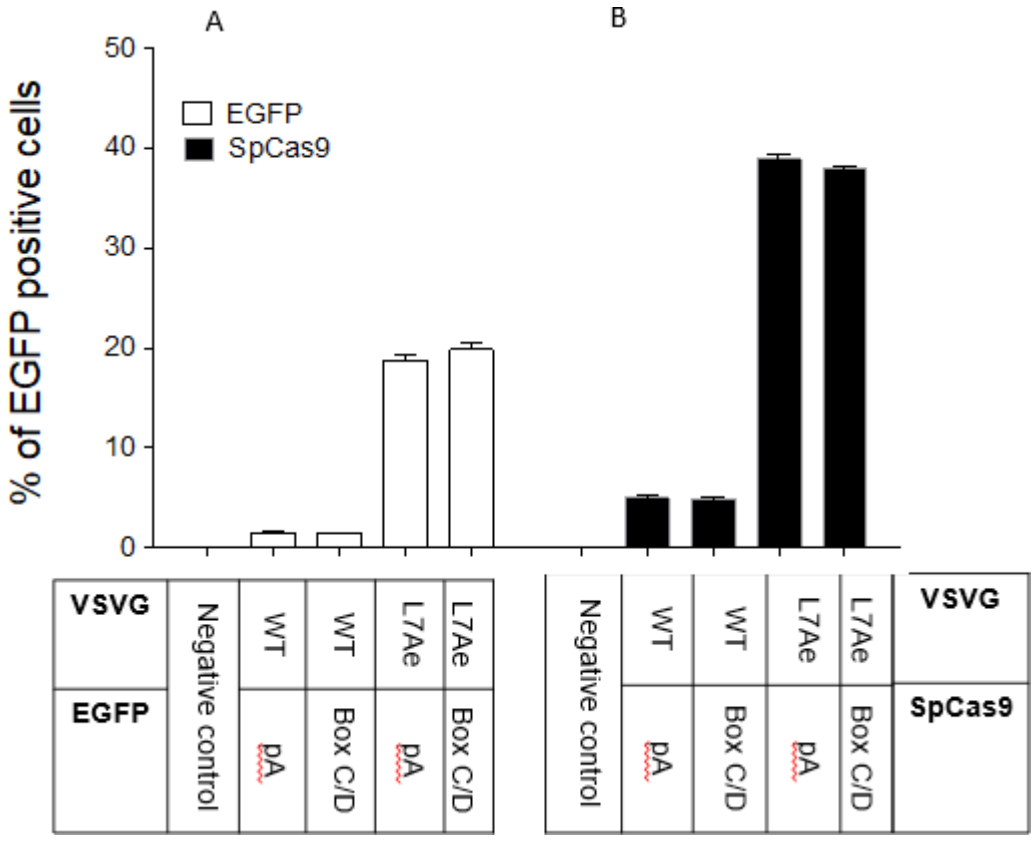

Figure 3.4 Potent efficiency of EGFP/SpCas9 delivery by VSVG-L7Ae VLPs does not require the presence of BoxC/D
EGFP fluorescent recipient HEK293T /HEK293T EGxxFP cells were measured by flow cytometer 24 hrs/72 hrs after inoculation with VLP samples bearing EGFP/SpCas9 with or without BoxC/D motif

3.3 Delivery by VSVG-L7Ae VLPs is mRNA-mediated

In attempt to elucidate the possible mechanism of action, we quantified the amount of mRNA in VLPs by qRT-PCR. As a result, EGFP/SpCas9 mRNA levels in VSVG-L7Ae VLPs were higher compared with wild-type VSV-G, regardless of the BoxC/D motif (Figures 3.5 and 3.6).

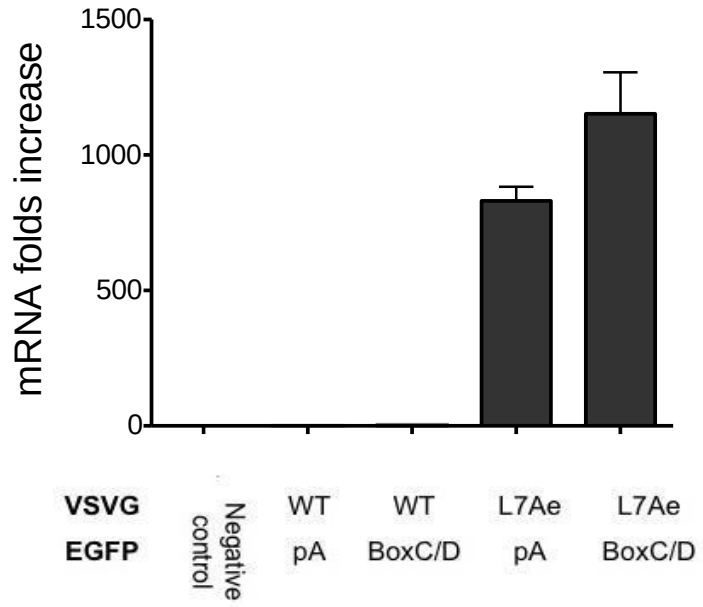

Figure 3.5 Relative EGFP mRNA quantification in VSVG-WT and VSVG-L7Ae VLPs VLPs of VSVG-WT and VSVG-L7Ae were lysed and utilized in qRT-PCR. The amount of mRNA EGFP was present regardless of BoxC/D motif presence.

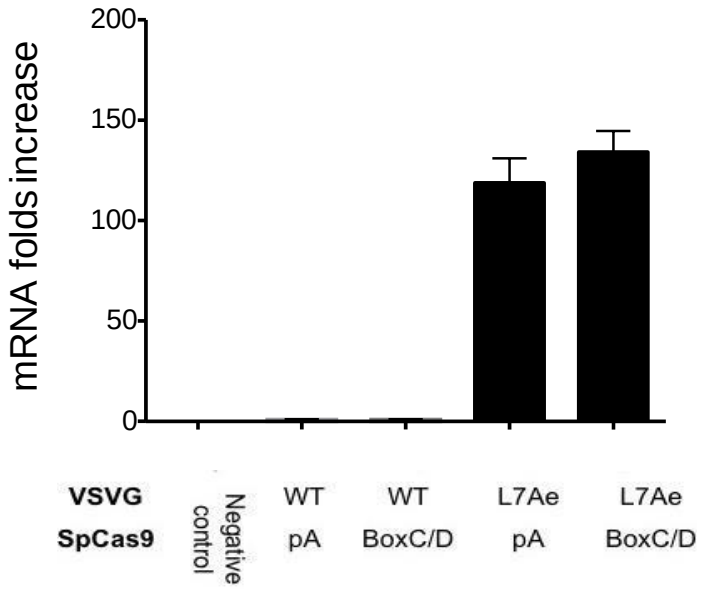

Figure 3.6 Relative SpCas9 mRNA quantification in VSVG-WT and VSVG-L7Ae VLPs VLPs of VSVG-WT and VSVG-L7Ae were lysed and utilized in qRT-PCR. The amount of EGFP mRNA was present regardless of BoxC/D motif presence.

Next, we aimed to assess the cargo protein loading of VSVG-L7Ae and VSVG-WT. Although qRT-PCR revealed increased incorporation of both EGFP and SpCas9 mRNA, we checked the protein amount of SpCas9 in the VLPs. Consistent with the previous experiment VSVG-L7Ae was less expressed in the producer cells and in the VLPs than VSVG-WT. Furthermore, we did not observe improved incorporation of SpCas9 protein into VSVG-L7Ae. Hence the increased delivery was likely not due to VLPs being enriched with the protein. This is consistent with qRT-PCR results which suggest that superior delivery by VSVG-L7Ae is due to enhanced mRNA incorporation, rather than protein incorporation.

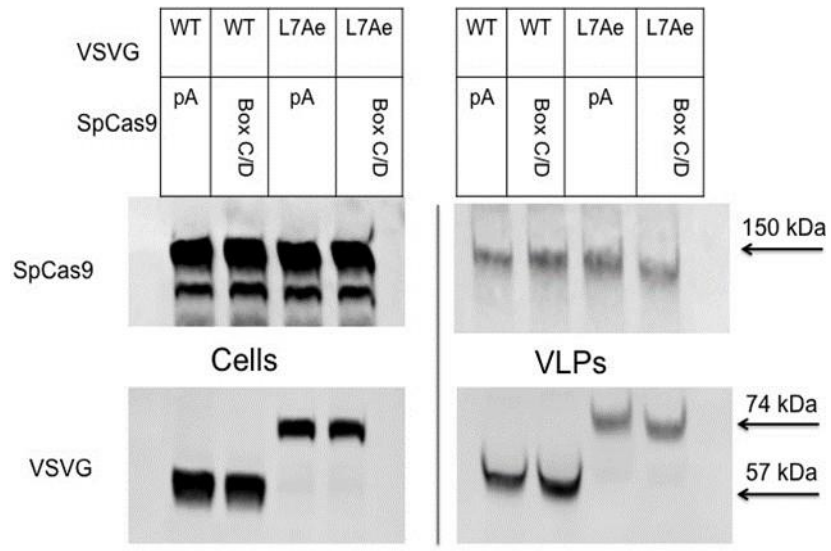

Figure 3.7 Western blot of cells and VLPs bearing SpCas9
Cells and VLPs of VSVG-WT and VSVG-L7Ae bearing SpCas9 were lysed, and Western blot was performed. No superior loading of SpCas9 into VSVG-L7Ae was observed.

Further we aimed to enrich the evidence basis for the enhanced mRNA rather than protein incorporation. We studied time dependence of EGFP positive cells after simultaneous inoculation with VSVG-WT and VSVG-L7Ae VLPs bearing EGFP (in 4, then 8, and 24 hrs). In case of protein delivery, the initial maximum number of EGFP positive cells should be decreased in a time-dependent manner as the protein degraded. Yet we observed that the number of EGFP positive cells kept rising with the time flow that confirmed mRNA-mediated delivery. That was another piece of evidence supporting the mRNA delivery (Figure 3.8)

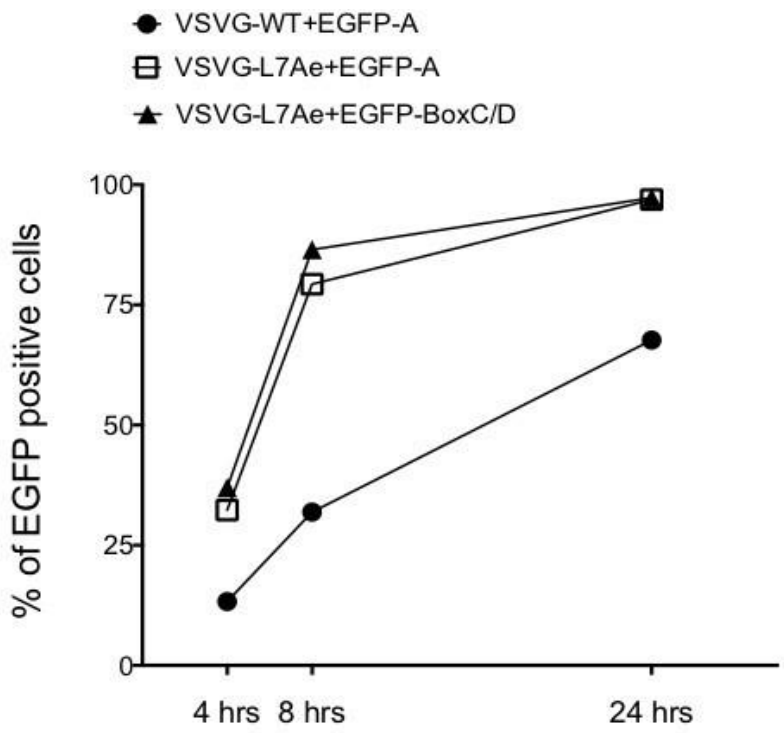

Figure 3.8 Time-course experiments with VSVG-WT and VSVG-L7Ae VLPs carrying EGFP
HEK293T cells were inoculated with the VLPs of VSVG-WT and VSVG-L7Ae system loaded with EGFP. The cells were analyzed by FACS in 4,8, and 24 hrs post inoculation.

At some point we could not understand why overexpressed mRNA molecules without any additional motifs non-specifically get incorporated into VLPs. Hence, we aimed to check if this phenomenon was driven by the switching of vesicular transport system and skewing the prevalence of secretion towards the exosome production. Hence, we utilized the exosomal inhibitors (Spiroepoxide, GW4869), yet observed no decline in VSVG-L7Ae performance (Figure 3.9)

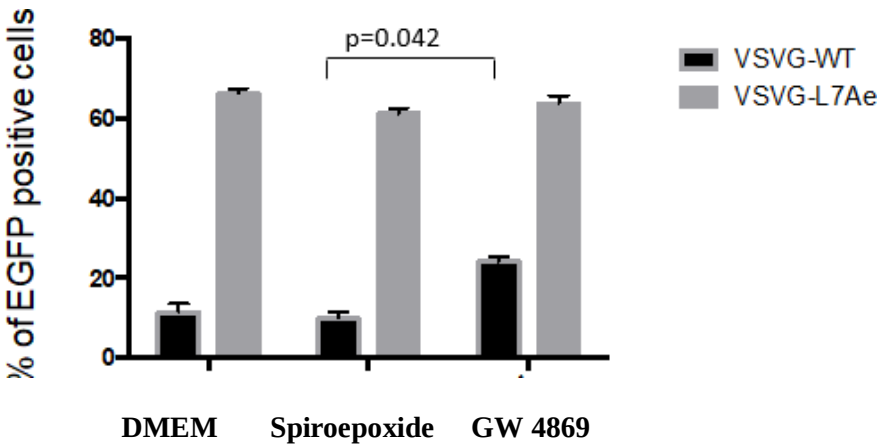

Figure 3.9 FACS analysis of recipient cells inoculated with VLPs (VSVG-WT vs VSVG-L7Ae), which were generated by producer 293T cells treated with exosomal inhibitor (Spiroepoxide, GW4869).

3.4 Delivery by VSVG-L7Ae VLPs is due to interaction with endogenous motif

At the following time during production of VSVG and VSVG-L7Ae VLPs, we decided to transfect the producer cells (293T cells) with L7Ae plasmid in addition to the common set of plasmids. Apart from L7Ae, cells were transfected as usual with VSVG/VSVG-L7Ae plasmid+ cargo plasmid of SpCas9. VLPs were collected and inoculated into 293T EG_FP+sgRNA cell line. After 72 hours, recipient cells were collected and underwent FACS analysis. Although the increased performance of VSVG-L7Ae was consistent with previous results, the second set of samples demonstrated poor delivery even in case of VSVG-L7AeVLPs. These results appeared puzzling and made us think that L7Ae might have occupied all binding centers on mRNAs of SpCas9 and that could account for why nothing was incorporated into VSVG-L7Ae VLPs. Hence, we needed to prove the binding with the upcoming CLIP experiment.

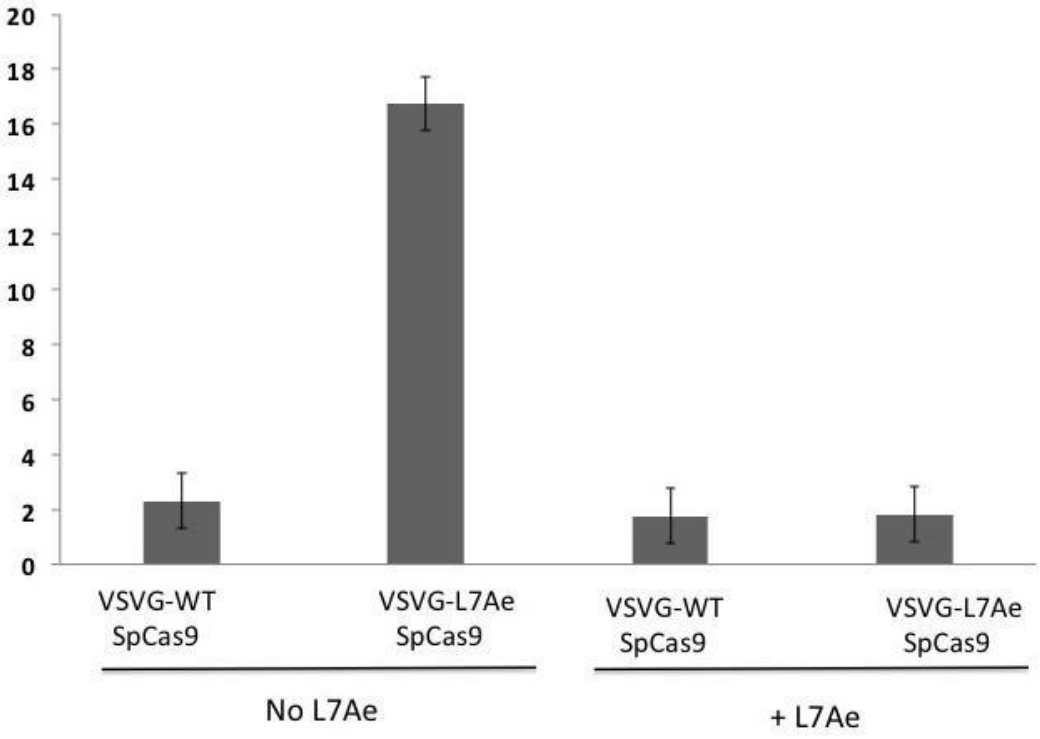

Figure 3.10. Free L7Ae added to VLP-producing cells abolished delivery of SpCas9 to EG_FP +sgRNA expressing cells.

293T EG_FP+sgRNA reporter cell lines demonstrated a decreased amount of EGFP positive cells after inoculation with VSVG-L7Ae VLPs generated from the producer cells additionally transfected with L7Ae plasmid. VSVG-L7Ae VLPs generated from producer cells which did not achieve additional free L7Ae transfection, demonstrated a performance superior to that of VSVG-WT VLPs that was consistent with the previous results.

Since EGFP mRNA without BoxC/D was enriched in VSVG-L7Ae particles, this prompted us to hypothesize that L7Ae fused with VSV-G might be binding with the EGFP mRNA independently of the BoxC/D motif and possibly with other endogenous mRNAs. To determine that the RNAs were binding with VSVG-L7Ae, we performed RNA CLIP assay.

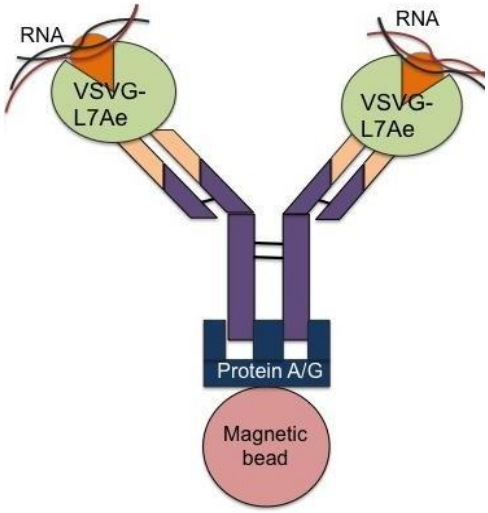

Figure 3.11 The schematic representation of magnetic beads with VSVG-L7Ae and RNAs bound through antibodies

After immunoprecipitating the whole complexes on the magnetic beads, we checked the loading equivalence by Western blotting in an attempt to identify and compare the amount of two samples (WT and VSVG-L7Ae) (Figure 3.11). We observed that the amount of VSVG-L7Ae expressed and absorbed on the beads did not exceed that of VSVG-WT. Being assured of the equal VSVG-WT/VSVG-L7Ae attachment to the magnetic beads (Figure 3.12), we proceeded with the qRT-PCR. EGFP mRNA was bound with VSVG-L7Ae and enriched more than 600-fold compared with the control VSVG-WT (Figure 3.13). However, the enrichment of the bound RNA was also observed in the endogenous mRNAs, such as GAPDH (~160-fold), β-actin (ACTB,~110-fold), and 7SL lncRNA (RN7SL1, ~90-fold) (Figure 3.13).

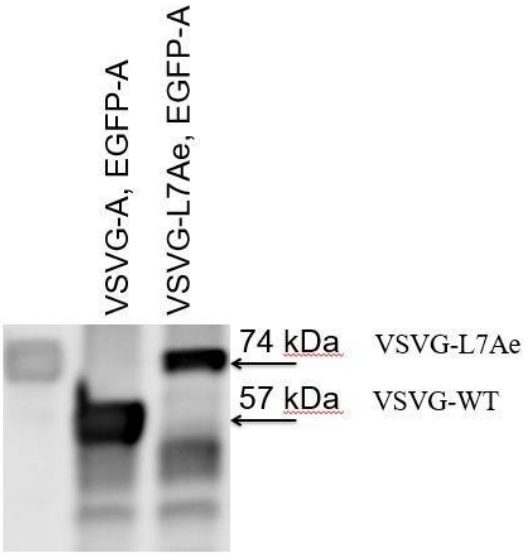

Figure 3.12 The amount of VSVG-WT/VSG-L7Ae, precipitated on the beads, measured by Western Blot.
The protein (either VSVG-WT or VSVG-L7Ae) was precipitated on the magnetic beads and measured by Western blot prior to proceeding with the assessment of bound RNAs level. This was required to ensure that VSVG-L7Ae sample did not contain more precipitated protein than that of VSVG-WT.

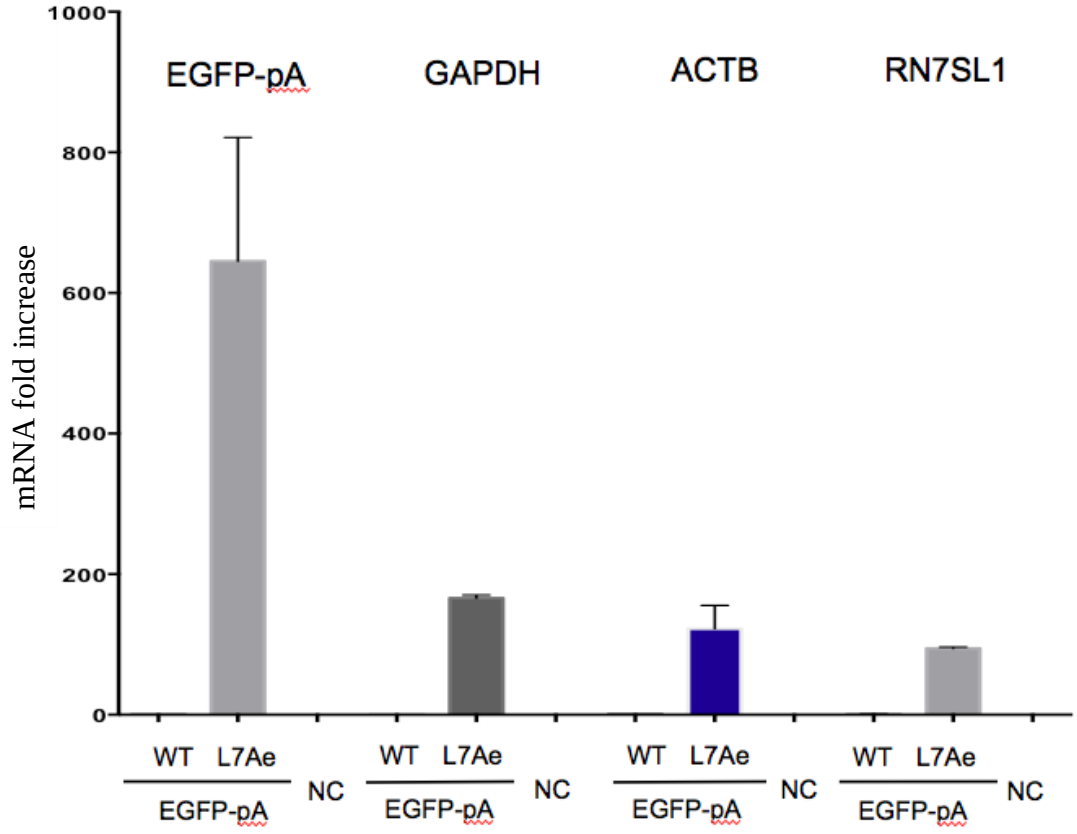

Figure 3.13 The relative amount of RNA (EGFP, GAPDH, ACTB, and L7Ae) in VSVG-WT vs VSVG-L7Ae precipitates

CLIP assay was performed to pull-down mRNAs directly bound with engineered pHL-EF1a-VSVG-L7Ae-pA co-transfected with pHL-EF1a-EGFP-pA in the producer HEK293T cells on 6-cm plates scale. The pulled-down mRNAs were assessed by qRT-PCR analysis for EGFP mRNA transgene, as well as endogenous housekeeping mRNAs GAPDH, ACTB, and RN7SL1. VSVG-WT sample was used as a control, and relative RNA enrichment is presented from technical triplicate experiment (n = 3, ± S.D.).

Elevated transcripts in VSVG-L7Ae VLPs

transcript	name	Log FC
ENST00000553637	*7SL RNA*	3,371
ENST00000580625	*RN7SL1*	3,140
ENST00000490232	*RN7SL2*	3,112
ENST00000581458	*RNA_7SL_Cytoplasmic 5*	2,937
ENST00000434805	*RPL5P4*	1,579
ENST00000396859	*GAPDH_204*	1,484
ENST00000396690	*RP11_75L1.2*	1,462
ENST00000372209	*RSP8*	1,449
ENST00000426182	*NME/NM23*	1,449
ENST00000351677	*PTPN11-201*	1,439
ENST00000509535	*GNB2L1*	1,418
ENST00000371146	*USP1-202*	1,388
ENST00000548787	*chaperonin containing TCP1 Subunit 2*	1,265
ENST00000373610	*taxilin alpha*	1,237
ENST00000546654	*ribosomal protein L41*	1,217
ENST00000480896	*pericentrin*	1,191
ENST00000437890	*ribosomal protein S13 pseudogene 2*	1,126
ENST00000368069	*COPA-202*	1,103

*Grey lines- contain BoxC (G/A ATGATG)+BoxD (CTGA)

Figure 3.14 Increased transcripts in VSVG-L7Ae VLPs in comparison with VSVG-WT VLPs.

In consistency with the CLIP results, when VSVG-L7Ae immunoprecipitated on magnetic beads was shown to be bound with 7SL, RNA-seq results demonstrated significantly higher incorporation of 7SL transcripts into VSVG-L7Ae.

3.5 K-turn domain of L7Ae plays a critical role in the work of VSVG-L7Ae system

Interaction of VSVG-L7Ae with endogenous RNAs raised the question whether this interaction was specific to the RNA-binding activity of L7Ae. To examine this, we mutated two lysine residues of L7Ae (K37A and K79A, termed as L7KK) known to be essential for interaction with BoxC/D RNA motifs [Hara, Saito, Inoueб 2013]. The mutations in these two residues are known to significantly decrease binding of L7Ae/L7KK with BoxC/D motifs from 1.6 nM (L7Ae: BoxC/D) to 680 nM (L7KK: BoxC/D)

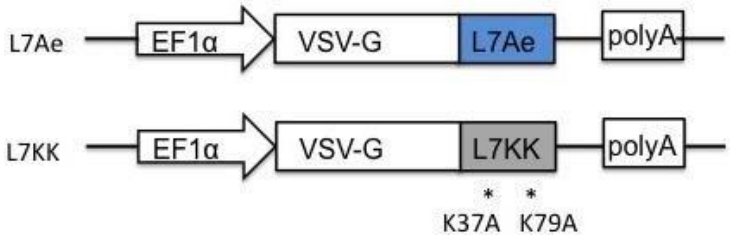

Figure 3.15. Schematic representation of VSGV-L7Ae and VSVG-L7KK vectors

Therefore, we generated a fusion with VSV-G similar to VSVG-L7Ae (Figure 3.15). VSVG-L7KK VLPs were produced side-by-side with VSVG-WT and VSVG-L7Ae VLPs and co-packaged with either EGFP or SpCas9 mRNA containing or not containing the BoxC/D motif. Then, VLPs were inoculated into HEK293T cells or HEK293T EGxxFP+sgRNA cells to analyze EGFP or SpCas9 delivery by flow cytometry 24 hours or 72 hours post inoculation. VSVG-L7KK VLPs demonstrated slightly higher delivery than VSVG-WT VLPs, whereas drastically decreased the delivery of EGFP (Figure 3.16 A) or SpCas9 (Figure 3.16 B) in comparison with VSVG-L7Ae.

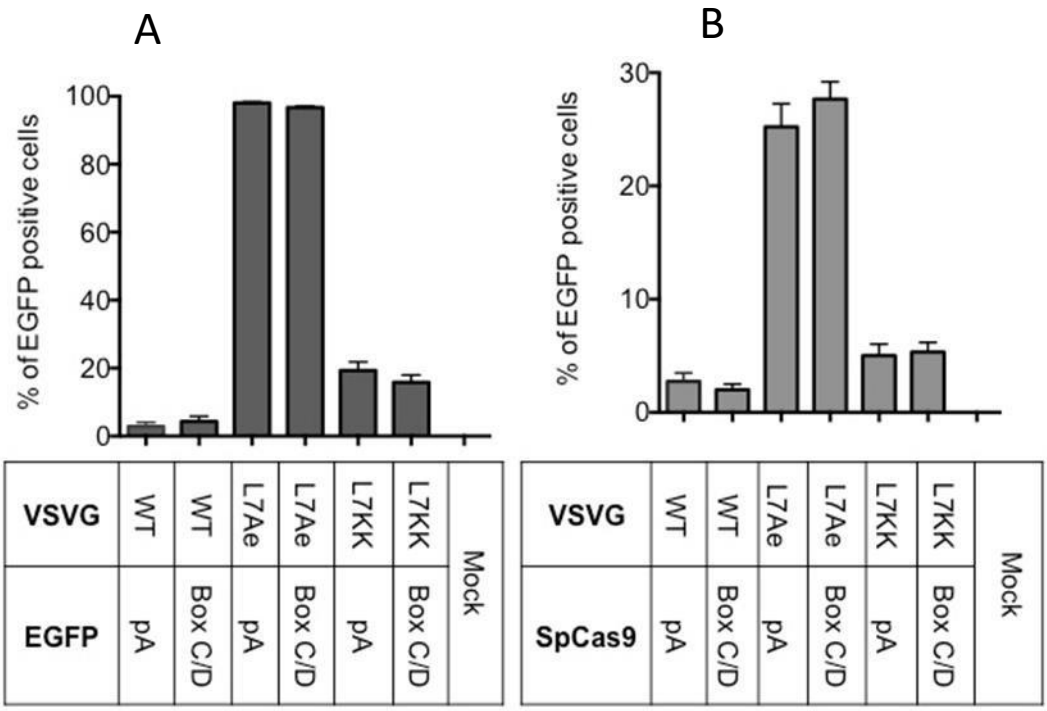

Figure 3.16. Enhanced delivery and mRNA incorporation were mediated by RNA-binding domain of L7Ae

EGFP-positive recipient HEK293T / HEK293T EGxxFP+sgRNA cells were measured by flow cytometry 24 hrs/72 hrs after inoculation with VLPs (n = 3, ± S.D.).

Consequently, we investigated the EGFP mRNA incorporation levels in VLPs by qRT-PCR. In comparison with VSVG-L7Ae VLPs, mutant VSVG-L7KK VLPs showed significantly lower level of mRNA packaging (Figure 3.16). Taken together, these results indicate that the two lysine residues (K37 and K79) of L7Ae may be important for mRNA delivery via VSVG-L7Ae VLPs.

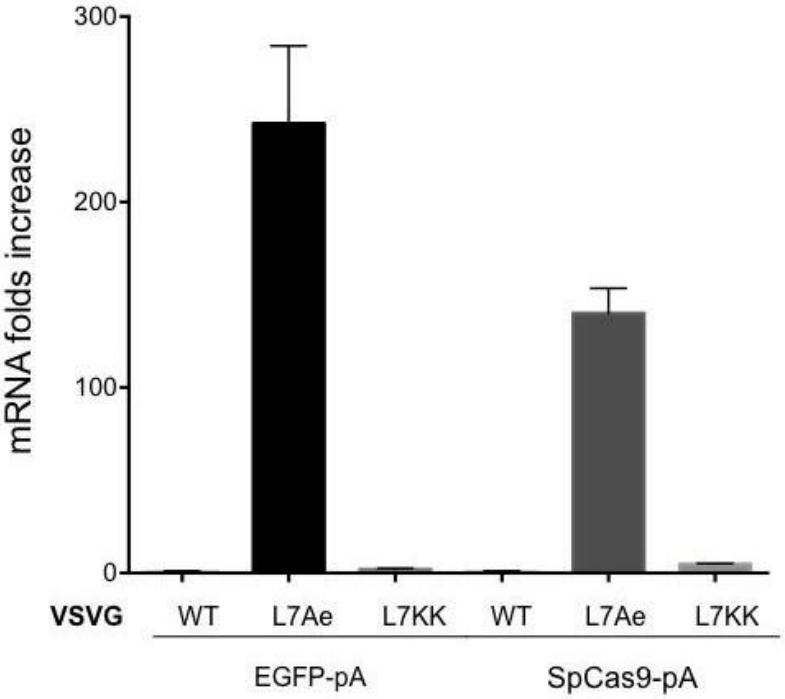

Figure 3.17. Enhanced delivery and mRNA incorporation were mediated by RNA-binding domain of L7Ae
qRT-PCR analysis of the amount of EGFP mRNA incorporated into VLPs demonstrated decreased incorporation into VSVG-L7KK VLPs (n = 3, ± S.D.)

3.6 Pseudotyping of retroviruses with VSVG-L7Ae abolishes their action

On a different note from investigating the mechanism of increased mRNA-mediated incorporation, we were curious about checking what would happen if we used VSVG-L7Ae instead of VSVG-WT for pseudotyping of HIV-1 and MLV viruses. Given that VSVG is commonly used in molecular biology labs for the pseudotyping HIV (mainly) and other viruses, we decided to test whether VSVG-L7Ae would demonstrate altered performance in comparison with VSVG-WT as a pseudo-coating agent. Surprisingly, exploiting VSVG-L7Ae instead of VSVG-WT completely abolished the delivery of EGFP not only by retro- but also by lentiviruses (Figure 3.18. and 3.19).

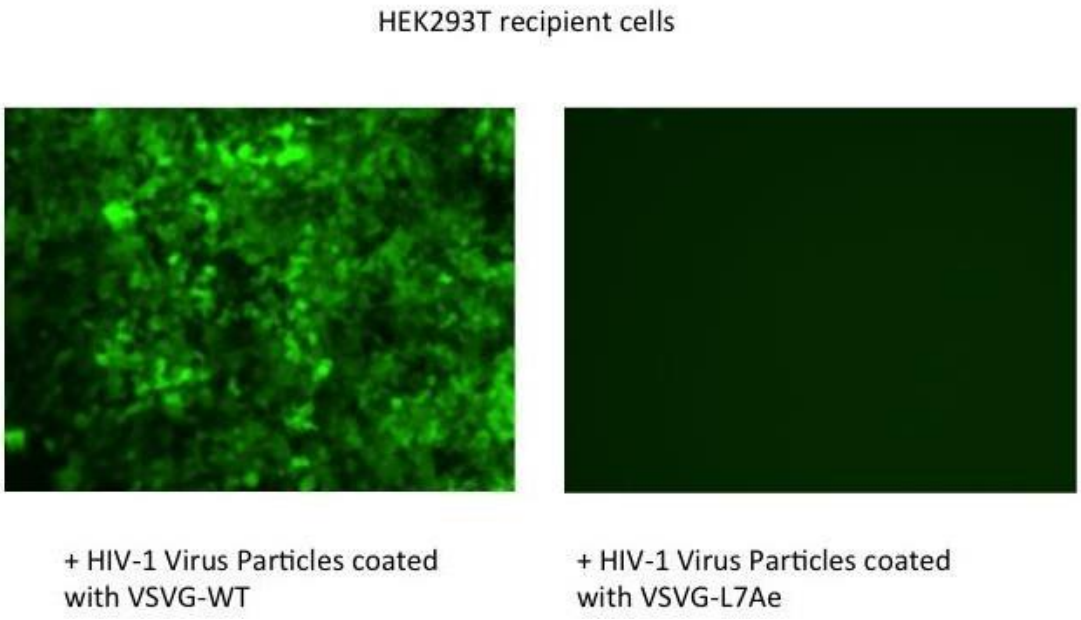

Figure 3.18 Keyence images of HEK293T cells infected with conventional HIV-1 particles vs virus particles with VSVG-L7Ae protein used for pseudo-coating

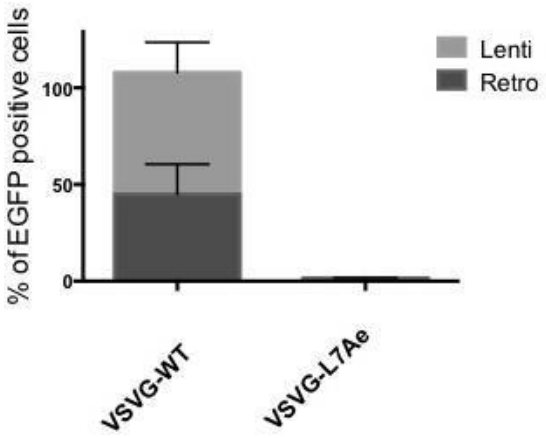

Figure 3.19 Abolished delivery of EGFP by HIV-1 and MLV particles
FACS analysis of the amount of EGFP positive cells was performed 72 hrs after infection of HEK293T cells with HIV-1 or MLV virus particles pseudo-coated with either VSVG-WT or VSVG-L7Ae (n = 3, ± S.D.)

3.7 Proteomics of VLPs

Having elucidated that the enhanced delivery by VSVG-L7Ae is due to the increased mRNA-incorporation which is BoxC/D independent, yet dependent on L7Ae k-turn binding domain, we

proceeded with Mass spectrometry of VLPs. Enriched entries were plotted (Figure 3.20) and analyzed. The top entries, which were enhanced the most in VSVG-L7Ae VLPs, were YBX-1, RPL22, PABC1, SYNCRIP, and SPR14. All of them represent mRNA binding proteins essential for translation and trafficking of the nascent chain complex to the ER of the cell. Importantly, analyzed VLPs were loaded with SpCas9. Consistent with our previous experiments (qRT-PCR of the VLPs, Western blot of VLPs), mass spec did not demonstrate significantly increased amount of SpCas9 protein in VSVG-L7Ae VLPs. This indicates that efficient delivery of a loaded cargo is indeed mRNA- rather than protein-mediated. Major participants of translation being at the top of the list and highly enriched in VSVG-L7Ae over VSVG-WT entries additionally confirm that it is mRNA-mediated delivery. mRNA is incorporated into the VLPs together with the whole transcriptional complex.

On contrary, some entities are highly enriched in VSVG-WT VLPs (RALA, CTNNB1, GNA13, RAB14). These are involved in GTP-dependent exocytosis (RALA), cell adhesion (CTNNB1), membrane trafficking between Golgi complex and endosomes (RAB13), and signal transduction (GNA13). This goes in accordance with the mechanism of VSV-G transport from ER to the cell membrane with a consequent exocytosis and VLPs formation. Lower passive incorporation of these proteins into VSVG-L7Ae VLPs might indicate altered mechanism of VLPs formation and substances incorporation due to the fusion of VSV-G with L7Ae.

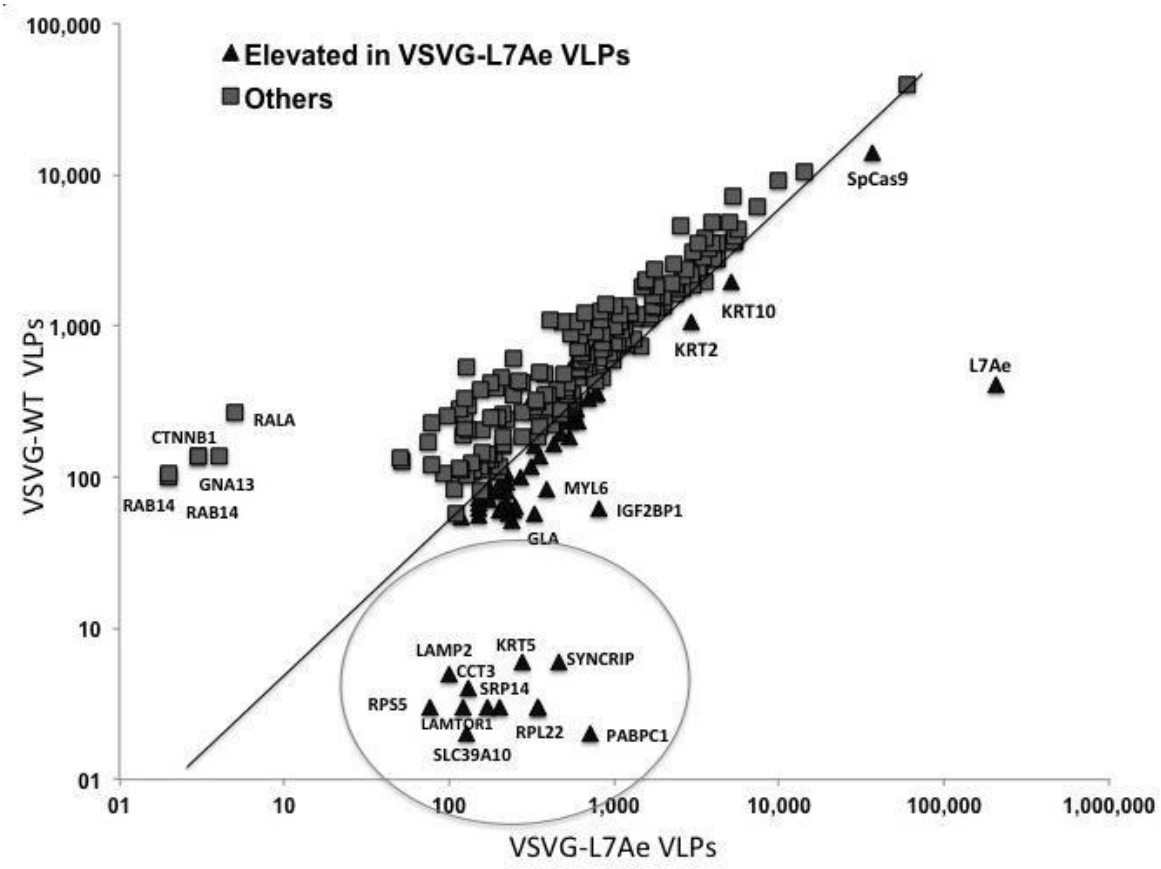

Figure 3.20 Increased protein amount in VSVG-L7Ae VLPs in comparison with VSVG-WT VLPs

Table 3.21 List of proteins, increased in VSVG-L7A VLPs

After trypsin digestion of samples, samples were labeled with iTRAQ and analyzed by nanoLC-MS/MS. Ion count for VSVG-WT/VSVG-L7Ae samples were measured and $\log^2$ calculated.

GeneName	Description	VSVG-WT	VSVG-L7Ae	VSVG-L7Ae/VSVG-WT log2
L7Ae		**405,2**	**206894,7**	**9**
YBX1	**Nuclease-sensitive element-binding protein 1**	**2**	**708,53**	**8,47**
RPL22	**60S ribosomal protein L22**	**3**	**346,43**	**6,85**
PABPC1	**Polyadenylate-binding protein 1**	**3**	**346,27**	**6,85**
SYNCRIP	**Heterogeneous nuclear ribonucleoprotein**	**6**	**458,41**	**6,26**
SRP14	**Signal recognition particle 14 kDa protein**	**3**	**201,96**	**6,07**
SLC39A10	**Zinc transporter ZIP10**	**2**	**127,52**	**5,99**
F10	**Coagulation factor X**	**3**	**171,9**	**5,84**
LAMTOR1	**Ragulator complex protein LAMTOR1**	**3**	**119,77**	**5,32**
CCT3	**T-complex protein 1 subunit gamma**	**4**	**130,04**	**5,02**
LAMP2	**Lysosome-associated membrane glycoprotein 2**	**5**	**100,01**	**4,32**
IGF2BP1	**Insulin-like growth factor 2 mRNA-binding protein 1**	**62,71**	**797,88**	**3,67**
GLA	**Alpha-galactosidase A**	**56,94**	**324,85**	**2,51**
MYL6	**Myosin light polypeptide 6**	**84,2**	**391,92**	**2,22**
ANP32E	**Acidic leucine-rich nuclear phosphoprotein 32 family member E**	**51,06**	**237,59**	**2,22**
NAP1L1	**Nucleosome assembly protein 1-like 1**	**60,92**	**247,13**	**2,02**
RPS26	**40S ribosomal protein S26**	**62,96**	**252,91**	**2,01**
JUP	**Junction plakoglobin**	**56,8**	**229,21**	**2,01**
TBCA	Tubulin-specific chaperone A	60,09	204,07	1,76
RPL9	60S ribosomal protein L9	61,67	205,7	1,74
VPS13B	Vacuolar protein sorting-associated protein 13B	182,83	534,18	1,55
CCT6A	T-complex protein 1 subunit zeta	81,13	223,54	1,46
SSRP1	Chromatin-specific transcription elongation factor 80 kDa subunit	55,35	151,8	1,46
BANF1	Breakpoint cluster region protein 1	100,92	271,74	1,43
TMED9	Transmembrane emp24 domain-containing protein 9	118,24	315,57	1,42
LAMP1	Lysosome-associated membrane glycoprotein 1	163,94	433,67	1,4
Cas9		14035,97	36756,57	1,39
PHGDH	D-3-phosphoglycerate dehydrogenase	234,89	602,06	1,36
PLS3	Plastin-3	138,32	353,48	1,35
TLN1	Talin-1	70,26	174,43	1,31
ANXA2	Annexin A2	193,72	469,66	1,28
UCHL1	Ubiquitin carboxyl-terminal hydrolase isozyme L1	93,55	223,14	1,25
CPNE1	Copine-1	80,03	190,76	1,25
HNRNPC	Heterogeneous nuclear ribonucleoproteins C1	62,76	149,25	1,25
PRDX6	Peroxiredoxin-6	234,8	550,49	1,23
CD276	CD276 antigen	85,65	198,71	1,21
CALR	Calreticulin	355,76	781,34	1,14
HSPA5	Endoplasmic reticulum lumenal Ca	258,54	570,74	1,14
TSPAN3	Tetraspanin-3	68,13	149,2	1,13
EHD3	EH domain-containing protein 3	54,08	118,23	1,13
CD47	Leukocyte surface antigen CD47	355,81	774,72	1,12
SOD1	Superoxide dismutase 1	329,19	701,74	1,09
ATP1B1	Sodium/potassium-transporting ATPase subunit beta-1	105,54	223,65	1,08
SRI	Sorcin	274,13	567,23	1,05
DPYSL5	Dihydropyrimidinase-related protein 5	282,3	582,32	1,04
RPS24	40S ribosomal protein S24	276,52	559,18	1,02
HSP90AA1	Heat shock protein HSP 90-alpha	247,48	501,38	1,02
SLC7A5	Large neutral amino acids transporter small subunit 1	84,9	172,42	1,02
GNA11	Guanine nucleotide-binding protein subunit alpha-11	73,46	149,3	1,02
CD81	CD81 antigen	284,96	573,07	1,01
RPSA	40S ribosomal protein SA	163,27	327,99	1,01

3.8. VSVG-L7Ae chimeric VLPs efficiently transduced hard-to-transfect cell lines including iPS cells and monocytes

Because of the highly efficient mRNA delivery of our VLP system in HEK293T cells, we set out to test our system on various human cell types. Human iPS cells are widely used for disease modeling, drug screening and drug toxicity testing *in vitro* due to their unlimited proliferative potential and pluripotency [Takahashi, Yamanaka, 2006]. Various transduction methods, such as electroporation or lentiviral vector transduction [Cao et al, 2010] have been utilized and optimized, but it is still difficult to achieve transduction efficiency higher than 70%. In our hands, when VSVG-L7Ae VLPs were inoculated into human iPS cells, the result was highly potent concerning the EGFP delivery and showed the highest EGFP+ portion, as well as higher mean fluorescence intensities than VSVG- WT VLP (Figure 3.22B).

As another target cell line, we used a human monocytic cell line, THP-1, which is derived from the peripheral blood of a childhood case of acute monocytic leukemia (M5 subtype) and has been widely used for immunological experiments. Again, when we inoculated our VLPs, we observed high transduction efficiency, over 90%, with our VSVG-L7Ae VLP system (Figure 3.22 C).

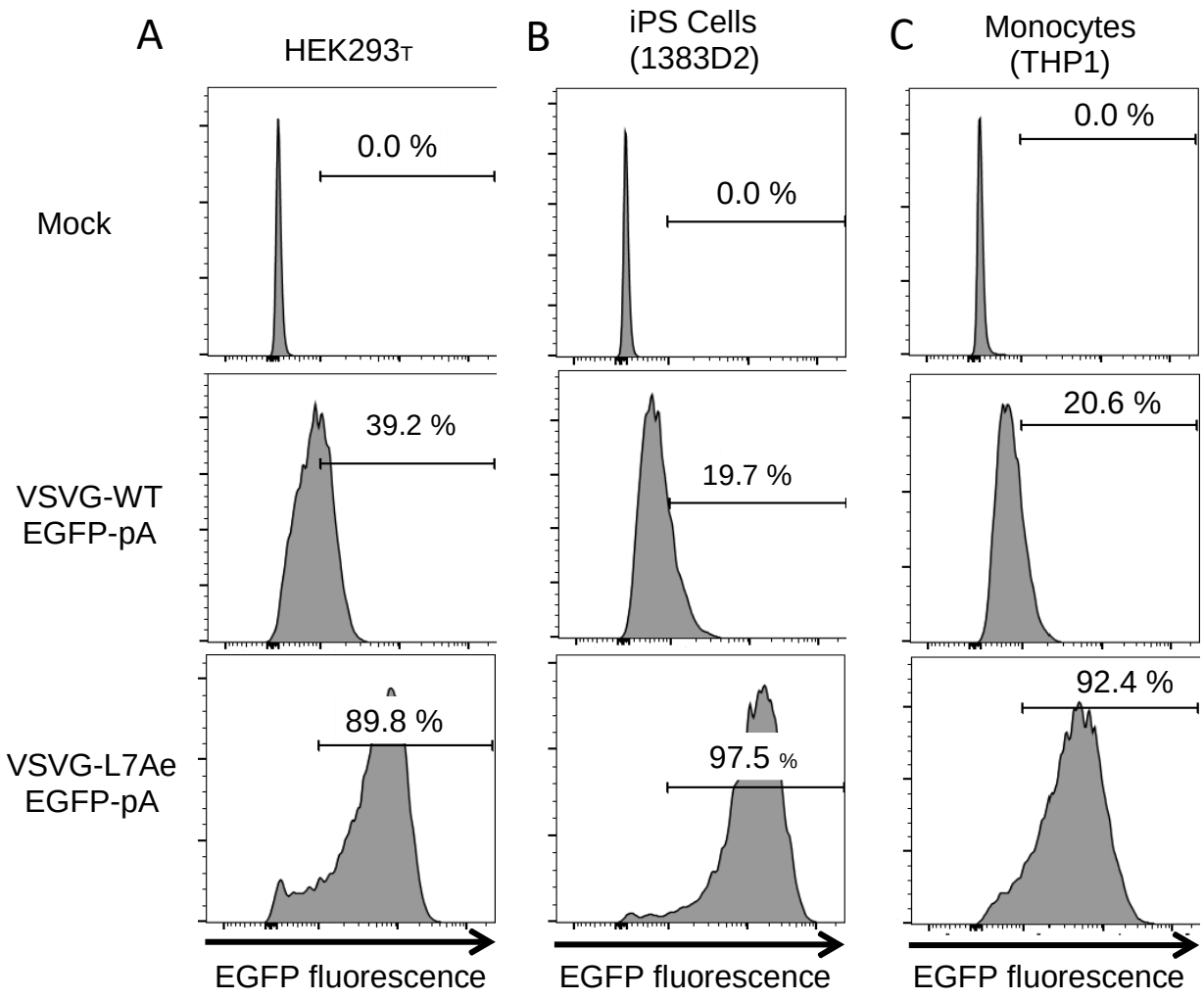

Figure 3.22. High transduction efficiencies by VSVG-L7Ae VLP in various human cell types

VSVG-WT or VSVG-L7Ae VLPs packed with EGFP mRNA were inoculated onto HEK293T cells (A), iPS cells (1383D2) (B), and THP-1 monocytes (C), and EGFP fluorescence intensities were measured after 24 hours.

Chapter 4

Discussion

mRNA delivery has several exciting applications, such as mRNA vaccines, cellular reprogramming, and genome editing [Stanton,2018]. mRNA translation is initiated promptly after the delivery to the cytoplasm. In case of exploiting mRNA as a delivery nucleic acid the risk of genomic integration is close to zero. To this end, there is an unmet need for an efficient delivery tool to introduce mRNA into various cell lines, especially for "hard-to-transfect" cell types. Therefore, we aimed to concentrate our research interest in the developing an mRNA delivery system.

Several platforms for mRNA-mediated transfer have been reported, such as lipofection, lipid nanoparticles, electroporation, RNA viral vectors, and reverse transcriptase-deficient lentiviral vectors [Slivac et al, 2017]. One such approach to mRNA delivery to the target cells is by exploiting virus-like particles (VLPs), which were already discussed above [Zeltins, 2013].

Mangeot et al. reported a novel VLP system termed as “gesicles” induced by the expression of an envelope glycoprotein G of Vesicular stomatitis virus (VSV-G) in HEK293 cells [Mangeot et al, 2011]. Gesicles could stochastically co-package overexpressed proteins of interest for the delivery. We set out to take advantage of the ability of VSV-G to induce VLP-formation by engineering them to deliver mRNA into target cells. For specific mRNA-incorporation, we fused VSV-G envelope protein with RNA-binding proteins. Two RNA-binding proteins were selected: bacteriophage MS2-binding protein (MS2BP) [Prel et al, 2015] and archaeal L7Ae ribosomal protein from *Archeoglobus fulgidus* [Saito et al, 2010].

MS2BP is an envelope protein of MS2 bacteriophage which inhibits replicase gene expression by binding to MS2-stem loop structures on its mRNA [Pickett, Peabody, 1993]. The interaction between MS2BP and MS2-stem loops has been previously exploited for mRNA delivery as VLPs *in vitro* and *in vivo* [Pickett, Peabody, 1993]. Another common area of MS2 system

utilization is tracking intracellular RNA molecules.

On the contrary, L7Ae protein is one of the large ribosomal subunit proteins of archaeal species. Apart from playing a vital role in ribosome structure, it is also involved in splicing, posttranscriptional modifications of ribosomal RNAs, and archaeal RNase P complex stabilization [Daume et al, 2017]. L7Ae is capable of binding RNA secondary structures, termed kink-turn motifs. A kink-turn is characterized by the formation of an axial bend into the RNA structure which provides for interaction with L7Ae protein [Klein et al, 2011]. There are various kink-turn motifs, including BoxC/D (Figure 4) and H/ACA motifs in snoRNAs, Kt motifs in ribosomal RNAs, and riboswitches [Klein et al, 2001].

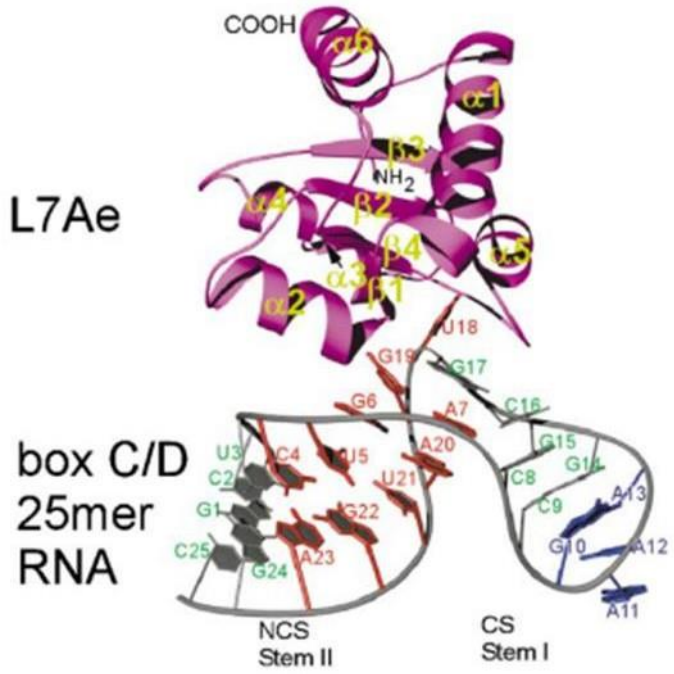

Figure 4. Schematic representation of L7Ae and BoxC/D interaction [Klein, 2001]

We created our VLP system by VSVG fusion with RNA-binding proteins: either L7Ae or MS2BP. To facilitate incorporation of RNA we cloned in its structure the cognate binding motifs : BoxC/D and MS2SL, respectively. While trying out two systems side-by-side, we

realized that VSVG-MS2BP system appeared not to be effective at all and could not manage cargo delivery to the recipient cells unlike VSVG- L7Ae (Figure 3.1). Interestingly, after we initiated this project another group also attempted to engineer the delivery system via chimeric VSVG-MS2BP VLPs [Hung, Leonard, 2016]. Hung and Leonard managed to achieve an increased incorporation of mTomato mRNA into VLPs by raising the number of MS2 stem loops in 3'UTR of mRNA. However, the delivery of mTomato to the recipient cells failed similar to our experiments. The authors supposed that the reason for this was poor endosomal escape of VSVG-MS2BP into the cytoplasm of the recipient cells. While this could definitely have been the case, by Western blotting we also observed diminished VSV- G protein amount in producer cells after it was fused with MS2BP in comparison with VSVG- WT (Figure 3.3). We hypothesized that it could be one of the reasons for the delivery failure. In addition, qRT-PCR analysis of the VLPs revealed only slightly increased amount of EGFP mRNA with 2 or 4 MS2 stem loops in comparison with wild type VSV-G VLPs (Gesicles) but greatly enhanced enrichment of EGFP mRNA with BoxC/D in VSVG-L7Ae VLPs (Figure 3.2).

Overall, VSVG-L7Ae VLPs demonstrated dramatically outperformed VSVG-WT or VSVG-MS2BP VLPs (Figure 3.1, 3.2). Strikingly, follow-up experiments showed that the presence of inserted BoxC/D motif in EGFP mRNA was not essential for the efficient performance (Figure 3.4). Given that L7Ae of VSVG-L7Ae was supposed to bind to/with its partner BoxC/D kink-turn motif, these results appeared very surprising. We then aimed to elucidate the mechanism that would explain this phenomenon. To do this we set out to answer the following questions: 1. Is the delivery mRNA- or protein- mediated? 2. Could it be that fusion of VSV-G with another protein completely skewed the exosome secretion pathway and hence improved VLPs production? If that was the case, could it benefit from pseudo-coating lenti- and retroviruses with VSVG-L7Ae instead of VSV-G?

By performing qRT-PCR (that demonstrated enhanced incorporation of EGFP and SpCas9 mRNA into VVSG-L7Ae particles in comparison to VSVG-WT VLPs- Figure 3.5-3.6), Western blot (that revealed not exceeding level of protein in VSVG-L7Ae VLPs- Figure 3.7), time-course experiment (that showed decrease of EGFP expression in the cells with the time flow- Figure 3.8), and Proteomics analysis (Figure 3.20-3.21)- we established that the delivery by VSVG-L7Ae was mainly mRNA- rather than protein-mediated. Given that mRNA greatly enhanced in the VLPs was lacking the L7Ae -binding motif (BoxC/D), the origin of this phenomenon remained to be elucidated.

We excluded the possibility that the pathway of exosome formation had been altered by applying a couple of exosome inhibitors to the VLP-producing cells (Figure 3.9). We hypothesized that if VSVG-L7Ae facilitated exosome production, this experiment would halt it. However, there was no drastic drop in samples with applied exosome inhibitors. Despite these results, we still hoped to improve retro- and lentiviral pseudo-coating procedure. However, utilizing VSVG-L7Ae instead of classical VSV-G completely abolished the infectivity of the viral medium collected 72 hours after transfection of viral plasmids (Figure 3.18-3.19). This may have happened due to the interaction of L7Ae with some critical stages of virus assembly and replication.

Further, we wanted to elucidate if some kind of specific or non-specific binding occurred between any internal cellular structures and VSVG-L7Ae. We observed that VSVG-L7Ae demonstrated enhanced performance not only in EGFP delivery, but also in that of SpCas9, hence it did not seem to be the property of particularly EGFP as we first thought.

CLIP experiment revealed binding of L7Ae of VSVG-L7Ae with EGFP mRNA, that was either direct or non-direct. (Figure 3.11). Noteworthy, in numerous qRT-PCR experiments we observed that the amount of mRNA of house-keeping genes (GAPDH and ACTB) and 7SL (RN7SL1)

were elevated in VSVG-L7Ae VLPs in comparison with VSVG-WT. Since housekeeping genes (GAPDH, ACTB, and RN7SL1) showed significant upregulation in VSVG-L7Ae VLP samples, standard $2^{\wedge(-ddCT)}$ method could not be applied. Having supposed that VLPs were enriched in all other types of mRNAs including other possible internal controls (tubulin, cyclophilin A, hypoxanthine-guanine phosphoribosyltransferase (HGPRT)), we decided to calculate the relative fold increase by $2^{\wedge(-dCt)}$ method. Although some non-coding housing-keeping genes, such as RNU12 (U12 small nuclear RNA) or Small Cajal body-specific RNA 5 (SCARNA5) should have been exploited, we did not do it. Instead, we calculated $2^{\wedge(-dCt)}$ values relative to VSVG-WT VLP as a reference sample, after normalization with the total input mRNA quantification to show semi-quantitative mRNA levels of EGFP [Huggett et al, 2005].

In the CLIP experiment, VSVG-L7Ae precipitated on the magnetic beads contained high amounts of not only EGFP mRNA, but also other types of mRNA (GAPDH, ACTB) and, again, non-coding 7SL RNA. This indicated that, indeed, either some specific binding occurred with a particularly abundant structure within the eukaryotic cells or non-specific interactions with various possible molecules took place.

There was a need to understand the potential binding partners of the archaeal protein L7Ae within eukaryotic cells. In fact, L7Ae is capable of interacting with various secondary RNA motifs termed kink-turns. The latter are ubiquitously spread in the cellular cytoplasm.

Kink-turn motifs are widely spread secondary structures of various RNA types within prokaryotic, archaeal and eukaryotic cells. K-turn consists of two conserved GA helices with an

asymmetrical bulge in the middle introducing the kink. K-turn generally serves as a binding motif for proteins, despite the capability of interacting with the cell metabolites as well (Fig 4.1)

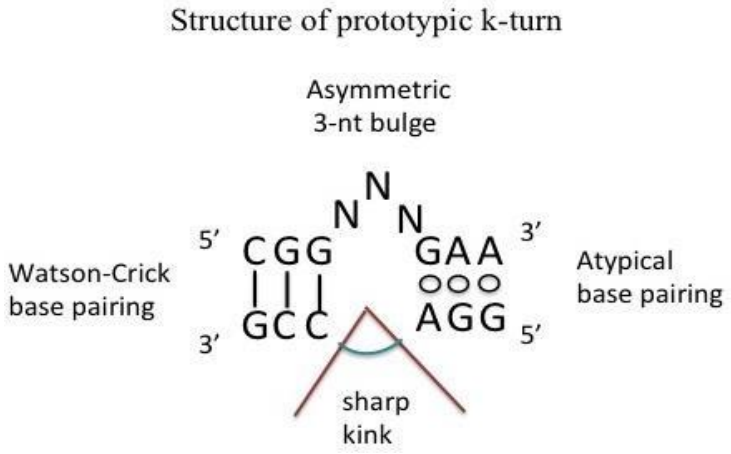

Figure 4.1. Structure of a typical k-turn motif

Kink-turn represents a duplex RNA that possesses asymmetric, usually 3nt long, bulge introducing a sharp angle in the axis of RNA. This bulge is flanked by helix with conventional Watson-Crick base-pairing and atypical GA base-pairing.

Initially, in 2001 Winkler and colleagues observed the similarity in the secondary structural motif among regulatory systems in the leader RNA regions of some prokaryotes. Box T and Box S serve as transcription terminator controls in Gram-positive bacteria. [Wels et al, 2008].These systems are involved in regulating gene expression responsible for aminoacyl-tRNA-synthetase and methionine biosynthesis, respectively [Grundy et al, 1998]. Winkler et al., observed highly conserved motifs within Box T and S systems including two short helices containing purine nucleotides, GA tandems, with the asymmetrical bulge in-between. Interestingly, the authors identified that such prototypical structural elements resembled BoxC/D motifs of snoRNAs, L30 binding site of rRNA, yeast Snup13 binding site of U4snRNA, and motifs on 23rRNA.

The term kink-turns, or K-turns, was introduced by Klein et al. later in 2001 [Klein et al, 2001]. In their work, the authors identified six k-turns on 23S rRNA of a large ribosomal subunit and two k-turns of 16s RNA of a small ribosomal subunit in *H. marismortui*. Although k-turns vary in structure, their consensus sequence defines key distinctive characteristics of the RNA element, which are the following: the asymmetrical, typically 3 nt long bulge, surrounded by canonical and non- canonical duplex helices. Canonical stem contains base pairs (usually CG) with the conventional Watson-Crick bonds, while non-canonical stem has tandem GA nucleotides with unusual pairing between two purine bases. The 3nt loop introduces a sharp bend in the RNA [Klein et al, 2001].

Interaction of L7Ae and homologs and kink-turn motifs

L7Ae of *H. Marismortui*, yeast Snu13p, and eukaryotic 15.5kDa are homologs, which all possess similarities in their RNA-binding domains and interact with k-turns in a similar manner.

- *15.5 kDa interaction with U4 snRNA k-turn*

Splicing occurs in the nucleus with the assistance of spliceosomal RNP complex. Divergent steps at splicing include formation of A, or ATP-dependent complex, consisting of U2 snRNAP and pre-mRNA, and further B-complex, involving U4, U5, and U6 snRNA and a pre-mRNA substrate. Yeast Snu13p and its human homolog 15.5kDa bind to the k-turn motif located at 5'end of U4 snRNA. This interaction is essential for the tri-snRNP (U4/U6, U5) complex formation and U4atac minor spliceosome function in humans. Precise matching between amino acid residues of 15.5 kDA and nucleotides U31, G32, A33, G43, and A44 on U4 snRNA internal loop is required. Internal loop structure is highly conserved within various species, therefore, mutations in these nucleotides abolish the interaction with 15.5 kDa [Vidovic et al, 2000].
15.5 kDa (L7Ae) interacts with BoxC/D and H/ACA k-turns on snoRNAs, hTR RNA.

- *Spliceosomal snoRNA molecules contain BoxC/D or H/ACA motifs*

Splicing is a process that occurs after transcription and allows the introns to be excised and the exons to be joined together [Nilsen, Graveley, 2010]. Splicing takes place in the nucleus with the assistance of spliceosomal complex consisting of small nuclear ribonucleoproteins (snRNPs). Other types of RNA transcripts containing introns which are catalytically active and are capable of being self- spliced are termed ribozymes. In eukaryotic mRNA transcripts, a typical intron contains a donor site at the 5'-end containing highly conserved GU sequence. At the 3'-end of the intron where branch site is located, there is a less conserved GA-rich sequence. Canonical splicing happens in the vast majority of all cases and allows interaction of donor GU and acceptor GA sites, forming a loop or a lariat, that is further excised by means of snRNPs [Nilsen, Graveley, 2010].

Apart from participating in splicing, human 15.5kDa (and yeast Snu3p) is also involved in posttranscriptional modification of ribosomal RNA via the interaction with k-turn motif. This is a k-turn element, typically around 10 nt long containing two highly conserved elements BoxC (A/CTGATGA) and BoxD (CTGA). Primarily, BoxC/D elements are found in snoRNAs, which are short 100 nt long non-coding RNAs residing in the nucleolus and involved in the rRNA processing. H/ACA snoRNAs is another type of snoRNA implicated in posttranslational modification of rRNA. Both elements: BoxC/D and H/ACA meet the standards of archetypical k-turns, and both bind with 15.5kDa protein (human)/L7Ae (archaea), respectively.

Human ribosomal RNAs (18S, 5.8S, and 28S) altogether have approximately 100 2'-O-ribosylmethylated and 100 pseudouridinylated sites. BoxC/D snoRNAs are short circular RNAs with BoxC located close to the 5'end, and BoxD - to the 3'end [Filipowicz et al, 1999]. While BoxC and BoxD sequences are highly conserved, there may be less conserved sequences that still resemble BoxC (A/CTGATGA) and BoxD (CTGA), yet carry some variations in the

structure referred to as BoxC' or D'. BoxC/D snoRNAs perform site-directed ribose 2'-O-methylation of rRNA with the help of protein orchestra, which in human includes 15.5kDa (L7Ae in archaea), Nop56, Nop58, and fibrillarin. Fibrillarin is the effector protein executing methylation. A short sequence, typically of 10-22 nt [Rozhdestvensky et al, 2003], upstream of BoxD/D' is complementary to the target rRNA, thus snoRNA serves as a guide RNA to lead the snRNP complex. The nucleotide which has to be methylated in rRNA is always located 5 nt upstream of BoxD/D'. Here fibrillarin exerts its functions. Ribosomal protein L7Ae is a homologue of 15.5 kDa in archaea with 33% identity and 60% similarity [Rozhdestvensky et al, 2003].

Likewise, H/ACA snoRNA also contains k-turn motif, involved in posttranscriptional rRNA pseudouridylation. H/ACA snoRNAs consist of two stem loops with two linear hinge motifs between them. These hinge regions contain conserved H sequence (ANANNA) and ACA motif. Similarly to BoxC in BoxC/D snoRNA, here H box is also located within the 5'end ofsnoRNA, while ACA motif is located close to the 3'end. H/ACA snoRNA performs similar functions to the BoxC/D complex, initiating the polyprotein assembly and guiding the complex to the required target site on rRNA, which is typically 14-16 nt upstream of ACA element. The effector protein performing the reaction is referred to as dyskerin (DKC1) in humans. Other proteins involved in H/ACA complex assembly include: NHP2 (homolog of archaeal L7Ae), Gar1, and Nop10.

- *Cajal bodies snoRNAs possess both: BoxC/D and H/ACA motifs*

Additionally, BoxC/D and H/ACA motifs were also found in snoRNAs of Cajal bodies involved in post-transcriptional modifications of other spliceosomal snoRNAs (i.e U2 and U5) [Ja et al, 2001; Ja et al, 2002; Ja et al, 2003]. These snoRNAs possess both types of kink-turn motifs at the same time.

- *Telomerase RNA (hTR) contains H/ACA motif on its 3'end*

Interestingly, H/ACA motifs are also localized in the RNA of the telomerase complex [Mitchell et al, 1999]. Telomerase represents a holoprotein complex including: catalytic enzyme subunit serving as a reverse transcriptase (hTERT), telomerase RNA (hTR), and associated protein Telomerase complex. It is required for the chromosome stability, namely, to prevent shortening of 3'-ends of chromosomes which otherwise would be inevitable with every cell division. DNA polymerase can only work from 5'->3' direction; hence only leading strand of DNA can be replicated unceasingly. DNA polymerase requires primers to initiate the synthesis of a complementary strand, which in case of the chromosome ends can be located only on a short sequence of nucleotides. This is possible for maintaining the leader strand (5'->3' end) but not the lagging strand, since there is not enough space for the primers to be located. For this reason, telomerase complex is essential for maintaining the ends of chromosomes by reverse-transcribing them from the template RNA of telomerase complex (hTR).

Deletion of hTR leads to inability of telomerase to maintain the stability of chromosomes, chromosomal shortening, instability, and carcinogenesis [Blasco et al, 1995; Mceachern, Blackburn, 1996; Singer ,Gottschling, 1994]. In mammals hTR is 450nt long and is highly conserved [Blasco et al, 1995]. Notably, hTR contains H/ACA motif at the 3'end [Mitchell, Cheng, Collins, 1999]. Moreover, proteins involved in the interaction with this H/ACA RNA were shown/demonstrated to be essentially the same as those required for the assembly of snRNP complex, which may serve for post-transcriptional modification of either rRNA or snoRNA: dyskerin, Nhp2 (homolog of archaeal L7Ae), Gar1, and Nop10 [Pogac, Filipowicz, 2000]. Although the minimum required elements for the telomerase catalytic activity *in vitro* are hTERT and hTR [Beattie et al, 1998; Weinrich et al, 1997], associated proteins are essential for the stability of telomerase complex *in vivo*, its transportation to telomeres, assembly, and activity.

- *RNA of RNase P contains a kink-turn motif*

Given its role as a pivotal factor in various catalytically active RNP complexes, it is not surprising that k-turn motif was also identified in RNaseP RNA of *Methanococcus maripaludis* (Mma) [Cho et al, 2010]. RNaseP was initially demonstrated to be a *trans*-acting ribozyme operating as endonuclease by Altman and Smith [Altman, Smith, 1971]. The authors discovered that it is capable of processing the 5'end of pre-tRNA. The fact that the RNA of the RNaseP complex has enzymatic activity supported the theory of RNA World, originally proposed by Alexander Rich (Rich, 1962). The RNA molecule of RNaseP complex, termed RPR, was capable of endonuclease activity of tRNA in the presence of Mg^{2+} cations. However, the associated proteins assembling the complex, termed RPPs, play a catalytic role in the enzymatic activity of RPR enabling its work in physiological concentrations of Mg^{2+} within the eukaryotic cell. Archaeal (POP5, RPP21, RPP29, and RPP30) and bacterial [Reiter et al, 2010] associated proteins were shown to be present in considerably lower amount than those of Eukaryotic RNaseP[Jarrous et al, 2010]. Archaeal L7Ae was demonstrated to play a role in the RNaseP function, since after the mutation in nucleotides critical to binding, the enzymatic cleavage of tRNA dropped to less than 1% of its activity [Cho, Lai, 2010]. A putative k-turn motif was also identified although it did not fully satisfy the k-turn structure criteria in the sense that there was rather a bulge than a helix as one of the sides of the angle (conventional kink-turn has a structure of helix-asymmetrical bulge-helix, while here it resembled rather bulge-asymmetrical bulge-helix). The same authors proposed a eukaryotic protein homologous to Archaeal L7Ae, in particular, RPP38, which had the highest similarity with L7Ae out of all others involved in RNase P complex.

- *K-turn of 7SL lncRNA of SRP*

Recently, archaeal L7Ae of *Sulfolobus acidocaldarius* was demonstrated to interact with 7SL lncRNA of Signal Recognition Particle (SRP) [Daume et al, 2017]. Daume et al. have pulled down all RNA precipitated with L7Ae and performed RIP-seq: one of the bound RNA turned out to be 7SL, and a putative k-turn motif for binding was identified.

The signal recognition particle is a ribonucleoprotein complex which consists of a non-coding 7SL RNA and associated proteins which in humans are: SRP9, SRP14, SRP19, SRP54, SRP68, and SRP72. SRP plays a pivotal role in trafficking a wide range of ribosome-nascent chain complexes from being freely dispersed in cytoplasm towards the translocon of endoplasmic reticulum. SRP is operational co-translationally.

7SL RNA is a long non-coding RNA whose structure can be divided into two domains: the one arising after Alu-sequences, Alu-domain, and the other domain–specific for 7SL, or S-domain. Interestingly, Alu-domain is characterized by high conservation throughout all kingdoms of life, for example, the similarity between Alu-domain of human 7SL and that of *Xenopus laevis* is 87%, and with that of Drosophila - 64% [Ullu, Tschudi, 1984]. Alu-domain interacts with SRP9 and SRP14, while less conserved S-domain -with the rest of the protein complex (SRP19, 54, 68, 72).

- *mRNA of L7Ae, fibrillin, Nop5p L30 contain k-turns*

The same study of sequencing RNA precipitates allowed another interesting interaction of archaeal L7Ae protein to be identified. A coordination of L7Ae with its own mRNA was demonstrated providing a negative feedback for the regulation of translation. Furthermore, L7Ae was also interacting with mRNA of fibrillin and Nop5 executing translational control as all of these essential players of sno BoxC/D complex required post-transcriptional modification of rRNA and snoRNA.

Another member of L7Ae family, yeast L30e ribosomal protein also possesses this ability of negative auto-regulation [Mao, White, Williamson, 1999].

- *K-turns occurrence in riboswitches*

Finally, k-turn motifs occur in riboswitches. Riboswitches are naturally occurring regulators of gene expression at posttranscriptional level. They are considered to be an ancient mechanism of influencing gene expression utilized by all three domains of life. Riboswitch is a region (aptamer) of RNA located in its non-coding region, usually 5'-UTR, which is sensitive to the presence of a particular metabolite and serves as its sensor. When the metabolite concentration increases, it can encounter the aptamer on RNA molecule. RNA aptamer is a complexly folded RNA sequence conventionally divided into two functional subunits which can be located either consecutively one after another or possess mutual overlapping. The upstream domain of the aptamer called "sensor" is the one responsible for recognizing and binding with the ligand molecule of a metabolite. This sequence is usually highly conserved among species and possesses high specificity towards the corresponding ligand. The downstream expression domain is the one that undergoes conformational changes after interaction of the sensor with a ligand and thus can affect the gene expression at the posttranscriptional level. Watson-Crick base pair interactions formed in the effector domain upon interaction of the ligand with the sensor, are unlikely to reverse to their non-active state without denaturation even if the ligand detaches from the sensor.

Riboswitches are unique k-turns in the way that they do not require a protein molecule serving as an adaptor hence they can directly bind to the metabolite ligand. The mechanism of action of riboswitches includes terminating transcription and preventing or facilitating translation by either revealing or obscuring ribosomal binding sites due to the RNA complex conformational changes. The first described riboswitches were those that bind to the vitamin derivatives, such as Thiamine pyrophosphate (TPP) (Vitamin B1 derivative), [Winkler, Nahvi, Breaker, 2002], Cobalamin (Vitamin B12) [Nahvi et al, 2002], and Flavin mononucleotide (FMN) [Winkler, 2002] (Vitamin B2 derivative). Thereafter, the plethora of ligands

for riboswitches was expanded to purines and their derivatives (i.e cyclic-diGMP riboswitch), S-adenosylmethionine (SAM), amino acids, theophylline, and cationic ions. However, in eukaryotic cells, TPP riboswitch common for prokaryotes serves for the coordination of alternative splicing rather than gene expression.

L7Ae binds with the following riboswitches, lysC, and SAM Kt [Saito et al, 2010] *in vitro*.

- *Artificial circuits and k-turns*

Kink-turn motifs and interaction of BoxC/D with its protein partner archaeal L7Ae have been widely exploited in synthetic biology. At first, L7Ae-BoxC/D k-turn switch was demonstrated to be beneficial for the translation regulation at post-transcriptional level, resembling the structure and functioning of naturally occurring ribonucleoprotein complexes [Stapleton et al, 2012]. By means of inserting the k-turn domain at the 5'-UTR with a following introduction of the effector protein (L7Ae), Saito et al. managed to create a system for the translation control of any mRNA of interest (Figure 4.2). Further, more complex multilayered circuits enabling regulation of mRNA translation were introduced [Wroblewska et al, 2015].

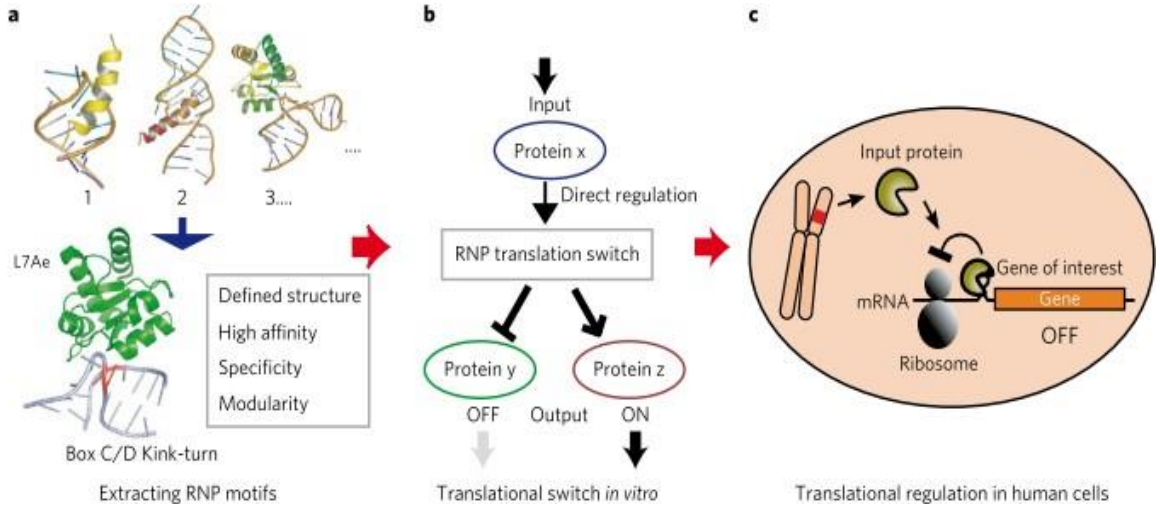

Figure 4.2. Schematic representation of L7Ae-BoxC/D translational ON/OFF switch
Figure is adapted from the reference Saito et al, 2010

To sum up, L7Ae has numerous potential binding partners within the eukaryotic cell. Furthermore, our experiments utilizing L7KK, the mutated form of L7Ae (where two lysine residues of L7Ae (K37A and K79A) are substituted to alanine) to generate VLPs demonstrated that such mutated VLPs could not deliver EGFP/Cas9 as efficiently as VSVG-L7Ae. Given that L7KK has two altered amino acid residues in the domain known to interact with kink-turn motifs, let us hypothesize that the binding may have relied on particular interaction of L7Ae with some endogenous kink-turn motif. Two mutated amino acids (out of 119 of the whole length of L7Ae) and thus drastically altered function suggested evidence towards the specific kink-turn binding rather than some non-specific interaction. As in the latter case, the mutation of two amino acids probably would not play such a key role.

As discussed above there are various endogenous kink-turn motifs occurring in eukaryotic cells. At the same time, we observed that the delivery was mainly mRNA-mediated; therefore, those k-turns mostly located in cytoplasmic RNAs and involved in transcription/ translation (7SL, rRNA k-turns) would be appropriate candidates as L7Ae binding partners. According to the results of RNA-seq, 300 bp- long non-coding 7SL RNA and its isoforms were prevalently enriched in VSVG-L7Ae VLPs (Figure 3.14). 7SL is a part of the Signal Recognition Particle complex carrying the whole composition of mRNA with nascent polysomes to the endoplasmic reticulum. Only secreted proteins were previously thought to be targeted to ER. However, additional research demonstrated that the vast majority of ribosomes with the nascent polypeptide chain in the exit tunnel enters SRP-targeted pathway and reaches ER in HEK293 T cells [Bornemann et al, 2008]. According to all our qRT-PCR experiments, 7SL was also increased and was demonstrated to have a kink-turn in its structure and to interact with L7Ae, at least, in archaeal organisms [Daume et al, 2017]. Despite high conservation of Alu domain of 7SL among species, we did not manage to demonstrate a particular kink-turn to interact with L7Ae in archaea in mammalian 7SL sequence [Daume, 2017].

On top of that, tentative interaction of VSVG-L7Ae with 7SL may be involved in the explanation of the abolished lenti- and retroviral function when pseudocoated with VSVG-L7Ae instead of VSV-G (Figure 3.19). It has long been recognized that retroviruses recruit endogenous RNA, in particular, 30% of RNA within a viral particle is comprised of endogenous RNA [Aronoff, Linial, 1991]. This RNA mass is presented by divergent non-coding RNAs, transcribed by cellular Polymerase III. Importantly, 7SL RNA of SRP is highly enriched in various retroviruses [Faras et al, 1973; Onafuwa-nuga, King, Telesnitsky , 2005]

Although this phenomenon of ncRNA incorporation has been recognized since the pioneer studies in 1970s [Faras et al, 1973], the exact mechanism and the role of this process remain unsolved. Still, it is known that interaction of Alu domain of endogenous 7SL with Gag of retroviral particle is crucial for the retroviral particle assembly [Keene, Telesnitsky, 2012]. Also, within the host mammalian cells Alu domain of 7SL interacts with SRP 9/14 (Figure 1S) nascent proteins of signal recognition particle. Interestingly enough, SRP 14 is among the top of the table of the proteins that are enriched in VSVG-L7Ae VLPs in comparison to VSVG-WT VLPs according to the LC-MS/MS data (Table 3.21).

Taken together that 7SL is known to be crucial for retroviral particles formation, that it interacts with Gag, we can assume that tentative interaction of VSVG-L7Ae with 7SL may have prevented 7SL interaction with Gag and thus retroviral particles formation. Although extremely interesting phenomenon, which we would like to study further, it is still very preliminary hypothesis that, however, may explain abolished retroviral delivery experiment (Figure 3.19).

On the other side, in archaea L7Ae plays a structural role in the large ribosomal subunit where it interacts with the kink-turns of ribosomal RNA [Moore et al, 2004]. Hence another potential candidate for the interaction with L7Ae could be the kink-turn of ribosomal RNA.

Further experiments will be required to identify the exact binding partner. For now, it can be said that VSVG-L7Ae VLP-based delivery system is a non-specific mRNA delivery that does

not require additional modifications of mRNA. It incorporates into VLPs and delivers any mRNAs highly abundant within the producer cell to the recipient cells. Therefore, although the packaging of desired cargo mRNA molecules is considerably more prevalent than that of other molecules (i.e. in CLIP experiment the EGFP mRNA amount was 4-5 times higher than that of GAPDH and ACTB mRNA in VSVG-L7Ae samples in comparison with VSVG-WT samples), some background delivery of the host cellular mRNAs and hence proteins should be taken into account and addressed in the further research.

Conclusion:

Messenger RNA is now being considered a promising therapeutic modality for the vaccine/ dendritic vaccine development, protein-replacement gene therapy, and, of course, genome editing [Kaczmarek, Kowalski, Anderson, 2017]. Therefore, the need to devise an efficient, easy-to-generate delivery tool for mRNA to work within cells is evident. Moreover, we need to have a potential to deliver messenger transcripts *in vivo* and not to be rapidly degraded by serum plasma enzymes, including complement cascade.

During my PhD work, we developed a platform for messenger mRNA delivery via virus-like particles, in particularly, VSVG-L7Ae. These VLPs have a superior performance compared with the currently existing VSVG-WT VLPs platform. The delivery is mRNA-mediated, which was proven by considerable evidence (qRT-PCR of the VLPs, Western blotting of the VLPs, and LC-MS/MS experiments). Surprisingly, incorporating mRNAs into VSVG-L7Ae VLPs was

completely independent of the presence of exogenously cloned cognate RNA motif, a kink-turn BoxC/D. An enhanced enrichment of VSVG-L7Ae VLPs with mRNA of either EGFP or SpCas9 did not require BoxC/D motif in the mRNA sequence. Still, BoxC/D- binding domain of L7Ae was demonstrated to be important for efficient mRNA delivery. Generated with the mutant form of L7Ae (L7KK), VLPs demonstrated a drastically decreased performance in comparison with VSVG-L7Ae VLPs in terms of delivering EGFP and SpCas9 to the target cells. Moreover, an enhanced incorporation of mRNA molecules was achieved through binding of L7Ae domain of VSVG-L7Ae protein to some internal structures, presumably, kink-turn motifs that are highly abundant within the eukaryotic cells. Surprisingly, pseudo-coating of lenti- and retroviral particles with VSVG-L7Ae instead of VSVG-WT abolished the infectivity of retroviral particles. The mechanism of this phenomenon requires further research as it might be helpful to understand retro particles assembly and factors preventing it. Overall, the exact binding partner of VSVG-L7Ae within the mammalian cell should be determined in further works.

Additionally, VSVG-L7Ae system was demonstrated to be effective in transfecting even hard-to-transfect cell lines, in particular, iPS cells and monocytes. It can non-specifically deliver any agent of interest to various cell lines without performing additional complicated cloning. In other words, this system should not be customized depending on the loaded cargo, which makes it universal and easy-to-use. We hope that VSVG-L7Ae VLPs system can be of a considerable interest and become a useful tool for basic research, especially to work with fragile and hard-to-transfect cell lines. It would be exciting to determine the exact binding partner of VSVG-L7Ae as well as to study if free L7Ae can disrupt retroviral assembly.

Concluding, we wish to reiterate: no matter the details and mechanics of the action should be further investigated and perfected the robust transgene delivery via our VSVG-L7Ae mRNA-delivery system opens up new ways for basic research and medicine.

Appendix A

Table 1. Primers sequences used for cloning

Template vector	Primers sequences		Tm
pMS2CP-myc-T2A-tagRFP	Fwd	ccgacttggaaagcttggatccatggcttctaactttactcagttc	55 ℃
	Rev	tgcggccttaaagcttagatctcagatcctcttctgaga	
pcDNA3.1-CMV-L7Ae-myc-His6-pA	Fwd	ccgacttggaaagcttggatccatgtacgtgagatttgaggttcc	54 ℃
	Rev	tgcggccttaaagcttatggtgatggtgatgatgaccg	
pL7KK-myc-T2A-tagRFP	Fwd	aacctcatttccatggacatcacc	56 ℃
	Rev	aagctgggtctagatctaacgcgtcttctgaaggcctttaatcttctcca	
pHL-EF1a-VSVG-L7Ae-myc-His-pA **pHL-EF1a-VSVG-L7KK-myc-pA**	Fwd	aacctcatttccatggacatcacc	55 ℃
	Rev	tggagaagattaaaggccttcagaagacgcgttag	

◦**Table 2**. Oligonucleotides used for cloning

Cloning			Tm
BoxC/D into sgRNA	Fwd	gtacagatctggatcgggcgtgATCcgaaagGtgacccgatcctaggcttaaG	55 ℃
	Rev	CTTAAGCCTAGGATCGGGTCACCTTTCGGATCACGCCCGATCCAGATCTGTAC	
MS2 into sgRNA	Fwd		56 ℃
	Rev	Gcccgggtttgaattcaaaaaaagatgggtgatcctcaccggatcgcaccgactcggtgccacttttcaagtt gataa cggactagccttattttaacttgctatttctagctc	

Table 3. MS2 and BoxC/D sequences

BoxC/D sequence	gggcgtgATCcgaaagGtgaccc
MS2SL sequence	gatccggtgaggatcacccatc

Supplementary

Description of the top entries of mass-spectrometry analysis of VSVG-L7Ae over VSVG-WT VLPs. The top of the list of the highly enriched proteins comprise proteins with RNA-binding properties.

1) YBX1

Although Y-box X (p50)binding protein was initially believed to have specificity for the particular motif (termed Y-box X (5'- CTGATTGGC/TC/TAA-3') on the DNA promoter regions and thus have an influence on the gene expression, it was later reported not to be the case, although the protein itself still remained its name as Y-box binding protein after the corresponding motif. After ChiP-seq experiments, it became evident that Y-Box protein had no preferential specificity to Y-Box DNA motif. Moreover, YB-1 protein appeared to be NF-Y transcription factor [Dolfini, Mantovani, 2013]

Effects of YB-1 protein on transcription are divergent and depend on the characteristics of DNA sequence. If there is a pyrimidine-rich sequence, YBX-1 facilitates involvement of transcription factors with the affinity to ss-DNA [Izumi et al,2001] Oppositely, in case of G-rich sequence of DNA, it promotes association of TF with affinity to ds-DNA [Zasedatelevaet al, 2002] The latter mechanism often the case for the TFs, i.e. E2F which activate genes involved in cellular proliferation and thus carcinogenesis[Lasham et al, 2011].

Also, due to exonuclease activity, YB-1 is engaged in DNA repair, in particular, it restores cross-linked DNA induced by radiation or chemotherapy (i.e. Cisplatin)[Gaudreault et al, 2004]. YB-1 has superior affinity to RNA than to DNA, hence it's defined mainly as RNA-binding protein. YB-1 was found in both spliceosome complexes A-complex, formed with U2 snRNA and pre-mRNA and

B-complex, which includes triRNP (with three various snoRNA U4, U5, U6). [Deckert et al,2006] By way of reviewing, U6 snRNA possesses BoxC/D and H/ACA motifs.

Although YB-1 was reported to participate into splicing, it is far not the key element of spliceosome. YBX-1 is rather considered as regulator of splicing in some mRNAs [Skabkin et al, 2004]

YBX-1 plays a pivotal role translation regulation and mRNA stability. It was observed to be the core protein in RNPs in cytoplasm. YB-1 exerts its effects based on its prevalence in relation to mRNA molecules. If YB-1/ mRNA ratio is low (YB-1 is not exceeding mRNA), then YB-1 facilitates translation by few mechanisms. Firstly, in interacts with duplex structures in 5'-UTR of mRNA with two domains: CTD and CSD (CTD- C-terminal RNA-binding domain, CSD-Cold shock protein RNA-binding domain of YB-1) and promotes dsRNA unwinding [Skabkin et al, 2004]. This enables initiation factors and ribosome binding. On top of that, YB-1 binding of mRNA is critical as it positions the initiation factors towards the 5'-UTR. In *in vitro* experiment in the conditions of absent YB-1 and bare RNA, initiation factors were spread along the mRNA molecule instead of concentrating at the 5'-UTR, and translation was impaired [Evdokimova et al, 1998]

In contrary to these effects, when YB-1 concentration is abundant and ratio YB-1/mRNA is high, YB-1 rather disables translation and ensures mRNA stability. With its CSD domain it remains bound to mRNA at the 5'UTR while with the other domains it forms multimeric complex with either YB-1 molecules, thus forming RNP. RNA with such YB-1 RNP complex is not accessible for initiation factors. In particular, YB-1 prevents eIF4G and PABP binding, inhibiting translation and stabilizing mRNA [Evdokimova et al, 2001].

2) RPL22

Ribosomal protein L22 is one of the major proteins, which constitute the big 60S in eukaryotes/40S in prokaryotes ribosomal subunit. This is the only ribosomal protein which

interacts with all 6 binding sites of 23s rRNA. [Ban et al, 2000, Selmer et al 2006]

L22 together with L4 form the walls of the channel used for the exit of polypeptide chain. Both of these proteins have multiple extensions and loops with which they interact with 23s rRNA and participate in the peptide exit tunnel structuring. Therefore, it has been suggested that they might have played a role into large ribosomal subunit assembly or affect polypeptide chain leaving the ribosome. However, it was shown not to be the case since: neither assembly, nor translation were affected in ribosomes formed with L22 and L4 with diminished extensions [Zengel et al, 2003].

In prokaryotes, another protein L23e is involved in the formation of the corridor for peptide chain exit. It was observed that acquired resistance to erythromycin is caused by bacterial mutations in L22. Indeed, mutations of L22 three amino acid residues in vitro lead to the development of such resistance [Davydova et al, 2002].

In addition to structural function in ribosome formation, L22 may play a role in the telomerase complex stability. By mean of review, telomerase a ribonucleoprotein that is comprised of the catalytically active protein with reverse transcriptase properties (hTERT) and 390-450 nt RNA (hTR) which serves as a template for replication of 3'ends of chromosomes (discussed in the introduction). In addition to the telomerase associated proteins which are required for the complex stability and transportation (dyskerin, Nhp2 (homolog of archaeal L7Ae), Gar1, and Nop10, it was also shown to interact with L22 [Le , Sternglanz, Greider, 2000]. In fact, L22 has been observed to localize in nucleoli [Materat, Wardt, Steitztf, 1994].

Taking into account notion that hTR is also located in the nucleus and possesses H/ACA motif [Mitchell, Cheng, Collins, 1999], Le et al demonstrated interaction of L22 and telomerase, suggesting that ribosomal protein plays here extra-ribosomal functions for RNA processing and stability

3) PABPC1c

Poly-adenylate binding proteins (PABP) is a group of ubiquitously expressed protein which play crucial role in translation regulation. The prototypic member of the family and the one which has been studies the most, is PABPC1. PABP consists of four RNA-recognition motifs (RRM), located at the N-terminal end of the protein, proline-rich linker, and C-terminal domain, located on the C-terminal end. All RRMs have increased affinity to AU-rich RNA-regions although specificity of RRM1 was reported to be the highest. [Resch, Holtmann, 2003; Sladic 2003].

Affinity towards AU-rich RNA regions enable PABPC1 proteins to interact with poly-A tail of mRNA. Proline-rich linker is required for the homodimerization of protein, while C-terminal domain is essential to cooperate with other proteins involved in translation initiation. Although PABPC1 binds to 3'-end of mRNA it still can be found in a close proximity to 5' m7G-Cap regions due to the protein-protein interactions PABPC1 is involved in. In particular, it coordinates with eIF4G to form a close-loop structure This collaboration between eIF4G and PAPBP1 is highly conserved. [Wilkie, Dickson, Gray, 2003]

Such configuration facilitates translation initiation. To be more precise, this promotes the small ribosomal subunit 40S recruitment [Tarun, Sachs, 1995].

Additional lines of evidence suggest that it also affects big ribosomal subunit (60S) binding [Brook et al, 2009]. PABP1 is located predominantly in the cytoplasm [Gorlach, Burd, Dreyfuss, 1994], although has been reported to shuttle to the nucleus[Afonina, Stauber, Pavlakis, 1998] where PABP family of proteins assist in poly-adenylation of newly-transcribed pre-mRNA. In addition to crucial role in translation initiation, PABPC1 is also involved in translation termination as it was reported to interact with eRF3. eRF3 activates eRF1 which promotes termination of translation. On top of that, some reports suggest that PABP1 interaction with eRF3 facilitates ribosome recycling with further repeated usage in translation [Uchida, Hoshino, 2002].

4) SYNCRIP

SYNCRIP (synaptotagmin binding, cytoplasmic RNA-interacting protein) (mouse) [Mizutani et al, 2000] or NSAP1 (humans) [Harris, Boden, Astell, 1999] is RNA-binding protein which similarly to PABP1 possesses high affinity to A/U-rich sequences of RNA. It binds to polyA-tail in a phosphorylation –dependent manner. SYNCRIP was reported to be bound with other RNA-binding protein, predominantly, with ribosomal proteins. The main role attributed to SYNCRIP is mRNA stabilization [Ikegami , Inoue, Mikoshiba, 2004]. However, in the immunoprecipitated complex of SYNCRIP bound to ribosomal proteins, there was no L22 found which suggests that L22 is not incorporated into VLP due to the interaction with SYNCRIP (and vice versa).

5) SRP14

7SL is a long non-coding RNA, which serves as a scaffold for the formation of Signal Recognition Particle RNP complex. 7SL, or SRP RNA, is 301 nt long, and can be divided into 3 domains: left-sided Alu domain, which remains highly conserved among species, right-sided S domain, which is specific for divergent species, and a hinge domain in the middle. In eukaryotes, SRP is formed via the assembly of 7SL with 6 proteins. Two of these proteins, SRP9 and SRP14, form a heterodimer (SRP9/14) and interact with Alu domain of 7SL, while the rest of the proteins, namely, SRP 19, 54,68, 72 binds with S-domain of 7SL. From the latter protein, SRP 68/72 also form heterodimeric complex, but SRP 19 and 54 are monomeric. Noteworthy, SRP 54 is conserved best throughout evolution and plays a major role of cooperating with the receptor for SRP, which located in translocon of ER (Sec61 in eukaryotes). It also differs from other proteins in that sense that requires SRP 19 for binding with nascent 7SL, while all of the other proteins can interact directly with 7SL. (Figure S1)

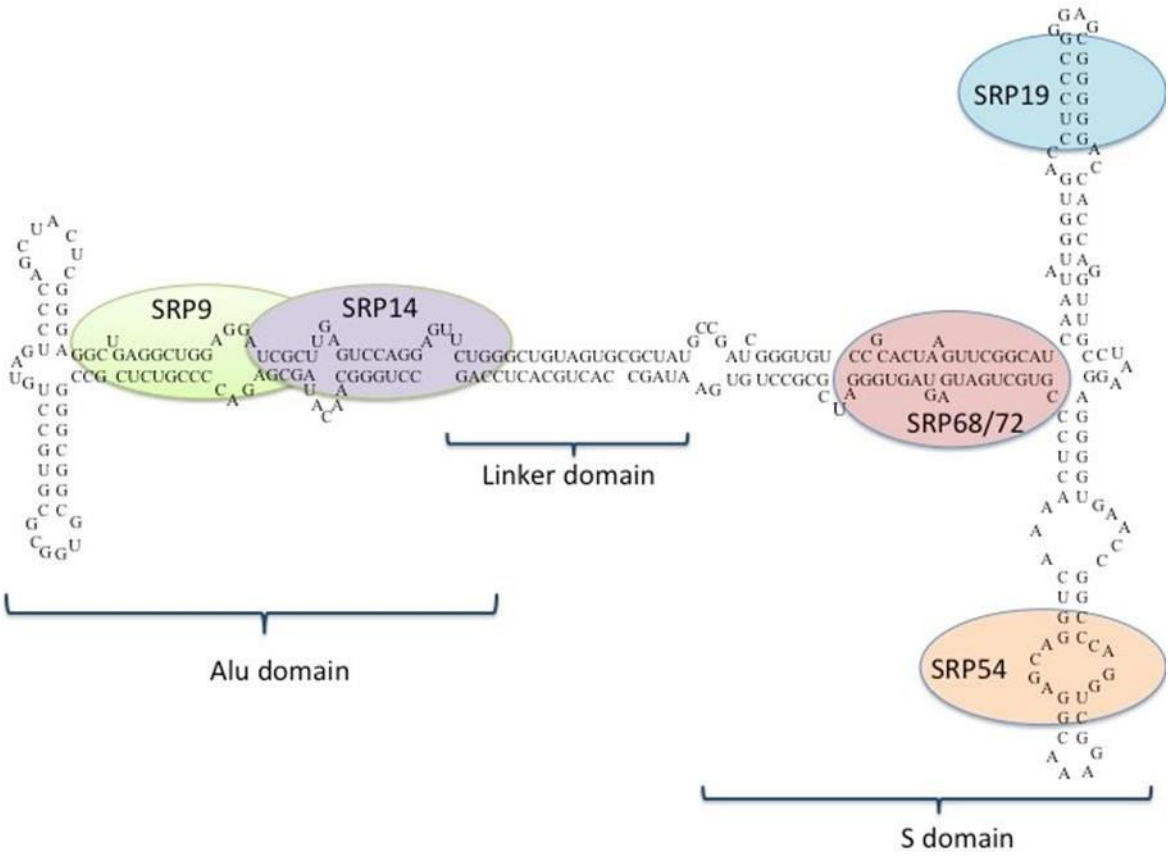

Figure S1 Structure of 7SL and associated proteins of SRP

Hydrophobic signal sequence [Martoglio, 1998] (hydrophobic anchor) is common for all proteins which are transmembrane, supposed to be secreted or localized into certain organelle (for example, lysosome). In other words, this sequence serves as a signal for its counterpart, signal recognition particles, that the protein should be delivered to the translocon, a special protein complex, of the endoplasmic reticulum, which would further distribute and transport the proteins to their final destination. Despite this pathway of trafficking proteins towards ER is common for all kingdoms of life, there is no universal signal sequence, rather its constructions resemble certain patterns. In most cases signal sequence is located on the N-terminal end of a polypeptide chain. It has 6-15 hydrophobic amino acid residues in the middle [Martoglio, 1998] On the N-terminal end, a variable in length

group of amino acid residues[Von Heijne, 1985] positioned. Usually, this region is polar and positively charged. The group of amino acid residues located closer to the C-terminal end from the hydrophobic core is hydrophilic and contain a cleavage site for the signal sequence to be trimmed from the protein.

Bibliography

Abraham A, U. Natraj, A.A. Karande, A. Gulati, M.R.N. Murthy, S. Murugesan, P. Mukunda, H.S. Savithri, Intracellular delivery of antibodies by chimeric Sesbania mosaic virus (SeMV) virus like particles, Sci. Rep. 6 (2016) 1–12. doi:10.1038/srep21803

Accola MA, B. Strack, Efficient Particle Production by Minimal Gag Constructs Which Retain the Carboxy-Terminal Domain of Human Immunodeficiency Virus Type 1 Capsid-p2 and a Late Assembly Domain, 74 J.Virol, (2000) 5395–5402.

Afonina E, R. Stauber, G.N. Pavlakis, The Human Poly (A) -binding Protein 1 Shuttles between the Nucleus and the Cytoplasm, JBC, 273 (1998) 13015–13021.

Altman S, J.D. Smith, Tyrosine tRNA precursor molecule polynucleotide sequence, Nat. New Biol. 233 (1971) 35–39. doi:10.1038/newbio233035a0.

Amin A, A.Z. Dudek, T.F. Logan, R.S. Lance, J.M. Holzbeierlein, J.J. Knox, V.A. Master, S.K. Pal, W.H. Miller Jr, L.I. Karsh, I.Y. Tcherepanova, M.A. DeBenedette, W.L. Williams, D.C. Plessinger, C.A. Nicolette, R.A. Figlin, Survival with AGS-003, an autologous dendritic cell-based immunotherapy, in combination with sunitinib in unfavorable risk patients with advanced renal cell carcinoma (RCC): Phase 2 study results, J. Immunother. Cancer. 3 (2015) 14. doi:10.1186/s40425-015-0055-3.

Andries O, S. Mc Cafferty, S.C. De Smedt, R. Weiss, N.N. Sanders, T. Kitada, N1-methylpseudouridine-incorporated mRNA outperforms pseudouridine- incorporated mRNA by providing enhanced protein expression and reduced immunogenicity in mammalian cell lines and mice, J. Control. Release. 217 (2015) 337–344. doi:https://doi.org/10.1016/j.jconrel.2015.08.051.

Aronoff R, M. Linial, Specificity of Retroviral RNA Packaging, Journal of virology, 65 (1991) 71–80.

Ban N, P. Nissen, J. Hansen, P.B. Moore, T.A. Steitz, The complete atomic structure of the large ribosomal subunit at 2.4 Å resolution, Science. 289 (2000) 905–920. doi:10.1126/science.289.5481.905.

Beattie TL, W. Zhou, M.O. Robinson, L. Harrington, Reconstitution of human telomerase activity in vitro, Current Biology, 1998, 177–180.

Bernal JA. RNA-based tools for nuclear reprogramming and lineage-conversion: towards clinical applications. J Cardiovasc Transl Res. 2013, 6:956-68

Blasco MA, W. Funk, B. Villeponteau, I lwolrmna Functional Characterization and Developmental Regulation of Mouse Telomerase RNA, Science (1995) 3–6.

Boczkowski D, S.K. Nair, D. Snyder, E. Gilboa, Dendritic cells pulsed with RNA are potent antigen-presenting cells in vitro and in vivo, J. Exp. Med. 184 (1996) 465–472.

https://www.ncbi.nlm.nih.gov/pubmed/8760800.

Boldin MP, K.D. Taganov, D.S. Rao, L. Yang, J.L. Zhao, M. Kalwani, Y. Garcia-flores, M. Luong, A. Devrekanli, J. Xu, G. Sun, J. Tay, P.S. Linsley, miR-146a is a significant brake on autoimmunity , myeloproliferation , and cancer in mice, JEM, 208 (2011). doi:10.1084/jem.20101823.

Bornemann T, J. Jöckel, M. V. Rodnina, W. Wintermeyer, Signal sequence- independent membrane targeting of ribosomes containing short nascent peptides within the exit tunnel, Nat. Struct. Mol. Biol. 15 (2008) 494–499. doi:10.1038/nsmb.1402.

Brook M, J.W.S. Smith, N.K. Gray, The DAZL and PABP families: RNA-binding proteins with interrelated roles in translational control in oocytes, Reproduction, 2009.,

Caldeira J, J. Bustos, J. Peabody, B. Chackerian, D.S. Peabody, Epitope-specific anti-hCG vaccines on a virus like particle platform, PLoS One. 10 (2015) 1–11. doi:10.1371/journal.pone.0141407.

Cao F, X. Xie, T. Gollan, L. Zhao, K. Narsinh, R.J. Lee, J.C. Wu, Comparison of Gene-Transfer Efficiency in Human Embryonic Stem Cells, (2010) 15–24. doi:10.1007/s11307-009-0236-x.

Chen CY, P. Sarnow, Initiation of protein synthesis by the eukaryotic translational apparatus on circular RNAs, Science. 268 (1995) 415 LP- 417. doi:10.1126/science.7536344.

Cho LM, L.B. Lai, D. Susanti, B. Mukhopadhyay, V. Gopalan, Ribosomal protein L7Ae is a subunit of archaeal RNase P, Proc. Natl. Acad. Sci. 107 (2010) 14573–14578. doi:10.1073/pnas.1005556107.

Cooper A, Y. Shaul, Recombinant viral capsids as an efficient vehicle of oligonucleotide delivery into cells, Biochem. Biophys. Res. Commun. 327 (2005) 1094–1099. doi:10.1016/j.bbrc.2004.12.118.

Crossey E, M.J.A. Amar, M. Sampson, J. Peabody, J.T. Schiller, B. Chackerian, D. Weinberg, K.E. Baker, B.R. Graveley, J. Coller, Codon optimality is a major determinant of mRNA stability, Cell. 160 (2015) 1111–1124. doi:10.1016/j.cell.2015.02.029.

D'Astolfo DS, R.J. Pagliero, A. Pras, W.R. Karthaus, H. Clevers, V. Prasad, R.J. Lebbink, H. Rehmann, N. Geijsen, Efficient Intracellular Delivery of Native Proteins, Cell. 161 (2015) 674–690. doi:10.1016/j.cell.2015.03.028.

Daume M, M. Uhl, R. Backofen, L. Randau, RIP-Seq Suggests Translational Regulation by L7Ae in Archaea, MBio, 8 (2017) e00730- 17. doi:10.1128/mBio.00730-17.

Davydova N, V. Streltsov, M. Wilce, A. Liljas, M. Garber, L22 Ribosomal Protein and Effect of Its Mutation on Ribosome Resistance to Erythromycin, JMB, 2836 (2002) 635–644. doi:10.1016/S0022-2836(02)00772-6.

Deckert J, K. Hartmuth, D. Boehringer, N. Behzadnia, C.L. Will, B. Kastner, H. Stark, H. Urlaub, R. Lu, Protein Composition and Electron Microscopy Structure of Affinity-Purified Human Spliceosomal B Complexes Isolated under Physiological Conditions, Molecular and Cellular Biology, 26 (2006) 5528–5543. doi:10.1128/MCB.00582-06.

Dolfini D, R. Mantovani, Targeting the Y / CCAAT box in cancer : YB-1 (YBX1) or NF-Y?, Cell Death and Differentiation (2013), 676–685. doi:10.1038/cdd.2013.13.

Doudna J.A, E. Charpentier, The new frontier of genome engineering with CRISPR-Cas9, Science 346(6213):1258096 (2014).

Endo K, J.A. Stapleton, K. Hayashi, H. Saito, T. Inoue, Quantitative and simultaneous

translational control of distinct mammalian mRNAs, Nucleic Acids Res. 41 (2013)

Essandoh K, L. Yang, X. Wang, W. Huang, D. Qin, Blockade of exosome generation with GW4869 dampens the sepsis-induced inflammation and cardiac dysfunction. Biochim Biophys Acta. 2015 Nov;1852(11):2362-71. doi: 10.1016/j.bbadis.2015.08.010.

Evdokimova V, P. Ruzanov, H. Imataka, B. Raught, Y. Svitkin, L.P. Ovchinnikov, N. Sonenberg, The major mRNA-associated protein YB-1 is a potent 5' cap-dependent mRNA stabilizer, The EMBO, 20 (2001) 5491–5502.

Evdokimova VM, E.A. Kovrigina, D. V Nashchekin, E.K. Davydova, J.W.B. Hershey, L.P. Ovchinnikov, The Major Core Protein of Messenger Ribonucleoprotein Particles (p50) Promotes Initiation of Protein Biosynthesis in Vitro, JBC, 273 (1998) 3574–3581.
F. Zhang, In vivo interrogation of gene function in the mammalian brain using CRISPR-Cas9, Nat. Biotechnol. 33 (2015) 102–106. doi:10.1038/nbt.3055.
Faras AJ, A.C. Garapin, W.E. Levinson, J.M. Bishop, H.M. Goodman, Characterization of the Low-Molecular-Weight RNAs Associated with the 70S RNA of Rous Sarcoma Virus, Journal of Virology, 12 (1973) 334–342

Fawell S, J.O.E. Seery, Y. Daikh, C. Moore, L.L. Chen, B. Pepinsky, Tat- mediated delivery of heterologous proteins into cells, Proc Natl Acad Sci U S A. 1994 Jan 18;91(2):664-8. 91 (1994) 664–668.

Filipowicz W, P. Pelczar, V. Pogacic, F. Dragon, Structure and biogenesis of small nucleolar RNAs acting as guides for ribosomal RNA modification, Acta Biochim. Pol. 46 (1999) 377–389.

Fotin-Mleczek M, K.M. Duchardt, C. Lorenz, R. Pfeiffer, S. Ojkic-Zrna, J. Probst, K.-J. Kallen, Messenger RNA-based Vaccines With Dual Activity Induce Balanced TLR-7 Dependent Adaptive Immune Responses and Provide Antitumor Activity, J. Immunother. 34 (2011).

Fusaki, N., Ban, H., Nishiyama, A., Saeki, K., & Hasegawa, M. (2009). Efficient induction of transgene-free human pluripotent stem cells using a vector based on Sendai virus, an RNA virus that does not integrate into the host genome. Proceedings of the Japan Academy. Series B, Physical and Biological Sciences, 85, 348.

Gaj T, D.S. Ojala, F.K. Ekman, L.C. Byrne, P. Limsirichai, D. V Schaffer, In vivo genome editing improves motor function and extends survival in a mouse model of ALS, Sci. Adv. 3 (2017) doi:10.1126/sciadv.aar3952.

Garcea RL, L. Gissmann, Virus-like particles as vaccines and vessels for the delivery of small molecules, Curr. Opin. Biotechnol. 15 (2004) 513–517. doi:10.1016/j.copbio.2004.10.002.

Garg AD, P.G. Coulie, B.J. Van den Eynde, P. Agostinis, Integrating Next- Generation Dendritic Cell Vaccines into the Current Cancer Immunotherapy Landscape, Trends Immunol. 38 (2017) 577–593. doi:10.1016/j.it.2017.05.006.

Gaudreault I, D. Guay, M. Lebel, M. Street, YB-1 promotes strand separation in vitro of duplex DNA containing either mispaired bases or cisplatin modifications , exhibits endonucleolytic activities and binds several DNA repair proteins, Nucleic Acids Research (2004) 316–327.

Gleiter S, H. Lilie, Coupling of antibodies via protein Z on modified polyoma virus-like particles., Protein Sci. 10 (2001) 434–444. doi:10.1110/ps.31101.

Gorlach M, G.C.Burd, G.Dreyfuss.The mRNA poly(A)- binding protein: Localization, Abundance, and RNA-binding Specificity, Experimental Cell Research, (1994).

Grundy FG, T.M. Henkin, The S box regulon : a new global transcription termination control system for methionine and cysteine biosynthesis genes in Gram-positive bacteria, Mol

Microbiol. (1998) 737–749.

H. Yin, G. Gao, C. Mueller, T.R. Flotte, W. Xue, In Vivo Genome Editing Partially Restores Alpha1-Antitrypsin in a Murine Model of AAT Deficiency, Hum. Gene Ther. 29 (2018) 853–860. doi:10.1089/hum.2017.225.

Hamann MV, N. Stanke, E. Müllers, K. Stirnnagel, S. Hütter, B. Artegiani, S. Bragado Alonso, F. Calegari, D. Lindemann, Efficient transient genetic manipulation in vitro and in vivo by prototype foamy virus-mediated non-viral RNA transfer, Mol. Ther. 22 (2014) 1460–1471. doi:10.1038/mt.2014.82.

Hara T, H. Saito, T. Inoue, Directed evolution of a synthetic RNA–protein module to create a new translational switch, Chem. Commun. 49 (2013) 3833. doi:10.1039/c3cc38688k.

Harris CE, R.A. Boden, C.R. Astell, A Novel Heterogeneous Nuclear Ribonucleoprotein-Like Protein Interacts with NS1 of the Minute Virus of Mice, Journal of Virology, 73 (1999) 72–80.

Harrison MS, T. Sakaguchi, A.P. Schmitt, Paramyxovirus assembly and budding: Building particles that transmit infections, Int. J. Biochem. Cell Biol. 42 (2010) 1416–1429. doi:10.1016/j.biocel.2010.04.005.

Heil F, H. Hemmi, H. Hochrein, F. Ampenberger, S. Akira, G. Lipford, H. Wagner, S. Bauer, Species-Specific Recognition of Single-Stranded RNA via Toll-like Receptor 7 and 8. Science. 2004 Mar 5;303(5663):1526-9. Epub 2004 Feb 19.

Hsu FJ, C. Benike, F. Fagnoni, T.M. Liles, D. Czerwinski, B. Taidi, E.G. Engleman, R. Levy, Vaccination of patients with B–cell lymphoma using autologous antigen–pulsed dendritic cells, Nat. Med. 2 (1996) 52. https://doi.org/10.1038/nm0196-52.

https://slideplayer.com/slide/13806387/

Huggett J, K. Dheda, S. Bustin, A. Zumla, Real-time RT-PCR normalisation; strategies and considerations, Genes Immun. 6 (2005) 279–284. doi:10.1038/sj.gene.6364190.

Hung ME, J.N. Leonard, A platform for actively loading cargo RNA to elucidate limiting steps in EV-mediated delivery, J. Extracell. Vesicles. 5 (2016) 31027. doi:10.3402/jev.v5.31027.

Ikegami T, T. Inoue, K. Mikoshiba, An RNA-interacting Protein , SYNCRIP (Heterogeneous Nuclear Ribonuclear Protein Q1/NSAP1) Is a Component of mRNA Granule Transported with Inositol 1 , 4 , 5-Trisphosphate Receptor Type 1 mRNA in Neuronal Dendrites, JBC, 279 (2004) 53427–53434. doi:10.1074/jbc.M409732200.

Iliakis, G., et al., Mechanisms of DNA double strand break repair and chromosome aberration formation. Cytogenet Genome Res, 2004. 104(1-4): p. 14-20.

Izumi H, T. Imamura, G. Nagatani, T. Ise, T. Murakami, H. Uramoto, T. Torigoe, H. Ishiguchi, Y. Yoshida, M. Nomoto, T. Okamoto, T. Uchiumi, M. Kuwano, K. Funa, K. Kohno, Y box-binding protein-1 binds preferentially to single-stranded nucleic acids and exhibits 3 ′ → 5 ′ exonuclease activity, Nucleic Acids Research, 29 (2001) 1200–1207.

Ja AE, A small nucleolar guide RNA functions both in 2'- O -ribose methylation and pseudouridylation of the U5 spliceosomal RNA,The EMBO Journal (2001) 20, 541-551

Ja AE, X. Darzacq, Â. Verheggen, A.M. Kiss, E. Bertrand, Cajal body-specific small nuclear RNAs : a novel class of 2' - O -methylation and pseudouridylation guide RNAs, The EMBO Journal (2002) 21, 2746-2756

Ja AE, X. Darzacq, K.E. Tucker, A.G. Matera, E. Bertrand, Modification of Sm small nuclear RNAs occurs in the nucleoplasmic Cajal body following import from the cytoplasm EMBO J.

2003 Apr 15; 22(8): 1878–1888.

Jarrous N, V. Gopalan, Archaeal / Eukaryal RNase P : subunits , functions and RNA diversification, Nucleic Acid Research, 38 (2010) 7885–7894. doi:10.1093/nar/gkq701.

John S, O. Yuzhakov, A. Woods, J. Deterling, K. Hassett, C.A. Shaw, G. Ciaramella, Multi-antigenic human cytomegalovirus mRNA vaccines that elicit potent humoral and cell-mediated immunity, Vaccine. 36 (2018) 1689–1699.

Kaczmarek J.C, P.S. Kowalski, D.G. Anderson, Advances in the delivery of RNA therapeutics : from concept to clinical reality, Genome Medicine (2017) 1–16. doi:10.1186/s13073-017-0450-0.

Keene SE, A. Telesnitsky, cis-acting Determinants of 7SL RNA Packaging by HIV-1, Journal of virology, 86 (2012) 7934–7942. doi:10.1128/JVI.00856-12.

Klein DJ, T.M. Schmeing, P.B. Moore, T.A. Steitz, The kink-turn: A new RNA secondary structure motif, EMBO J. 20 (2001) 4214–4221. doi:10.1093/emboj/20.15.4214.

Koido S, M. Kashiwaba, D. Chen, S. Gendler, D. Kufe, J. Gong, Induction of Antitumor Immunity by Vaccination of Dendritic Cells Transfected with MUC1 RNA, J. Immunol. 165 (2000) 5713 LP-5719.

Kormann MSD, G. Hasenpusch, M.K. Aneja, G. Nica, A.W. Flemmer, S. Herber-Jonat, M. Huppmann, L.E. Mays, M. Illenyi, A. Schams, M. Griese, I. Bittmann, R. Handgretinger, D. Hartl, J. Rosenecker, C. Rudolph, Expression of therapeutic proteins after delivery of chemically modified mRNA in mice, Nat. Biotechnol. 29 (2011) 154. https://doi.org/10.1038/nbt.1733.

Ladell K, E. Gostick, K. Vermeulen, K. Pieters, G. Nijs, B. Stein, E.L. Smits, Kaczmarczyk SJ, K. Sitaraman, H. a Young, S.H. Hughes, D.K. Chatterjee, Protein delivery using engineered virus-like particles, Pnas. 108 (2011) 16998– 17003. doi:10.1073/pnas.1101874108/

Lasham A, W. Samuel, H. Cao, R. Patel, R. Mehta, J.L. Stern, G. Reid, A.G. Woolley, L.D. Miller, M.A. Black, A.N. Shelling, C.G. Print, A.W. Braithwaite, YB-1, the E2F Pathway , and Regulation of Tumor Cell Growth, JNCI (2011) 133– 146. doi:10.1093/jnci/djr512.

Le S, R. Sternglanz, C.W. Greider, Identification of Two RNA-binding Proteins Associated with Human Telomerase RNA, Molecular biology of the cell, 11 (2000) 999–1010.

Leonhardt C., G. Schwake, T.R. Stögbauer, S. Rappl, J.T. Kuhr, T.S. Ligon, J.O. Rädler, Single-cell mRNA transfection studies: Delivery, kinetics and statistics by numbers, Nanomedicine Nanotechnology, Biol. Med. 10 (2014) 679–688. doi:10.1016/j.nano.2013.11.008.

Li HL, N. Fujimoto, N. Sasakawa, S. Shirai, T. Ohkame, T. Sakuma, M. Tanaka, N. Amano, A. Watanabe, H. Sakurai, T. Yamamoto, S. Yamanaka, A. Hotta, Precise correction of the dystrophin gene in duchenne muscular dystrophy patient induced pluripotent stem cells by TALEN and CRISPR-Cas9, Stem Cell Reports. 4 (2015) 143–154. doi:10.1016/j.stemcr.2014.10.013.

Li X, M.T. Brooks, S. Dharmaiah, A.B. Herr, C. Kao, P. Li, The RIG-I-like Receptor LGP2 Recognizes the Termini of double-stranded RNA, J Biol Chem, 284 (2009) 13881–13891. doi:10.1074/jbc.M900818200.

Li, L, Chen, X. and Li, Y. (2010), MicroRNA-146a and Human Disease. Scandinavian Journal of Immunology, 71: 227-231. doi:10.1111/j.1365-3083.2010.02383.x

Lin G, Y. Han, J. Li, Novel miR-122 delivery system based on MS2 virus like particle surface displaying cell-penetrating peptide TAT for hepatocellular carcinoma, Oncotarget. 7 (2016) 59402–59416. doi:10.18632/oncotarget.10681.

Long C, L. Amoasii, A.A. Mireault, J.R. McAnally, H. Li, E. Sanchez-Ortiz, S. Bhattacharyya, J.M. Shelton, R. Bassel-Duby, E.N. Olson, Postnatal genome editing partially restores dystrophin expression in a mouse model of muscular dystrophy, Science. 351 (2016) 400–403. doi:10.1126/science.aad5725.

MKotaka, T. Takaki, M. Umeda, C. Okubo, M. Nishikawa, A. Oishi, M. Narita, M. Way, G. Schiavo, C. Reis, Activation of MDA5 Requires Higher-Order RNA Structures Generated during Virus Infection , Journal of Virology. 83 (2009) 10761–10769. doi:10.1128/JVI.00770-09.

Mangeot P.E, S. Dollet, M. Girard, C. Ciancia, S. Joly, M. Peschanski, V. Lotteau, Protein Transfer Into Human Cells by VSV-G-induced Nanovesicles, Mol. Ther. 19 (2011) 1656–1666. doi:10.1038/mt.2011.138.

Mao H, S.A. White, J.R. Williamson, A novel loop-loop recognition motif in the yeast ribosomal protein L30 autoregulatory RNA complex, Nat. Struct. Biol. 6 (1999) 1139–1147. doi:10.1038/70081.

Martoglio B, Signal sequences : more than just greasy peptides, Trends in Cell Biology, 8 (1998) 14119– 14123.

Materat AG, D.C. Wardt, J.A. Steitztf, The Epstein-Barr virus (EBV) small RNA EBER1 binds and relocalizes ribosomal protein L22 in EBV-infected human B lymphocytes, PNAS, 91 (1994) 3463–3467.

Mceachern MJ, E.H. Blackburn, Cap-prevented recombination between terminal telomeric repeat arrays (telomere CPR) maintains telomeres in Kluyveromyces lactis lacking telomerase, Genes and development, (1996) 1822–1834.

Miki K, K. Endo, S. Takahashi, S. Funakoshi, I. Takei, S. Katayama, T. Toyoda,

Mitchell JR, J. Cheng, K. Collins, A Box H / ACA Small Nucleolar RNA-Like Domain at the Human Telomerase RNA 3' End, Molecular and Cellular Biology Jan 1999, 19 (1) 567-576
Miyashita I, K. Asano, K. Hayashi, K. Osafune, S. Yamanaka, H. Saito, Y. Yoshida, Efficient Detection and Purification of Cell Populations Using Synthetic MicroRNA Switches, Cell Stem Cell. 16 (2015) 699–711. doi:10.1016/j.stem.2015.04.005.

Mizutani A, M. Fukuda, K. Ibata, Y. Shiraishi, K. Mikoshiba, SYNCRIP , a Cytoplasmic Counterpart of Heterogeneous Nuclear Ribonucleoprotein R , Interacts with Ubiquitous Synaptotagmin Isoforms, JBC, 275 (2000) 9823–9831.

Monroe EB, S. Kang, S.K. Kyere, R. Li, P.E. Prevelige, Hydrogen/Deuterium Exchange Analysis of HIV-1 Capsid Assembly and Maturation, Structure. 18 (2010) 1483–1491. doi:https://doi.org/10.1016/j.str.2010.08.016.

Moolten FL, Tumor Chemosensitivity Conferred by Inserted Herpes Thymidine Kinase Genes : Paradigm for a Prospective Cancer Control Strategy Tumor Chemosensitivity Conferred by Inserted Herpes Thymidine Kinase Genes : Paradigm for a Prospective Cancer Control Strategy, Cancer Res. 1986 Oct; 46(10):5276-81. (1986) 5276–5281.

Moore T, Y. Zhang, M.O. Fenley, H. Li, Molecular basis of box C/D RNA- protein interactions: Cocrystal structure of archaeal L7Ae and a box C/D RNA, Structure. 12 (2004) 807–818. doi:10.1016/j.str.2004.02.033.

Moreno AM, P. Mali, Therapeutic genome engineering via CRISPR-Cas systems, Wiley Interdiscip. Rev. Syst. Biol. Med. 9 (2017) e1380. doi:10.1002/wsbm.1380.

Müllers E, The Foamy Virus Gag Proteins: What Makes Them Different?, Viruses. (2013)

1023–1041. doi:10.3390/v5041023.

Nahvi A, N. Sudarsan, M.S. Ebert, X. Zou, K.L. Brown, R.R. Breaker, Genetic control by a metabolite binding mRNA, Chem. Biol. 9 (2002) 1043–1049. doi:10.1016/S1074-5521(02)00224-7.

Nelson CA, C.H. Hakim, D.G. Ousterout, P.I. Thakore, E.A. Moreb, R.M. Castellanos Rivera, S. Madhavan, X. Pan, F.A. Ran, W.X. Yan, A. Asokan, F. Zhang, D. Duan, C.A. Gersbach, In vivo genome editing improves muscle function in a mouse model of Duchenne muscular dystrophy, Science. 351 (2016) 403–407. doi:10.1126/science.aad5143.

Nilsen TW, B.R. Graveley, Expansion of the eukaryotic proteome by alternative splicing, Nature. 463 (2010) 457. https://doi.org/10.1038/nature08909.

Nishishita, N., Takenaka, C., Fusaki, N., & Kawamata, S. (2011). Generation of human induced pluripotent stem cells from cord blood cells. Journal of Stem Cells, 6, 10
Onafuwa-nuga, S.R. King, A. Telesnitsky, Nonrandom Packaging of Host RNAs in Moloney Murine Leukemia Virus, Journal of virology, 79 (2005) 13528–13537. doi:10.1128/JVI.79.21.13528.
P. Mukunda, H.S. Savithri, Intracellular delivery of antibodies by chimeric Sesbania mosaic virus (SeMV) virus like particles, Sci. Rep. 6 (2016) 1–12. doi:10.1038/srep21803.

Pan Y, T. Jia, Y. Zhang, K. Zhang, R. Zhang, J. Li, L. Wang, MS2 VLP-based delivery of microRNA-146a inhibits autoantibody production in lupus-prone mice, Int. J. Nanomedicine. 7 (2012) 5957–5967. doi:10.2147/IJN.S37990.

Pan Y, Y. Zhang, T. Jia, K. Zhang, J. Li, L. Wang, C.L. Wang, Development of a microRNA delivery system based on bacteriophage MS2 virus-like particles, FEBS, 2012. doi:10.1111/j.1742-4658.2012.08512.x.

Pattanayak V, S. Lin, J.P. Guilinger, E. Ma, J.A. Doudna, D.R. Liu, High- throughput profiling of off-target DNA cleavage reveals RNA-programmed Cas9 nuclease specificity, Nat. Biotechnol. 31 (2013) 839–843. doi:10.1038/nbt.2673.
Peabody DS, Immunogenic display of diverse peptides, including a broadly cross-type neutralizing human papillomavirus L2 epitope, on virus-like particles of the RNA bacteriophage PP7.Vaccine, 28 (2010) 4384–4393. doi:10.1016/j.vaccine.2010.04.049.

Peretti S, I. Schiavoni, K. Pugliese, M. Federico, Cell Death Induced by the Herpes Simplex Virus-1 Thymidine Kinase Delivered by Human Immunodeficiency Virus-1-Based Virus-like Particles, 12 (2005) 1185–1196. doi:10.1016/j.ymthe.2005.06.474.

Pichlmair A, O. Schulz, C. Tan, J. Rehwinkel, H. Kato, O. Takeuchi, S. Akira, Pickett GG, D.S. Peabody, Encapsidation of heterologous rnas by bacteriophage MS2 coat protein, Nucleic Acids Res. 21 (1993) 4621–4626. doi:10.1093/nar/21.19.4621.

Plummer EM, D. Thomas, G. Destito, L.P. Shriver, M. Manchester, Interaction of cowpea mosaic virus nanoparticles with surface vimentin and inflammatory cells in atherosclerotic lesions, Nanomedicine. 7 (2012) 877–888. doi:10.2217/nnm.11.185.

Pogac V, W. Filipowicz, Human H / ACA Small Nucleolar RNPs and Telomerase Share Evolutionarily Conserved Proteins NHP2 and NOP10, Molecular and Cellular Biology, Dec 2000, 20 (23) 9028-9040; DOI: 10.1128/MCB.20.23.9028-9040.2000

Prel A, V. Caval, R. Gayon, P. Ravassard, C. Duthoit, E. Payen, L. Maouche- Chretien, A. Creneguy, T.H. Nguyen, N. Martin, E. Piver, R. Sevrain, L. Lamouroux, P. Leboulch, F. Deschaseaux, P. Bouillé, L. Sensébé, J.-C. Pagès, Highly efficient in vitro and in vivo delivery of functional RNAs using new versatile MS2-chimeric retrovirus-like particles, Mol. Ther. Methods Clin. Dev. 2 (2015) 15039. doi:10.1038/mtm.2015.39.

Presnyak V., N. Alhusaini, Y.-H. Chen, S. Martin, N. Morris, N. Kline, S. Olson, R.J. Lebbink, H. Rehmann, N. Geijsen, Efficient Intracellular Delivery of Native Proteins, Cell. 161 (2015) 674–690. doi:10.1016/j.cell.2015.03.028.

Ramaswamy S, N. Tonnu, K. Tachikawa, P. Limphong, J.B. Vega, P.P.Karmali, P. Chivukula, I.M. Verma, Systemic delivery of factor IX messenger RNA for protein replacement therapy, Proc. Natl. Acad. Sci. U. S. A. 114 (2017) E1941–E1950. doi:10.1073/pnas.1619653114.

Reiter NJ, A. Osterman, A. Torres-larios, K.K. Swinger, A. Mondragón, Structure of a bacterial ribonuclease P holoenzyme in complex with tRNA Nature, 2010
Remaley AT, A cholesterol-lowering VLP vaccine that targets PCSK9, Vaccine. 33 (2015) 5747–5755. doi:10.1016/j.vaccine.2015.09.044.

Resch K, H. Holtmann, Affinity purification of ARE-binding proteins identifies poly(A)-binding protein 1 as a potential substrate in MK2-induced mRNA stabilization, BBRC, 301 (2003) 665–670.

Rich A. "On the problems of evolution and biochemical information transfer." In: Kasha M., Pullman B., editors. Horizons in Biochemistry. Academic Press; New York, NY, USA: 1962. pp. 103–126

Richard JP, K. Melikov, E. Vives, C. Ramos, B. Verbeure, M.J. Gait, L. V Chernomordik, B. Lebleu, Cell-penetrating Peptides, J Biol Chem 278 (2003) 585–590. doi:10.1074/jbc.M209548200.

Robert MA, V. Lytvyn, F. Deforet, R. Gilbert, B. Gaillet, Virus-Like Particles Derived from HIV-1 for Delivery of Nuclear Proteins: Improvement of Production and Activity by Protein Engineering, Mol. Biotechnol. 59 (2017) 9– 23. doi:10.1007/s12033-016-9987-1.

Rozhdestvensky TS, T.H. Tang, I. V. Tchirkova, J. Brosius, J.P. Bachellerie, A. Hüttenhofer, Binding of L7Ae protein to the K-turn of archaeal snoRNAs: A shared RNA binding motif for C/D and H/ACA box snoRNAs in Archaea, Nucleic Acids Res. 31 (2003) 869–877. doi:10.1093/nar/gkg175.

Ruan GX, E. Barry, D. Yu, M. Lukason, S.H. Cheng, A. Scaria, CRISPR/Cas9-Mediated Genome Editing as a Therapeutic Approach for Leber Congenital Amaurosis 10, Mol. Ther. 25 (2017) 331–341. doi:10.1016/j.ymthe.2016.12.006.

Rulli SJ, C.S. Hibbert, J. Mirro, T. Pederson, S. Biswal, A. Rein, Selective and Nonselective Packaging of Cellular RNAs in Retrovirus Particles, J. Virol. 81 (2007) 6623–6631. doi:10.1128/JVI.02833-06.

Saito H, T. Kobayashi, T. Hara, Y. Fujita, K. Hayashi, R. Furushima, T. Inoue, Synthetic translational regulation by an L7Ae–kink-turn RNP switch, Nat. Chem. Biol. 6 (2010) 71–78. doi:10.1038/nchembio.273.

Schlee M, A. Roth, V. Hornung, C.A. Hagmann, W. Barchet, C. Coch, M. Janke, G. Wardle, S. Juranek, H. Kato, T. Kawai, H. Poeck, K.A. Fitzgerald, O. Takeuchi, S. Akira, T. Tuschl, E. Latz, J. Ludwig, G. Hartmann, Recognition of 5' triphosphate by RIG-I helicase requires short blunt double-stranded RNA as contained in panhandle of negative-strand virus. Immunity. 2009 Jul 17;31(1):25-34 doi:10.1016/j.immuni.2009.05.008.

Schmidt A, T. Schwerd, W. Hamm, J.C. Hellmuth, S. Cui, M. Wenzel, F.S. Hoffmann, M. Michallet, R. Besch, K. Hopfner, S. Endres, S. Rothenfusser, 5'-triphosphate RNA requires base-paired structures to activate antiviral signaling via RIG-I, Proc Natl Acad Sci USA. 2009 Jul 21;106(29):12067-72.

Schmitt PT, G. Ray, A.P. Schmitt, The C-terminal end of parainfluenza virus 5 NP protein is important for virus-like particle production and M-NP protein interaction., J. Virol. 84 (2010)

12810–23. doi:10.1128/JVI.01885-10.

Schuberth-Wagner C, J. Ludwig, A.K. Bruder, A.M. Herzner, T. Zillinger, M. Goldeck, T. Schmidt, J.L. Schmid-Burgk, R. Kerber, S. Wolter, J.P. Stümpel, A. Roth, E. Bartok, C. Drosten, C. Coch, V. Hornung, W. Barchet, B.M. Kümmerer, G. Hartmann, M. Schlee, A Conserved Histidine in the RNA Sensor RIG-I Controls Immune Tolerance to N1-2'O-Methylated Self RNA, Immunity. 43 (2015) 41–52. doi:10.1016/j.immuni.2015.06.015.

Seki, T., Yuasa, S., Oda, M., et al. (2010). Generation of induced pluripotent stem cells from human terminally differentiated circulating T cells. Cell Stem Cell, 7, 11.

Selmer M, C.M. Dunham, F. V. Murphy IV, A. Weixlbaumer, S. Petry, A. C. Kelley, J.R. Weir, V. Ramakrishnan, Structure of the 70S Ribosome Complexed with mRNA and tRNA, Science, (2006). doi:10.1126/science.1131127.

Singer MS, D.E. Gottschling, TLC1 : Template RNA Component of Saccharomyces cerevisiae Telomerase, Science, 509 (1994).

Singh K, H. Evens, N. Nair, M.Y. Rincón, S. Sarcar, E. Samara-Kuko, M.K. Chuah, T. Vanden, Driessche, Efficient in Vivo Liver-Directed Gene Editing Using CRISPR/Cas9, Mol. Ther. 26 (2018) 1241–1254. doi:10.1016/j.ymthe.2018.02.023.

Skabkin MA, O.I. Kiselyova, K.G. Chernov, A. V Sorokin, E. V Dubrovin, I. V Yaminsky, V.D. Vasiliev, L.P. Ovchinnikov, Structural organization of mRNA complexes with major core mRNP protein YB-1, Nucleic Acids Research, 32 (2004) 5621–5635. doi:10.1093/nar/gkh889.

Sladic RT, C.A. Lagnado, C.J. Bagley, G.J. Goodall, Human PABP binds AU- rich RNA via RNA-binding domains 3 and 4, FEBS, (2003) 450–457. doi:10.1046/j.1432-1033.2003.03945.x.

Slivac I, D. Guay, M. Mangion, J. Champeil, B. Gaillet, Non-viral nucleic acid delivery methods, Expert Opin. Biol. Ther. 17 (2017) 105–118. doi:10.1080/14712598.2017.1248941.

Song CQ, D. Wang, T. Jiang, K. O'Connor, Q. Tang, L. Cai, X. Li, Z. Weng,

Souza VD M.F. Summers, How Retroviruses select their genomes, Nature Reviews Microbiology (2005) 643–655. doi:10.1038/nrmicro1210.

Stanton MG, Reviews Current Status of Messenger RNA Delivery Systems, 28 Nucleic Acid Therapeutics (2018) 1–8. doi:10.1089/nat.2018.0726.

Stapleton JA, K. Endo, Y. Fujita, K. Hayashi, M. Takinoue, H. Saito, T. Inoue, Feedback control of protein expression in mammalian cells by tunable synthetic translational inhibition, ACS Synth. Biol. 1 (2012) 83–88. doi:10.1021/sb200005w.

Strenkowska M, R. Grzela, M. Majewski, K. Wnek, J. Kowalska, M. Lukaszewicz, J. Zuberek, E. Darzynkiewicz, A.N. Kuhn, U. Sahin, J. Jemielity, Cap analogs modified with 1,2-dithiodiphosphate moiety protect mRNA from decapping and enhance its translational potential, Nucleic Acids Res. 44 (2016) 9578–9590. http://dx.doi.org/10.1093/nar/gkw896.

Suffian IF, J.T.W. Wang, N.O. Hodgins, R. Klippstein, M. Garcia-Maya, P. Brown, Y. Nishimura, H. Heidari, S. Bals, J.K. Sosabowski, C. Ogino, A. Kondo, K.T. Al-Jamal, Engineering hepatitis B virus core particles for targeting HER2 receptors in vitro and in vivo, Biomaterials. 120 (2017) 126–138. doi:10.1016/j.biomaterials.2016.12.012

Sun Y, Y. Sun, R. Zhao, Establishment of MicroRNA delivery system by PP7 bacteriophage-like particles carrying cell-penetrating peptide, J. Biosci. Bioeng. 124 (2017) 242–249. doi:10.1016/j.jbiosc.2017.03.012.

Swiech L, M. Heidenreich, A. Banerjee, N. Habib, Y. Li, J. Trombetta, M. Sur,

Takahashi K, S. Yamanaka, Induction of Pluripotent Stem Cells from Mouse Embryonic and Adult Fibroblast Cultures by Defined Factors, Cell. 126 (2006) 663–676. doi:10.1016/j.cell.2006.07.024.

Tarun S, A.B. Sachs, A common function for mRNA 5 ' and 3 ' ends in translation initiation in yeast, Genes and Development, (1995) 2997–3007.

Tavernier G, O. Andries, J. Demeester, N.N. Sanders, S.C. De Smedt, J. Rejman, mRNA as gene therapeutic: How to control protein expression, J. Control. Release. 150 (2011) 238–247. doi:https://doi.org/10.1016/j.jconrel.2010.10.020.

Thess A, S. Grund, B.L. Mui, M.J. Hope, P. Baumhof, M. Fotin-Mleczek, T. Schlake, Sequence-engineered mRNA Without Chemical Nucleoside Modifications Enables an Effective Protein Therapy in Large Animals, Mol. Ther. 23 (2015) 1456–1464. doi:10.1038/mt.2015.103.

Tycko J, V.E. Myer, P.D. Hsu, Methods for Optimizing CRISPR-Cas9 Genome Editing Specificity, Mol. Cell. 63 (2016) 355–370. doi:10.1016/j.molcel.2016.07.004.

Uchida N, S. Hoshino, H. Imataka, N. Sonenberg, T. Katada, A Novel Role of the Mammalian GSPT / eRF3 Associating with Poly (A) -binding Protein in Cap / Poly (A) -dependent Translation, JBC, 277 (2002) 50286–50292. doi:10.1074/jbc.M203029200.

Ullu E, C. Tschudi, Alu sequences are processed 7SL RNA genes, Nature, (1984)
V.A. Master, S.K. Pal, W.H. Miller Jr, L.I. Karsh, I.Y. Tcherepanova, M.A. DeBenedette, W.L. Williams, D.C. Plessinger, C.A. Nicolette, R.A. Figlin, Survival with AGS-003, an autologous dendritic cell-based immunotherapy, in combination with sunitinib in unfavorable risk patients with advanced renal cell carcinoma (RCC): Phase 2 study results, J. Immunother. Cancer. 3 (2015) 14. doi:10.1186/s40425-015-0055-3.

Van Tendeloo VF, A. Van de Velde, A. Van Driessche, N. Cools, S. Anguille,

Vidovic I, S. Nottrott, K. Hartmuth, R. Lührmann, R. Ficner, Crystal structure of the spliceosomal 15.5kD protein bound to a U4 snRNA fragment, Mol. Cell. 6 (2000) 1331–1342. doi:10.1016/S1097-2765(00)00131-3

Von Heijne G, Signal Sequences The Limits of Variation, JMB, (1985) 99–105.
W.A. Schroyens, A.P. Gadisseur, I. Vrelust, P.G. Jorens, H. Goossens, I.J. de Vries, D.A. Price, Y. Oji, Y. Oka, H. Sugiyama, Z.N. Berneman, Induction of complete and molecular remissions in acute myeloid leukemia by Wilm's tumor 1 antigen-targeted dendritic cell vaccination, Proc. Natl. Acad. Sci. U. S. A. 107 (2010) 13824–13829. doi:10.1073/pnas.1008051107.

Wang G, T. Jia, X. Xu, L. Chang, R. Zhang, Y. Fu, Y. Li, X. Yang, K. Zhang,

Weinrich SL, R. Pruzan, L. Ma, M. Ouellette, V.M. Tesmer, S.E. Holt, A.G. Bodnar, S. Lichtsteiner, N.W. Kim, J.B. Trager, R.D. Taylor, R. Carlos, W.H. Andrews, W.E. Wright, J.W. Shay, C.B. Harley, G.B. Morin, Reconstitution of human telomerase with the template RNA component hTR and the catalytic protein subunit hTRT, Nat. Genet. 17 (1997) 498. http://dx.doi.org/10.1038/ng1297-498.

Wels M, T.G. Kormelink, M. Kleerebezem, R.J. Siezen, C. Francke, An in silico analysis of T-box regulated genes and T-box evolution in prokaryotes , with emphasis on prediction of substrate specificity of transporters, 16 (2008). doi:10.1186/1471-2164-9-330.

Wilkie GS, K.S. Dickson, N.K. Gray, Regulation of mRNA translation by 5'- and 3'-UTR-binding factors, Trends in Biomedical Science, 28 (2003) 182–188. doi:10.1016/S0968-0004(03)00051-3.

Winkler W, A. Nahvi, R.R. Breaker, Thiamine derivatives bind messenger RNAs directly to regulate bacterial gene expression, Nature. 419 (2002) 952– 956. doi:10.1038/nature01145.

Winkler WC, S. Cohen-Chalamish, R.R. Breaker, An mRNA Structure That Controls Gene Expression by Binding FMN, Proc. Natl. Acad. Sci. U. S. A. 99 (2002) 15908–15913. doi:10.2307/3073881.

Wroblewska L, T. Kitada, K. Endo, V. Siciliano, B. Stillo, H. Saito, R. Weiss, Mammalian synthetic circuits with RNA binding proteins for RNA-only delivery, Nat. Biotechnol. 33 (2015) 839–841. doi:10.1038/nbt.3301.

Wu DT, M.J. Roth, MLV based viral-like-particles for delivery of toxic proteins and nuclear transcription factors, Biomaterials. 35 (2014) 8416–8426. doi:10.1016/j.biomaterials.2014.06.006.

Yang Y, L. Wang, P. Bell, D. McMenamin, Z. He, J. White, H. Yu, C. Xu, H. Morizono, K. Musunuru, M.L. Batshaw, J.M. Wilson, A dual AAV system enables the Cas9-mediated correction of a metabolic liver disease in newborn mice, Nat. Biotechnol. 34 (2016) 334–338. doi:10.1038/nbt.3469.

Yao Y, T. Jia, Y. Pan, H. Gou, Y. Li, Y. Sun, Using a Novel MicroRNA Delivery System to Inhibit Osteoclastogenesis, JMS, 6 (2015) 8337–8350. doi:10.3390/ijms16048337.

Yin H, C. Song, J.R. Dorkin, L.J. Zhu, Y. Li, Q. Wu, A. Park, J. Yang, S. Suresh, A. Bizhanova, A. Gupta, M.F. Bolukbasi, S. Walsh, R.L. Bogorad, G. Gao, Z. Weng, Y. Dong, Therapeutic genome editing by combined viral and non- viral delivery of CRISPR system components in vivo, Nat. Biotechnol. (2016) 1– 7. doi:10.1038/nbt.3471.

Yin H, W. Xue, S. Chen, R.L. Bogorad, E. Benedetti, M. Grompe, V. Koteliansky, P.A. Sharp, T. Jacks, D.G. Anderson, Genome editing with Cas9 in adult mice corrects a disease mutation and phenotype, Nat. Biotechnol. 32 (2014) 551–553. doi:10.1038/nbt.2884.

Zangi L, K.O. Lui, A. von Gise, Q. Ma, W. Ebina, L.M. Ptaszek, D. Später, H. Xu, M. Tabebordbar, R. Gorbatov, B. Sena, M. Nahrendorf, D.M. Briscoe, R.A. Li, A.J. Wagers, D.J. Rossi, W.T. Pu, K.R. Chien, Modified mRNA directs the fate of heart progenitor cells and induces vascular regeneration after myocardial infarction, Nat. Biotechnol. 31 (2013) 898–907. doi:10.1038/nbt.2682.

Zasedateleva OA, A.S. Krylov, D. V Prokopenko, M.A. Skabkin, Specificity of Mammalian Y-box Binding Protein p50 in Interaction with ss and ds DNA Analyzed with Generic Oligonucleotide Microchip, JMB (2002) 73–87. doi:10.1016/S0022-2836(02)00937-3.

Zeltins, A Construction and characterization of virus-like particles: A review, Mol. Biotechnol. 53 (2013) 92–107. doi:10.1007/s12033-012-9598-4.

Zengel JM, A. Jerauld, A. Walker, M.C. Wahl, L. Lindahl, The extended loops of ribosomal proteins L4 and L22 are not required for ribosome assembly or L4- mediated autogenous control, RNA (2003) 1188–1197. doi:10.1261/rna.5400703.High- resolution.

Zhan S, J. Li, R. Xu, L. Wang, K. Zhang, R. Zhang, Armored long RNA controls or standards for branched DNA assay for detection of human immunodeficiency virus type 1, J. Clin. Microbiol. 47 (2009) 2571–2576. doi:10.1128/JCM.00232-09.